VSB Technical University of Ostrava
Faculty of Materials Science and Technology

DISSERTATION THESIS

2019 **Ing. Diana Lazecka**

VSB Technical University of Ostrava
Faculty of Materials Science and Technology

Biofilm creation study on polymeric nanocomposites

Ing. Diana Lazecka

Study program: Process Engineering

Supervisor: doc. Ing. Grazyna Simha Martynková, Ph.D.

Ostrava 2019

Bibliography identification

Name and surname of the author:
Ing. Diana Lazecka

Name of the dissertation thesis:
Biofilm creation study on polymeric nanocomposites

Name of the dissertation thesis in Czech:
Studium tvorby biofilmu na polymernich nanokompozitech

Faculty:
Faculty of Materials Science and Technology

Study program:
Process Engineering

Supervisor:
doc. Ing. Grazyna Simha Martynková, Ph.D.

Year of defense:
2019

Keywords in English:
Nanocomposite; Biofilm; Polymeric matrix; Biliary stents; Clay minerals; Nanoparticles; Thin film; Antimicrobial agent; Cancer treatment

Keywords in Czech:
Nanokompozit; Biofilm; Polymerní matrice; Biliární stenty; Jílové minerály; Nanočástice; Tenký film; Antimikrobiální látka; Léčba rakoviny

Prohlášení/Statement

Já, Diana Lazecka, prohlašuji, že jsem tuto práci vypracovala samostatně. Veškerou literaturu a ostatní prameny, z nichž jsem při přípravě práce čerpala, řádně cituji a uvádím v seznamu použité literatury.

I, Diana Lazecka, confirm that I have elaborated this work on my own. I cite and keep the references of all literature and other sources that I used during the preparation of this thesis.

Ostrava, 2019 Podpis

Acknowledgment

I would like to thank my supervisor, doc. Ing. Gražyna Simha Martynková, Ph.D., for attention, advisory, supervision, support and patience, which she kindly provided during the years of my study. I would like also to thank my kind colleagues in the Nanotechnology Center who helped me anyhow during this time.

Special thanks to Thomas Bata University of Zlin (Czech), Zdravotni Ustav Ostrava (Czech), Ustav geoniky (Czech), IT4Innovations (Czech), University of Jaen (Spain), University of Leeds (UK) and all the wonderful people I have met there, which gave me inspiration, knowledge and support.

I want to believe that the time and energy I have spent on this research will bring a drop of knowledge to the ocean of unexplored and unknown. I am thankful to life for such an experience and proud of being a part of scientific community.

I must also warmly thank my parents and my husband for deep understanding, endless support and care.

Acknowledgement of the support by projects: the National Programme of Sustainability (NPU II) project “IT4Innovations excellence in science-LQ1602” and to projects MŠMT SP 2016/75, SP2017/86, SP 2018/112, SP 2019/50

Abstract

The dissertation thesis focuses on the problematic of biliary stents functional coating, which may play an essential role in the life prolongation of cancer patients with bile duct types of cancer tumors. The developed coating represents a polymeric nanocomposite thin film prepared via *in-situ* polymerization, re-polymerization and extrusion methods.

Prepared number of samples with different types of antimicrobial agents, clay particles and polymeric matrices is characterized by X-Ray diffraction, FT Infrared Spectroscopy, Differential scanning calorimetry, Scanning Electron and Atomic Force Microscopy techniques as well as tested on microbial activity via special microbiological techniques. The charecterization provides the data about stability, morphology and structure of the developed materials. Several “in-body simulation” experiments are performed such as bile salts simulation, real-time liquid flow biofilm growing and visualization of the effect of the selected nanocomposite sample on the growth. The results show the actual antimicrobial functionality of the developed materials in case of ciclopirox olamine, less in case of imidazole and clotrimazole antimicrobial agents. Molecular modeling was used to prove the thermodynamical stability, it showed that the system gets more stable with greater antitumoral drug amount.
Molecular modeling was used to demonstrate the thermodynamic stability of drug system, it showed that the system becomes more stable with more antitumoral drug. An attempt to experimentally prepare an antitumoral polymeric nanocomposite was made.

Keywords: Nanocomposite, Biofilm, Polymeric matrix, Biliary stents, Clay minerals, Nanoparticles, Thin film, Antimicrobial agent, Cancer treatment

Abstrakt

Disertační práce se zaměřuje na problematiku funkčního povlaku žlučových stentů, který může hrát zásadní roli v prodloužení života pacientů s rakovinou s rakovinou žlučových cest. Vyvinutý povlak představuje polymerní nanokompozitní tenký film připravený metodami *in-situ* polymerace, re-polymerace a extruze.

Připravené vzorky s různými typy antimikrobiálních látek na jílových částicích zakomponované do tří různých polymerních matric je charakterizován rentgenovou difrakcí, FT infračervenou spektroskopií, diferenciální skenovací kalorimetrií, skenovací elektronovou mikroskopií a mikroskopií atomárních sil. Vzorky jsou dále testovanými na mikrobiální aktivitu pomocí speciálních mikrobiologických technik. Vyhodnocením výsledků analýz a testů jsme získali údaje o stabilitě, morfologii a struktuře vyvinutých materiálů. Dále byly uskutečněny testy *in vitro*, jako je simulace žlučových solí, růst biofilmu v tekutém toku v reálném čase a vizualizace účinku vybraného vzorku nanokompozitu na růst. Výsledky ukazují skutečnou antimikrobiální funkčnost vyvinutých materiálů v případě ciclopirox olaminu, méně v případě imidazolových a klotrimazolových antimikrobiálních látek.
Molekulární modelování bylo použito k prokázání termodynamické stability polymerního systému s léčivem, ukázalo se, že systém se stává stabilnějším s větším množstvím protinádorového léčiva. Byl proveden pokus experimentálně připravit protinádorový polymerní nanokompozit.

Klíčová slova: Nanokompozit, Biofilm, Polymerní matrice, Biliární stenty, Jílové minerály, Nanočástice, Tenký film, Antimikrobiální látka, Léčba rakoviny

Table of Contents

List of abbreviations

UV – ultraviolet

EPS - extracellular polymeric substance

ERCP - endoscopic retrograde cholangiopancreatography pancreatitis

PTC - percutaneous transhepatic cholangiography

SEMS - self-expanding metallic stent

FISH - fluorescence in situ hybridization

PLS - polymer/layered silicate

DNA - deoxyribonucleic acid

RNA - ribonucleic acid

PVAL – polyvinyl alcohol

PVAc – polyvinyl acetate

PEO - polyethylene oxide
PEG - Polyethylene glycol

FDA - Food and Drug Administration

AIPEA - Association Internationale pour l'Étude des Argiles

VMT – vermicuilte

BEN – bentonite

MMT – montmorillonite

PBPs - Penicillin- binding proteins

ESBLs - Extended-spectrum P lactum

CPX; ciclo – ciclopirox olamine

ATPase - adenosine triphosphatase

IMI – imidazole

BRO - Trihexyltetradecylphosphonium bromide

TROL – trolamine

CLO – clotrimazole

ERL – erlotinib

EGFR - epidermal growth factor receptor

SLM - supported liquid membranes

NSCLC - Non-small cell lung cancer

QS - quorum sensing

XRD - X-ray diffraction

ATR - attenuated total reflectance Fourier transform infrared spectroscopy

FTIR; FT-IR - A Fourier Transform InfraRed

FT - Fourier Transform

IR – Infra Red

DSC - Differential Scanning Calorimetry

OIT - oxidation induction time

DTA - differential thermal analysis

EM – electron microscopy

SPM – scanning probe microscopy

SFM - scanning force microscopy

PNC – polymeric nanocomposite

SEM - Scanning Electron Microscopy

EDS - energy dispersive spectroscopy

STM - scanning tunneling microscope

AFM - atomic force microscopy

MIC - Minimum inhibitory concentration

MBC - Minimum bactericidal concentration

CFU - Colony-forming unit

VA – vinyl acetate

BP – benzoyl peroxide

PCL-PEG-PCL - polycaprolactone polyethylene glycol polycaprolactone

PCL-PGA-PCL - polycaprolactone polyglycolic acid polycaprolactone

CED - cohesive energy density

1. INTRODUCTION

"Solve et coagula"

The materials science in field of medicine has made humongous progress in last few decades. The innovation in advanced materials and design of devices used for surgery and prosthetics is helping to extend human life and improve quality of patient's life.

The main risk areas of the surgery and following recovery from the illness are the infection. The infection can be caused via several life endangering bacterial strains and some yeast species.

Bacteria and the risk of infection is a significant concern for medical plastic components inserted into the body. Applications of greatest concern are those exposed to bodily fluid for extended periods of time, including but not limited to catheters, wound dressings, hospital bedding, surgical drapes, and hospital gowns. The risk of infection is particularly high for those tubes and components that are left in place for three or more days (i.e. in-dwelling catheters).

In this case, handling and exposure of these devices can influence time of onset and severity of infection. Infections often occur at incision points, where enter the blood vessel and bacteria is introduced into blood stream.

The general mechanism of infection related to in-dwelling polymers can be summarized as follows: Free floating microorganisms attach to the plastic surface. Colonies of bacteria grow and permanently anchor to plastic surface. A biofilm formation results as colonies grow and mature. Infection occurs when biofilm detaches from plastic substrate.

Antimicrobial technologies using both silver and polymer-based solutions are designed to fight infection and prevent the development of bacteria on contact surfaces. Formulations are custom developed to achieve specific application requirements.

Biofilms are of great importance in control of healthcare associated and other infections. This is not only due to their ability to act as a safe-haven for those microorganisms that are of public health significance, but also due to their inherent tolerance of and 'resistance' to antimicrobials. The diagnosing of a biofilm infection represents an area of grave concern significantly easier on abiotic surfaces following removal of a medical device than on biotic surfaces. For example, evidencing a biofilm within a chronic wound is complex and presently there is no 'gold standard' for that (Percival et al., 1999; Percival et al., 2010; Percival et al., 2015).

The main issue for successful and long-term elimination of the bacterial infection connected to the biofilm creation, is careful selection of materials of the medical device. Recent development of advanced materials is being more and more related to nanotechnology options. Utilization of materials which contains functional nanoparticles or have nanostructured surface/bulk is getting

very advantageous for many applications in medicine. As the wide range of materials used for medical devices are either metallic of polymeric, the main interest will be focused in improving of those materials.

In case of metallic devices, the research and discussion are heading to the modification of surfaces with appropriate coating. The coating should have except functionality very good adhesion to the metal surface material.

The polymeric surface will have more options for modification. Except attaching or depositing other functional layer we can play with base material itself to modify upper layer of the bulk.

To mitigate the infections associated with the implanted devices, a variety of antimicrobial device coatings have been developed with the goal of inhibiting the growth of biofilms on the devices both with and without drugs. Antimicrobial device coatings have dramatically evolved over the past couple of years. While early technologies focused on diffusion-based antibiotic-eluting coatings that provide short-term antimicrobial therapy, recent technologies have shifted their focus to coatings with more long-term antibiotic-eluting capabilities and materials that show intrinsic antimicrobial activity. The growing trend in the annual number of scientific journal publications on antimicrobial coatings over the past 17 years. Specifically, from 1997 to 2014, there has been a nearly 30-fold increase in the number of articles annually published on antimicrobial coatings, demonstrating the large number of innovations that have recently been developed in the field. In particular, the increase in publications over the past five years can be partially attributed to the legislative changes of the Patient Protection and Affordable Care Act (2010) (Cyphert et al., 2017).

THE WORK AIMS

The presented work is focused on materials suitable for medical applications, where the rapidly growing microbial biofilm is one of the serious dangers for health and life of a human. Since the range of the materials and applications in the field of prosthetics inserted in the body is large, this work will specialize only on one type of medical devices which are gastronentheorological stents applicable in case of damaged bile duct.

The research in this field will focus on study and optimization of polymeric stent material in respect to the conditions in the body.

The polymeric stent with antimicrobial/antitumoral filler may prolong the lifetime of the stent inside the body and therefore intense the treatment (Fig.1).

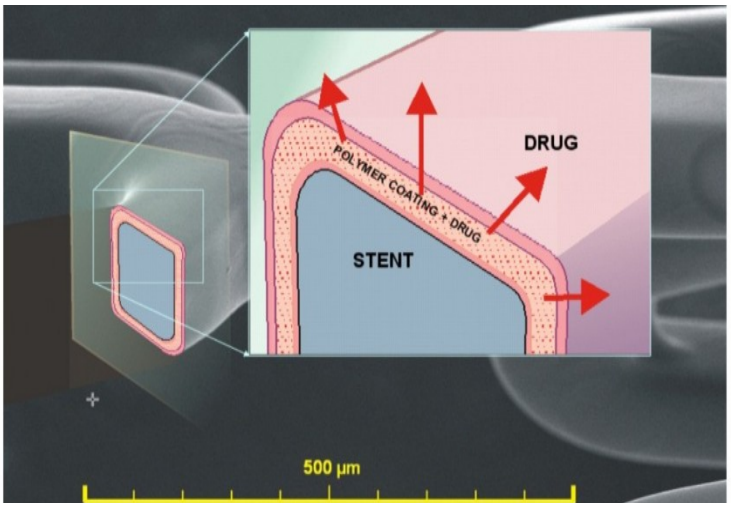

Figure 1. The schematic concept of the stent coating with drug elimination.

The partial goals of the work are:

- Molecular modeling of selected interaction
- Based on the known clinical facts and literature recherche select optimal basic materials and modifying compounds for experimental part
- Laboratory synthesis of functional antimicrobial materials suitable for incorporation to the polymeric matrix
- Laboratory preparation of polymeric nanocomposite
- Nanocomposite testing for stability
- Antimicrobial testing of selected nanocomposite
- Finding the most effective combinations of contents in nanocomposites
- Testing *in-vivo*

The experimental part of work presents the preparation and optimization of the polymeric film with antibacterial compounds. The formation and behavior of biofilms are tested via special microbiological methods.

2. THEORETICAL PART

The theoretical part first briefly explains the problematics of microbial biofilm along with related medical aspects. Then it continues in description of the materials selected for the research and shows the preparation methods of recently used polymeric nanocomposites. The chapter ends by showing the mechanisms of action of antimicrobial drugs, methods for further elimination of microbial film and points at usage of antitumoral drugs in chemotherapy.

2.1 BIOFILM ALARM

The modern society is focused on increasing the level of life and its quality. Although the population of the planet is rapidly growing and in current moment there is almost 8 billions of people, we all want to be healthy and have a chance to survive all possible and impossible conditions. As the humanity develops and adapts to a new reality, so do the bacterial strains and other living beings. The microorganisms are getting resistant to medicines and the consequences from it are dangerous for the whole of society.

Antibiotics were first synthesized in the beginning of 20th century, the very first one was called Arsphenamine and was used against syphilis (Gibaud et al., 2010). For more than a century the pharmaceutical industry was actively developing the treatments against all possible diseases associated with bacterial strains. Millions of people's lives have been saved, many deadly infections have been beaten. Nowadays, antimicrobials can be found almost everywhere, even in the chicken bought for dinner in supermarket.

The World Health Organization claims that the excessive usage of antimicrobial agents will be reduced to a reasonable minimum (O'Neill, 2016).

By 2050 the deaths from resistant bacterial infections are expected to overcome the lethal cancer cases (Fig.2).

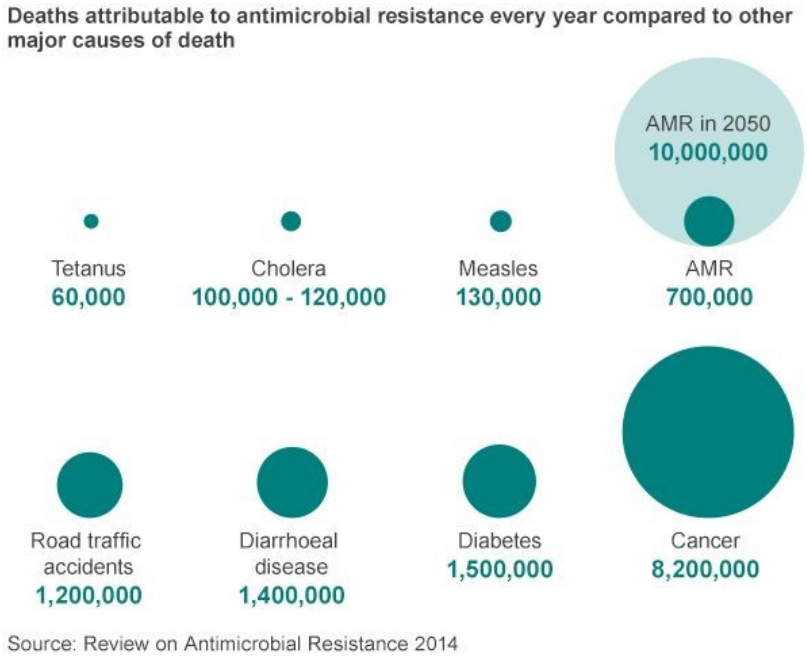

Figure 2. Antimicrobial resistance caused deaths compared to other major death causes (Cyphert et al. 2017).

BIOFILM DEFINITION

In comparison to higher life forms microorganisms can be seen as simple ones. But the investigations show their incredible ability to develop into complex systems to have a chance to survive different stresses (temperatures, UV-light etc.). These complex systems are known as bacterial biofilms. Opposite from laboratory conditions when the bacteria are isolated on specific media, in nature they are surviving mainly by attaching to and developing on many kinds of surfaces including human tissues and medical devices such as catheters and stents. It is considered a reason of numerous diseases like pneumonia and many tract and bloodstream infections. As a consequence, the complexity of biofilm brings lower susceptibility to antimicrobial agents if compared with planktonic organisms. When a medical device is colonized by a biofilm there is often a need of its removal and replacement operation (O'Toole et al., 2000; Olson et al., 2002).

Biofilms grow in several stages shown on Fig.3.

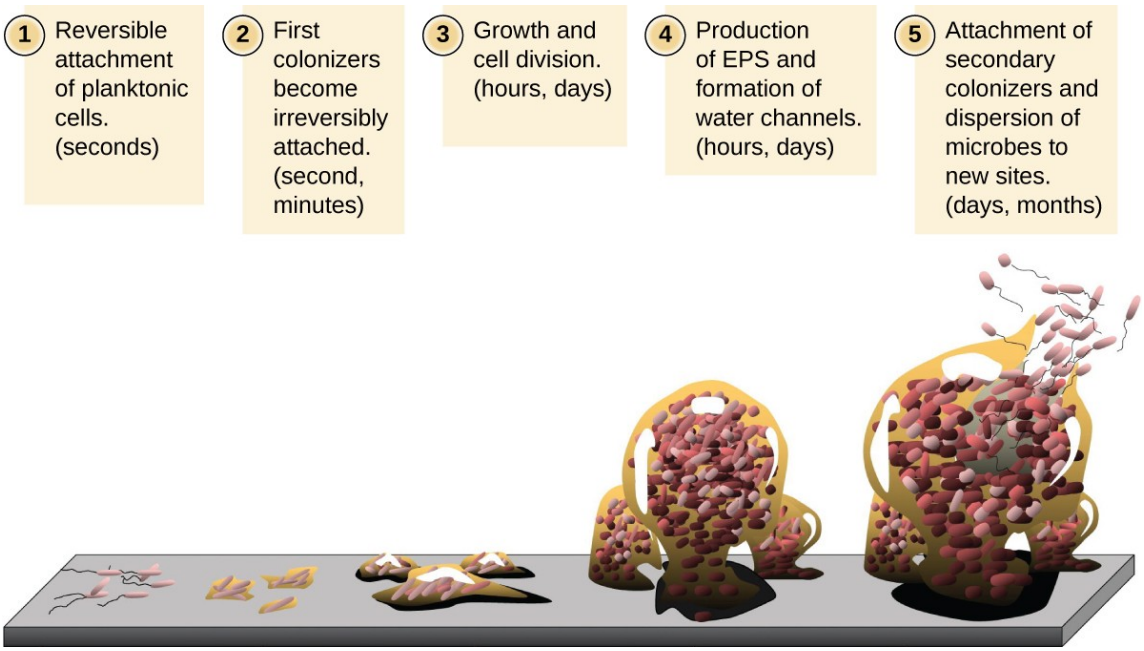

Figure 3. Stages of biofilm development. 1. *Initial attachment* 2. *Irreversible attachment* 3. *Maturation* I 4. *Maturation* II 5. Dispersion (O'Toole, 2000).

A biofilm can be defined as the extracellular polymers produced by microcolonies attached to the surface. The extracellular polymeric substance (EPS) contains polysaccharides and is very hydrated. The structure is heterogeneous and contains channels for nutrient and oxygen transportation (Lewandowski, 2000). It can be called "slime", which is causing so much difficulties with treatment. Infiltration of this slime is problematic for many antibiotics and chemicals, furthermore, on the slime's surface are the electrical charges which can create a barrier for antimicrobials. Also, antibiotics are efficient mostly on actively growing cells but the cells hidden behind the biofilm are slow because of oxygen and nutrient starvation, therefore they have lower susceptibility to antibiotics.

Obviously, it is not that simple to get rid of biofilms on surfaces, but there are several options. For example, removal of implant can help, if the biofilm haven't spread to a living tissue (Donlan, 2001). Other methods include different coatings for implants such as silver layers, different antimicrobial drugs, nanoparticles or nanocomposites.

The severity of the infection depends upon the type of bacteria or fungi involved as well as the maturity of the biofilm they may develop upon bacterial/fungal colonization on the device. In particular, Gram-positive *Staphylococcus aureus* (*S. aureus*) and *epidermidis* (*S. epidermidis*) are some of the most common bacterial strains responsible for forming biofilms on the devices (Naber,

2009). For fungal biofilms, *Candida albicans* (*C. albicans*) is the most prevalent. Once the biofilms are established, they can be very difficult to treat with conventional antibiotic treatments since the bacteria in the biofilm are metabolically inactive, rendering the biofilms less responsive to antibiotics (Cohen et al., 2013). Under these circumstances, the infected device often fails and must be removed from the patient to eradicate the infection. Therefore, the goal of antimicrobial device coatings is to prevent the infection, since treatment after infection occurs is challenging. While only a small percentage of patients develop infections, the cost of treating these infections surpasses $11 billion every year with nearly 2 million infection cases annually (Schierholz et al., 2001).

2.2 MEDICAL ISSUES – BILIARY STENTS

2.2.1 THE BILE DUCT

The biliary tract, (biliary tree or biliary system) includes the liver, gall bladder and bile ducts, altogether they are able to make, store and secrete bile (Fig.4). Bile consists of water, electrolytes, bile acids, cholesterol, phospholipids and conjugated bilirubin. Some components are synthesized by liver cells (hepatocytes), the rest liver extracts from the blood.

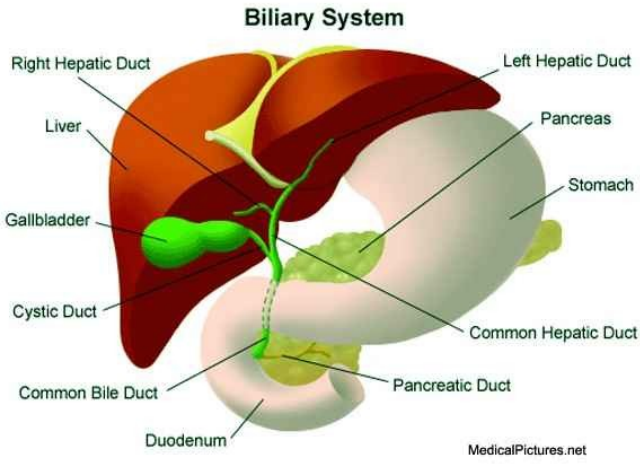

Figure 4. Biliary system scheme.

2.2.2 BILE AND ITS FUNCTION

Bile is made in the liver and stored in the gallbladder. The system of bile fluids includes water (97%), fats such as cholesterol, lecithin, phospholipids and fatty acids (0.51%), bile salts (0.7%), bilirubin (0.2%) and some inorganic salts (Barret et al., 2012). When lipids enter the small intestines, this triggers the release of bile. A

bile acid has two sides, a hydrophilic side and a hydrophobic side (Fig.5). To allow lipids to travel in an aqueous environment, the hydrophobic side binds to the lipid and surrounds it, creating an emulsion. Bile aids the digestive process by making it easier for enzymes to digest the fat, but is necessary for lipid absorption. After bile is absorbed and utilized, it can be recycled by the body and reused. Liver secretes the bile into small ducts which form the common hepatic duct.

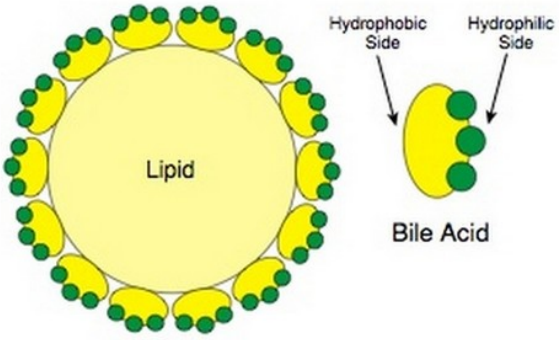

Figure 5. Lipid-bile acid interaction.

The bile duct is long tube-like structure that connects the liver to the intestine. The liver makes bile that is required for the digestion of food. The bile from the liver is transported to the intestine by the bile duct. It contains a mix of products such as bilirubin, cholesterol, and bile acids and salts.
The top half of the bile duct is associated with the liver while the bottom half of the bile duct is associated with the pancreas through which it passes on its way to the intestine. It opens in the part of the intestine called the duodenum into a structure called the Ampulla.
A variety of diseases can affect the bile ducts. All block the bile ducts in some way, which is why the various diseases cause similar symptoms.

Less common causes of blockages include cancers of the bile duct (cholangiocarcinomas) and strictures (scars that narrow the ducts after infection, surgery or inflammation).
Jaundice is commonly caused by conditions such as pancreatic cancer caused by blockage of the bile duct passing through the cancerous portion of the pancreas, bile duct cancer, blockage by a stone in patients with gallstones and from scarring after injury to the bile duct during gallbladder removal. The disease allows the skin and eyes to become yellow from the accumulated bile in the blood. This condition also causes severe itchiness.

Other bile duct diseases are uncommon, and include primary sclerosing cholangitis and primary biliary cirrhosis. Typically diagnosed in mid-adulthood, these conditions create ongoing inflammation in the bile duct walls, which can narrow and scar the walls. Primary sclerosing cholangitis is more common in people with inflammatory bowel disease (ulcerative colitis or Crohn's disease). Primary biliary cirrhosis is more common in women (Poupon, 2010). It is sometimes associated with autoimmune diseases such as Sjögren's syndrome, thyroiditis, scleroderma or rheumatoid arthritis.

Biliary atresia is a rare form of bile duct blockage that occurs in some infants two weeks to six weeks after birth, a time when the bile ducts have not completed their development normally.
The chronic conditions of primary sclerosing cholangitis, primary biliary cirrhosis and biliary atresia can result in inflammation and scarring of the liver, a condition known as cirrhosis.
Certain parasite infections mostly common in Southeast Asia (*Clonorchis sinensis* and *Opisthorchis viverrini*, also known as Chinese liver fluke) are associated with a higher risk of bile duct diseases.

2.2.3 BILIARY STENT APPLICATION

Stent is a short narrow metal or plastic tube often in the form of a mesh that is inserted into the lumen of an anatomical vessel (such as an artery or a bile duct) especially to keep a previously blocked passageway open.
Recent years many types of stents have been investigated, all have advantages and disadvantages which have to be discussed.
Biliary and pancreatic plastic or metal stents are used primarily to establish patency of an obstructed bile duct or main pancreatic duct but may also be used to treat biliary or pancreatic leaks, cholecystitis, large non-removable common bile duct stones, pancreatic fluid collections and to prevent post endoscopic retrograde cholangiopancreatography (ERCP) pancreatitis (Mangiavillano, 2015). This has become established as a treatment to resolve obstructive jaundice by a non-surgical approach. As this technique allows the relief of preoperative acute biliary obstruction, it is useful for stabilizing patients before surgery and enhancing their quality of life by enabling internal drainage in those who are not eligible for surgery. Although it is a beneficial method of treatment, it also can cause some further complications.
Biliary stenting is an effective solution of relieving obstruction, and is the preferred method of alleviating patients with malignancy (Barkay et al., 2013) as well as in benign conditions such as biliary fistulas or benign biliary strictures (Dumonceau et al., 2011).
As (Coté et al., 2016) said in their research "*among patients with benign biliary strictures of 6 mm or larger in whom the covered metallic stent would not overlap the cystic duct, cSEMS (covered self-expanding metallic stent) were not inferior to multiple plastic stents in achieving stricture resolution after no more than 12 months of endoscopic therapy*".

The efficacy of both types of biliary stents is high and frequent. Plastic stents are of interest because of economic reasons, they are at least 10 times cheaper than SEMSs. Developed plastic stents could not only help in expanding of vessels and unblocking the pathways for liquids but also to prevent occurring of various complications and to increase the efficacy of treatment itself. SEMSs are associated with a statistically significantly lower occlusion rate, less therapeutic failure, less need for reintervention, and lower cholangitis incidence (Sawas et al., 2015).

On the other hand, an important problem is the negative effect of metal ions or fretting debris, which can be released from the stainless steel implant devices because of corrosion, wear or other

reasons. Nickel and chromium are known as potentially harmful elements in the medical stainless steel. Nickel ions act as the allergens, which may cause cutaneous inflammations such as swelling, reddening, eczema and itching on skins, and may also lead to allergy reactions, teratogenicity and carcinogenicity in human body (Yang et al., 2010). The optimization of the metal-based stents, as well as plastic-based, is developing rapidly and there are already some solutions for the reduction of nickel release and increasing of biocompatability (Gill et al., 2015).

In comparison with metallic stents according to recent publications there is a higher probability of different stent failures in plastic-based stents (Table 1).

Stent failure is associated with recurrent morbidity, and often necessitates repeat endoscopy with stent retrieval and replacement. These procedures carry an increased risk for procedural complications such as pancreatitis, and can result in additional hospital admissions (Shatzel, 2016).

Table 1. Current stent failure rates.

Stent type	Stent failure rates in malignant obstruction
Plastic stents	30%-70%
Self expanding metal stents	19%-46%

Stent failure can be stratified into four primary etiologies: Internal stent failure from biliary clogging, external failure caused by tumour ingrowth or overgrowth of excessive epithelial or malignant cells, and stent migration. The incidence of each type of failure in malignant obstruction has been documented in several small prospective trials (Table 2).

Table 2. Causes of stent failure.

Causes of stent failure	Percent of total failures
Tumor ingrowth	66%-68%
Epithelial ingrowth	-
Biliary clogging	17%-21%
Tumor overgrowth	2%-11%
Stent migration	0%-4%

Although the biliary plastic stents were first introduced in 1979 and the very first coronary stent was implanted in 1986 (Serruys et al., 2006), the further research on stents didn’t go too far. As a solution to prevent the failures of implanted biliary stents the usage of several drugs has been performed. None of them nowadays are ideally fitting the conditions of the biliary environment. Ideal agents to incorporate into the stent exterior would help to effectively inhibit the growth of malignant pancreaticobilary cells, retard the proliferation of biliary epithelial hyperplasia and display favorable histologic changes when exposed to biliary epithelium, without necrosis or risk of

biliary perforation (Shatzel, 2016).

There are two ways to place a bile duct stent: ERCP (endoscopic retrograde cholangiopancreatography) and PTC (percutaneous transhepatic cholangiography).

Endoscopic treatment includes radial dilation with balloon dilators followed by the placement of post-stricture stents that must be maintained for at least three months. The control for evaluation of biliary duct patency may be performed through magnetic resonance cholangiography or endoscopic cholangiography. This treatment is less invasive than surgery with success rates ranging from 70% to 80% (Vitale et al., 2008). In general, 80-90% of biliary strictures can be treated through endoscopy. The predictors for endoscopic treatment failure include lesions above the hilum, long stenoses, late postoperative presentation (more than 3 months), anatomic variations of the upper gastrointestinal tract or of the biliary ducts, and clinical conditions of patients that affect the safety of prolonged sedation or general anesthesia (Artifon et al., 2012).

The main disadvantage of plastic stents is their limited diameter. This is set by the working channel in the duodenoscope, which prevents use of plastic stents with an outer diameter of more than ~4mm or 12 Fr (French scale or French gauge system commonly used to measure the size of a catheter) (Raijman, 2003). This can be a major issue for patients who require long-term placement of a stent. Stents with a larger diameter have longer patency because it takes longer for the inner cavity to fill with foreign substances (Speer et al., 1988). However, it is impossible to endlessly extend the diameter of the working channel of an endoscope due to its design, and thus the maximum outer diameter of a plastic stent is 11.5 Fr at most. Then 10 Fr plastic stents require a duodenoscope with an accessory channel of 3.7 mm, and 11.5 Fr plastic stents require a duodenoscope with an accessory channel of 4.2 mm (Pfau et al., 2013). According to several studies no major difference in the outcome between 10- and 11.5-Fr stents was found, and the mean duration of stent patency was 3 to 6 months (Kadakia et al., 1992). Despite the opinions that the composition of the plastic stent might affect its patency, some previous studies have suggested that patency was not significantly affected by composition (Teflon, polyurethane, or polyethylene) or shape (Terruzzi et al., 2000; England, 2000).

TREATMENTS FOR BILE DUCT CANCER

It is not usually possible to cure bile duct cancer because it is often diagnosed after it has grown and spread. But even in these cases, the treatment can help to control the symptoms for months or years. The main treatments for bile duct cancer are:

- surgery to remove the affected area – this is only suitable for a small number of people, but could get rid of the cancer completely
- *inserting a hollow tube (stent) into the bile duct to stop it becoming blocked – this can help relieve symptoms such as jaundice* (Fig.6)

- chemotherapy – where medication is given to stop the cancer cells growing and to relieve your symptoms
- radiotherapy – where a beam of radiation is carefully aimed at the cancer cells to stop them growing and to relieve your symptoms

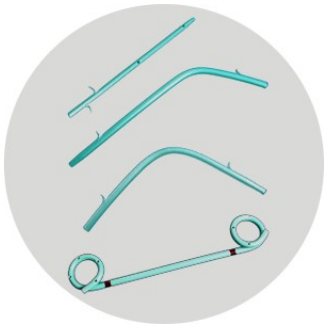

Figure 6. How the bile duct polymeric stent may look like.

2.2.4 Bacterial strains in biofilms

The popular theory is that bacterial biofilm and biliary sludge both play major roles, along with the extent of bacterial infection and duodenobiliary reflux of dietary fiber (Raijman, 2003; Leung et al., 2000).
The regular biliary sludge is different from cholesterol-rich sludge, which is related to gallstone formation. The biliary sludge that causes stent occlusion mainly consists of crystals of calcium bilirubinate and calcium palmitate produced by bacterial enzymes (Leung et al., 1988; Groen et al., 1987; Guaglianone et al., 2010). It is also known that several types of proteins (such as fibronectin, vitronectin, laminin, fibrin, and collagen), which are derived from bacteria of a specific origin but are not naturally present in bile, form a film, making the bacteria more adhesive and also work with the bacteria to produce biliary sludge (Yu et al., 1996; An et al., 1998). The development of a biofilm that occurs because of attachment of these proteins onto the inner surface of a stent is known to play an important role in the initiation of sludge accumulation.

Microorganisms isolated from occluded biliary stents include anaerobic bacterial species, fungi, and aerobic bacterial species. As aerobic species there are most commonly the gram-positive *Enterococcus* species, and gram-negative *Escherichia coli* and *Klebsiella* species, among anaerobic bacteria - *Clostridium* species (Fig.7).

Bacteria			
Gram-positive species	**Double pigtail stents (polyurethane)**	**Straight stents (polyethylene)**	**P value**
Enterococcus faecalis	56/113 (49.6%)	51/100 (51%)	0.834
Enterococcus faecium	37/113 (32.7%)	26/100 (26%)	0.282
Enterococcus casseliflavus	12/113 (10.6%)	5/100 (5%)	0.204
Enterococcus avium	10/113 (8.8%)	5/100 (5%)	0.224
Enterococcus gallinarum	8/113 (7.1%)	3/100 (3%)	0.224
Enterococci (other species)	2/113 (1.8%)	4/100 (4%)	0.423
Streptococcus anginosus	20/113 (17.7%)	16/100 (16%)	0.741
Streptococcus parasanguinis	5/113 (4.4%)	6/100 (6%)	0.604
Streptococcus oralis/mitis	3/113 (2.7%)	7/100 (7%)	0.195
Streptococcus constellatus	4/113 (3.5%)	1/100 (1%)	0.374
Streptococci (other species)	8/113 (7.1%)	7/100 (7%)	0.982
Staphylococcus aureus	2/113 (1.8%)	3/100 (3%)	0.667
Staphylococcus epidermidis	5/113 (4.4%)	5/100 (5%)	1.000
Staphylococcus haemolyticus	2/113 (1.8%)	4/100 (4%)	0.423
Staphylococci (other species)	0/113 (0%)	3/100 (3%)	0.102
Others	10/113 (8.8%)	8/100 (8%)	0.824
Gram-negative species	**Double pigtail stents (polyurethane)**	**Straight stents (polyethylene)**	**P value**
Escherichia coli	55/113 (48.7%)	34/100 (34%)	0.030
Enterobacter cloacae	16/113 (14.2%)	15/100 (15%)	0.862
Klebsiella oxytoca	14/113 (12.4%)	10/100 (10%)	0.582
Klebsiella pneumoniae	9/113 (8%)	11/100 (11%)	0.448
Citrobacter spp.	8/113 (7.1%)	6/100 (6%)	0.751
Hafnia alvei	7/113 (6.2%)	4/100 (4%)	0.470
Pseudomonas aeruginosa	6/113 (5.3%)	6/100 (6%)	0.827
Proteus vulgaris	5/113 (4.4%)	6/100 (6%)	0.604
Proteus mirabilis	5/113 (4.4%)	2/100 (2%)	0.452
Morganella morganii	2/113 (1.8%)	4/100 (4%)	0.423
Others	13/113 (11.5%)	16/100 (16%)	0.340
Anaerobes	**Double pigtail stents (polyurethane)**	**Straight stents (polyethylene)**	**P value**
Bacteroides spp.	11/113 (9.7%)	6/100 (6%)	0.316
Prevotella spp.	6/113 (5.3%)	7/100 (7%)	0.607
Veilonella spp.	4/113 (3.5%)	1/100 (1%)	0.374
Others	8/113 (7.1%)	7/100 (7%)	0.982
Fungi	**Double pigtail stents (polyurethane)**	**Straight stents (polyethylene)**	**P value**
Candida albicans	55/113 (48.7%)	48/100 (48%)	0.922
Candida glabrata	13/113 (11.5%)	10/100 (10%)	0.724
Candida kefyr	5/113 (4.4%)	0/100 (0%)	0.062
Candida tropicalis	1/113 (0.9%)	4/100 (4%)	0.189
Candida (other species)	6/113 (5.3%)	4/100 (4%)	0.753
Others	3/113 (2.7%)	1/100 (1%)	0.624
Multi-drug resistant species	**Double pigtail stents (polyurethane)**	**Straight stents (polyethylene)**	**P value**
Vancomycin-resistant enterococci (VRE)	18/125 (14.4%)	12/94 (12.8%)	0.728
Methicillin-resistant Staphylococcus aureus (MRSA)	2/2 (100%)	1/3 (33.3%)	0.400
ESBL-producing *Enterobacteriaceae*, resistant to 3 of 4 major antibiotic classes[§] (3MRGN)	17/129 (13.2%)	15/101 (14.9%)	0.716
Carbapenemase producing *Enterobacteriaceae*, resistant to 4 of 4 major antibiotic classes[§] (4MRGN)	1/129 (0.8%)	0/101 (0%)	1.000
Azole-resistant *Candida* species	25/80 (31.3%)	23/66 (34.8%)	0.645

Figure 7. Spectrum of microorganisms isolated from biliary stents (Lübbert et al., 2016)

Surprisingly, antibiotics, although there is a theoretical possibility for decreasing bacterial colonization, didn't show any effect in decreasing internal failure rates when given both systemically or locally through drug elution (Lee et al., 2016). As bacterial colonization is considered to be the most important cause of biliary plastic stent occlusion, in vitro and in vivo studies have been conducted with various antibiotics; however, none were found to prolong stent patency (Donelli et al., 2007). There were several trials to induce synergistic effects by combining

antibiotics with choleretic agents such as ursodeoxycholic acid or terpene. However, the review of Galandi et al. including a meta-analysis of 5 randomized trials reported no significant effect on stent patency or mortality rate (Galandi et al., 2002).

The process of biofilm formation in general is very complex (obstruction of biliary stents is more complex and involves not only bacteria and their products but bilirubin complexes, cholesterol complexes and ingrowth of tissue) (Fig.8). Biofilms are multicellular, three-dimensional aggregates that form on surfaces in both nature and the clinic. The ability to form biofilms in a variety of environments is a common defensive characteristic of several bacteria. The proximity of cells within the biofilm creates the opportunity for coordinated behaviors through cell-to-cell communication using a spectrum of diffusible signals, the most well documented being the so-called “quorum sensing” (Miller et al., 2001).

Chemical–physical conditions created by the biofilm make the bacteria up to 1000 times more resistant to antimicrobials than the planktonic cells; thus, bacterial biofilms sustain chronic infections, especially because they show augmented tolerance to antibiotics.

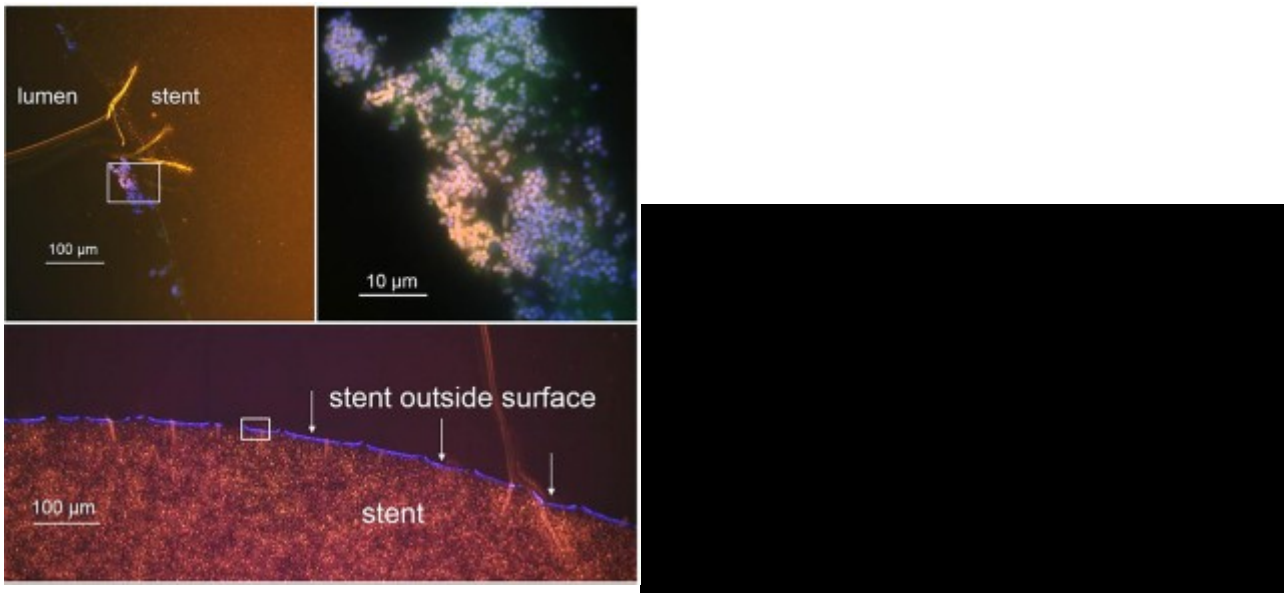

Figure 8. Presence of biofilm formation on a biliary polyethylene stent in a 62-year-old liver transplant recipient with anastomotic bile duct stenosis, visualized by fluorescence *in situ* hybridization (FISH). Using cultures, *Enteroccus faecalis* and *Escherichia coli* were detected (Lübbert, 2016).

2.3 POLYMERIC NANOCOMPOSITES FOR BIOFILM ELIMINATION

Many of the coatings rely on the encapsulation of various antibiotics or antifungal drugs to prevent device infection by locally delivering the drug. While there are many benefits to locally delivering

the drug to prevent device infection, these coatings have the potential to cause off target long-term toxicities, and can lead to the development of drug-resistant bacteria when the antibiotic is delivered at a subinhibitory dose and has a limited window of activity.

A number of successful polymer-based coatings have been developed using different quaternary ammonium salts and cationic polymers. These coatings primarily function through either a disruption of the bacterial membrane using cationic charges or hydrophobic interactions repelling the adherence of bacteria. The benefit of these coatings is that they are primarily non-leaching coatings and therefore demonstrate long-term intrinsic antibacterial activity, are biocompatible, and do not cause any significant cytotoxicity.

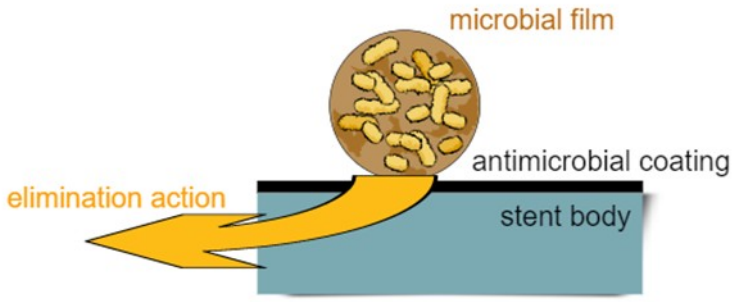

Figure 9. Scheme of proposed functionality of polymeric coating.

The focus is on polymeric antibacterial nanocomposite coating of inner bulk material of polymeric stent (Fig.9). Since we decided to tailor and develop functional sustainable coating the preference was given to biodegradable polymers as a matrix for nanocomposite film, because we believe that via gradual degradation of matrix the constant functionality of nanocomposite coating can be assured.

2.3.1 Polymeric nanocomposites with layered fillers

In polymer-inorganic nanocomposites, the synthetic routes are usually related to the conditions for polymerization. The polymerization conditions or technologies for the nanocomposites are usually the same as those for the pristine. An important aspect of preparing nanocomposites is the particle surface treatment as described in other sections. A primary mechanism in compatibilization of phase separated polymer blends involves lowering the interfacial tension between the phases and preventing coalescence of the particles during melt processing (Paul et al., 2008). The function of surfactant can be explained by its characteristic structure: surfactants usually have a structural group that has very little attraction for the solvent, known as a lyophobic group, and a group that has strong attraction for the solvent, called the lyophilic group. This is known as an amphipathic structure. Often used are deposition reaction modification, surface chemical modification, and mechanical force chemical modification, modification by high energy and modification by polymer surface grafting and intercalation. These modifications solve the

problems of heterogeneous aggregation. The interactions between the reacting groups of the polymer and the nanoparticles depend on the chemical structure of the polymer, the nanoparticle surface charge:

- *Covalent bonds*: carboxyl groups, sulfonating groups, amide or amine groups can form a covalent bond with, e.g., hydroxyl, groups on the nanoparticles.

- *Ionic bonds*: a chemical bond formed by coulombic attraction between positive and negative charges. Generally, the selected polymer chains and nanoparticles have opposite charges, and the ionic interaction between them stabilizes the nanocomposites systems.

- *Chiral bonds*: organic matrices usually have pair electrons, which have chiral interactions with empty electron orbitals through which a chemical interaction occur. The chiral interaction effect is used to prepare nanocomposites by in situ polymerization.

- *Affinity effect*: The surface affinity of nanoparticles for groups in polymer chains forms a strong interaction. This affinity ensures the homogenous dispersion of nanoparticles into the polymer matrix or their combinations.

Nanoparticles can be synthesized from a variety of materials. Owing to their high specific surface area and low surface energy, nanoparticles are not stable in ambient circumstances, and it is suitable to incorporate them in certain kinds of materials. Reverse micelles, glass, zeolites, and polymers can be used as the substrate to prepare composite materials containing nanoparticles. This substrate not only can prevent the nanoparticles from aggregation, but also can accurately control their size, shape and surface structure (Yang et al., 2009).

In general, polymer/layered silicate nanocomposites are of three different types, namely intercalated nanocomposites, for which insertion of polymer chains into a layered silicate structure occurs in a crystallographically regular fashion, with a repeat distance of few nanometers, regardless of polymer to clay ratio, flocculated nanocomposites, for which intercalated and stacked silicate layers flocculated to some extent due to the hydroxylated edge–edge interactions of the silicate layers, and exfoliated nanocomposites, for which the individual silicate layers are separated in the polymer matrix by average distances that depend only on the clay loading (Sinha Ray et al., 2003).

Nowadays utilization of clays in nanocomposites is very in demand. Natural clay particles are hydrophilic and are sensitive to mechanical–chemical treatments. The commonly used layered silicates for the preparation of polymer/layered silicate (PLS) nanocomposites belong to family of 2:1 layered silicates or phyllosilicates. Their crystal structure consists of layers made up of two tetrahedrally coordinated silicon atoms fused to an edge-shared octahedral sheet of either aluminum or magnesium hydroxide (Fig, 10).

The layer thickness is around 1 nm, and the lateral dimensions of these layers may vary from 30

nm to several microns or larger, depending on the particular layered silicate. Stacking of the layers leads to a regular van der Waals gap between the layers called the interlayer or gallery. Polymeric nanocomposites containing homogenously dispersed clay platelets present material with enhanced mechanical, chemical, and physical properties in comparison with conventional polymeric material. However, the fabrication of such nanocomposites still brings in basic obstacles. Therefore, fundamental knowledge of clay minerals and behavior in various chemical and physical environments will be here presented.

The pretreatment of clays for following usage in nanocomposites represents several specific techniques for example, exfoliation and delamination, intercalation with inorganic and organic species, and/or leaching (Sinha Ray et al., 2003; Pavlidou et al., 2008; Sinha Ray, 2003).

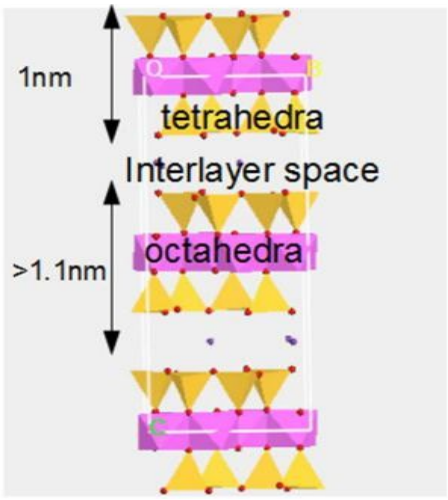

Figure 10. Model of 2:1 layered phyllosilicate.

The most popular clay minerals are smectites for long time. Especially montmorillonite is keeping its position as nanofiller for polymeric matrices, modified sorbent or carrier for other inorganic nanoparticles. Since, in their pristine state layered silicates are only miscible with hydrophilic polymers, such as poly(ethylene oxide) and poly(vinyl alcohol), in order to render them miscible with other polymers, one must exchange the alkali counter-ions with a cationic-organic surfactant (Šupová et al., 2011). The organic cations lower the surface energy of the silicate surface and improve wetting with the polymer matrix. Moreover, the long organic chains of surfactants, with positively charged ends, are anchored to the surface of the negatively charged silicate layers, resulting in an increase of the gallery height.

Two characteristics of layered silicates play an important role in the creation of nanocomposites: the first is the ability of silicate sheets to disperse into individual layers, and the second is the possibility to modify their surface chemistry through ion exchange reactions with organic and inorganic cations. The simple mixing of polymer and layered silicates does not always result in the generation of a nanocomposite, as this usually leads to dispersion of stacked sheets. This failure is due to the weak interactions between the polymer and the inorganic component. The surfactant cations lower the surface energy of the inorganic reinforcement, improve the wetting

characteristics of the polymer matrix, and result in larger interlayer spacing (Fig. 11). Additionally, the surfactant cations can provide functional groups that react with the polymer matrix or, in some cases, can initiate the polymerisation of monomers to form the polymer in-situ (Choudalakis et al., 2011); Bitinis et al., 2011).

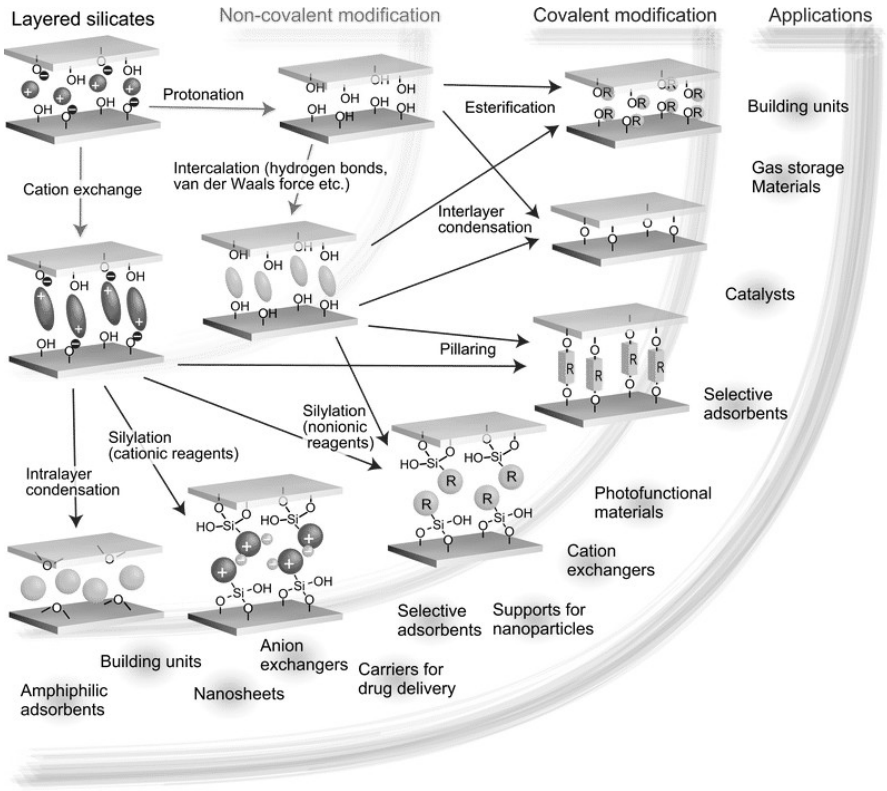

Figure 11. Silicate layer modification (Takahashi et al., 2011).

Polymer nanocomposites containing layered silicates have been considered as a new generation of composite materials due to their expected unique properties attributed to the high aspect ratio of the inorganic platelets. Nevertheless, addition of layered silicates to polyolefins mostly results in phase separated systems because of the incompatibility of the silicates with the non-polar polyolefins. Functional compatibilizers are required to enhance the interactions and alter the structure from phase separated micro-composites to intercalated and exfoliated nanocomposites (Simha Martynková et al., 2007).

Commercial macromolecular compatibilizers (mainly maleic-anhydride-functionalized polyolefins) are most commonly used to improve the interfacial bonding between the fillers and the polymers whereas specifically synthesized functional homopolymers or copolymers have been utilized as well. In this article, we are reviewing a number of investigations, which studied the influence on the composite structure of various parameters like the compatilizer to inorganic ratio, the type and content of the functional groups and the molecular weight of the functional additive, the miscibility between the matrix polymer and the compatibilizer, the kind of surfactants modifying the inorganic surface, the processing conditions, etc. (Valaskova et al., 2009).

It is a great challenge to characterize the structure and to manipulate the fabrication of polymer nanocomposites. The development of such materials is still largely empirical and therefore, computer modelling and simulation will play an ever-increasing role in predicting and designing material properties and guiding such experimental work as synthesis and characterization. Computer modelling and simulation are especially useful in the thermodynamics and kinetics of the formation of polymer nanocomposites; the hierarchical characteristics of the structure; dynamics at the interface between nanoparticles and polymer matrix; the dependence of polymer rheological behavior and the molecular origins of the reinforcement mechanisms of nanoparticles in polymer nanocomposites. (Zeng et al., 2008) at first introduced some computational methods, covering from molecular scale (e.g., molecular dynamics, Monte Carlo), microscale (e.g., Brownian dynamics, dissipative particle dynamics, lattice Boltzmann, time-dependent Ginzburg–Landau method, dynamic density functional theory method) to mesoscale and macroscale (e.g., micromechanics, equivalent-continuum and self-similar approaches, finite element method) and summarized the recent advances in the fundamental understanding of polymer nanocomposites reinforced by different types of nanofillers.

2.3.2 BIODEGRADABLE POLYMERS

Biodegradable polymers have innumerable uses in the biomedical field, particularly in the fields of tissue engineering and drug delivery (Lendlein et al., 2011; Tian et al., 2012). In order to be used as a therapeutic, the biodegradable polymer must meet several criteria:

1) be non-toxic in order to eliminate foreign body response;
2) the time it takes for the polymer to degrade is proportional to the time required for therapy;
3) the products resulting from biodegradation are not cytotoxic and are readily eliminated from the body;
4) the material must be easily processed in order to tailor the mechanical properties for the required task;
5) be easily sterilized;
6) and have acceptable shelf life (Vroman et al., 2009; Middleton et al., 2000)

Biodegradable polymers are of great interest in the field of drug delivery. The great benefit of a biodegradable drug delivery system is the ability of the drug carrier to target the release of its payload to a specific site in the body and then degrade into nontoxic materials that are then eliminated from the body via natural metabolic pathways (Caballero-George et al., 2013). The polymer slowly degrades into smaller fragments, releasing a natural product, and there is controlled ability to release a drug. The drug slowly releases as polymer degrades. Encapsulating the therapeutic in a polymer and adding targeting agents decreases the toxicity of the drug to healthy cells.

In addition to tissue engineering, biodegradable polymers are being used for orthopedic applications, such as bone and joint replacement (Navarro et al., 2008). A wide variety of non-biodegradable polymers have been used for orthopedic applications including silicone rubber, polyethylene, acrylic resins, polyurethane, polypropylene, and polymethylmethacrylate. The primary role of many of these polymers was to act as biocompatible cement in the fixation of prostheses and in the replacement of joints.

The first polymers to be used in biomedical applications, naturally-occurring polymers, far out-date the use of synthetic polymers which first appeared around the 1960s. They can be divided into the following three groups: proteins (e.g. silk, collagen, soy, and fibrin gels), polysaccharides (e.g. chitin/chitosan, alginate and hyaluronic acid derivatives) and polynucleotides (e.g. DNA and RNA). The main advantage of natural polymers is their high degree of scaffold–tissue compatibility due to the positive biological recognition of their chemical make-up. However, the use of these polymers also carries the potential for inciting an immune response due to any impurities in the material gained during processing. Clinical applications require the use of medical grade materials and, in any instances where immunogenic fragments are detected within the material, it is imperative that they are removed (Ozdil et al., 2014).

Synthetic polymeric biomaterials may not always come as cheaper alternative to biological polymers due to less availability, however, they are much more easily reproducible and have a longer shelf-life and therefore are often more viable sources of polymeric biomaterials. Uniformity of microstructure, degradation rate and mechanical structure with large-scale production are the key advantages of these polymers. The most extensively used synthetic biomedical polymers is the family of linear aliphatic polyesters: polyvinyl alcohol (PVAL), poly(lactic acid), poly(glycolic acid), poly(hydroxybutyrate) etc. Numerous combination options of these polymers, both with each other and/or various other elements, generate a great assortment of composite scaffolds with varying chemical, structural and mechanical properties that can be suited to specific tissues and tasks.

POLYVINYL ACETATE (PVAC)

Polyvinyl acetate is an aliphatic rubbery synthetic polymer with the formula $(C_4H_6O_2)_n$. It belongs to the polyvinyl esters family with the general formula -[RCOOCHCH$_2$]-. It is a type of thermoplastic.

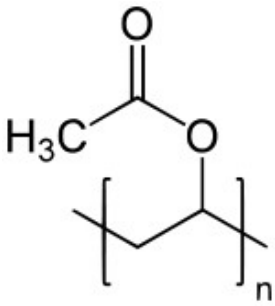

Figure 12. Polyvinyl acetate molecule.

PVAc is a vinyl polymer. Polyvinyl acetate is prepared by polymerization of vinyl acetate monomer (Fig.12) (free radical vinyl polymerization of the monomer vinyl acetate).

The degree of polymerization of poly(vinyl acetate) is typically 100 to 5000 while its ester groups are sensitive to base hydrolysis and will slowly convert PVAc into polyvinyl alcohol and acetic acid.
A number of microorganisms can degrade polyvinyl acetate; most commonly, damage is caused by filamentous fungi however there are also algae, yeasts, lichens and bacteria that have been shown to degrade polyvinyl acetate (Hoffman, 2012).
PVAc has been widely studied because of its excellent optical properties, biocompatibility, and few foreign-body reactions *in vivo* (Yeum et al., 2005), therefore it was selected for the presented research as well as two following polymers.

POLYVINYL ALCOHOL (PVAL)

Polyvinyl alcohol (Fig.13) is a water-soluble synthetic polymer. It has the idealized formula $[CH_2CH]_n$. It is used in papermaking, textiles, and a variety of coatings. It is white and odorless. It is sometimes supplied as beads or as solutions in water. Hydrogels being used as basic materials for manufacturing of wound dressings were invented in 1989 by (Rosiak et al., 1989). PVAL hydrogel is one of the well-known polymer gel that due to its good biocompatibility, has been used in numerous biomedical applications, for example as implants, artificial organs, contact lenses, drug delivery devices, and also wound dressings in wounds management. There is a number of variety of methods for crosslinking PVAL chains in order to produce PVAL hydrogels, including electron beam irradiation, bulk mixing with crosslinking agents such as glutaraldehyde and also freezing–thawing cyclic process (Kokabi et al., 2007).

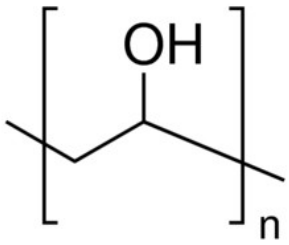

Figure 13. Polyvinyl acetate molecule.

POLYETHYLENE OXIDE (PEO)

Poly(ethylene glycol) (PEG), otherwise known as poly(oxyethylene) or poly(ethylene oxide) (PEO), is a synthetic polyether that is readily available in a range of molecular weights. Materials with Mw<100,000 are usually called PEGs, while higher molecular weight polymers are classified as PEOs. These polymers are amphiphilic and soluble in water as well as in many organic solvents (e.g., methylene chloride, ethanol, toluene, acetone, and chloroform). Low molecular weight (Mw<1,000) PEGs are viscous and colorless liquids, while higher molecular weight PEGs are waxy, white solids with melting points proportional to their molecular weights to an upper limit of about 67 °C.

PEG (Fig.14) has been found to be nontoxic and is approved by the FDA for use as excipients or as a carrier in different pharmaceutical formulations, foods, and cosmetics. Most PEGs with Mw<1,000 are rapidly removed from the body unaltered with clearance rates inversely proportional to polymer molecular weight. This property, combined with the availability of PEGs with a wide range of end-functions, contributes to the wide use of PEGs in biomedical research: drug delivery, tissue engineering scaffolds, surface functionalization, and many other applications. This section lists PEG and PEO polymers classified by end-group functions. Note that methyl-terminated PEGs are classified as monofunctional PEGs.

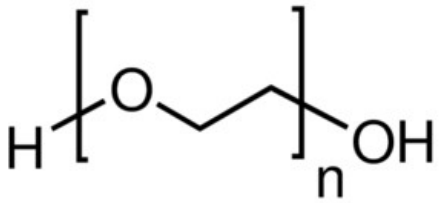

Figure 14. Polyvinyl acetate molecule.

2.3.3 NANOFILLERS FOR NANOCOMPOSITES - HYBRID NANOCLAYS

Clay minerals are the characteristic minerals of the earths near surface environments. They form in soils and sediments, and by diagenetic and hydrothermal alteration of rocks. Water is essential for clay mineral formation and most clay minerals are described as hydrous alumino silicates. Structurally, the clay minerals are composed of planes of cations, arranged in sheets, which may be tetrahedrally or octahedrally coordinated (with oxygen), which in turn are arranged into layers

often described as 2:1 if they involve units composed of two tetrahedral and one octahedral sheet or 1:1 if they involve units of alternating tetrahedral and octahedral sheets. Additionally some 2:1 clay minerals have interlayers sites between successive 2:1 units which may be occupied by interlayer cations, which are often hydrated. The planar structure of clay minerals give rise to characteristic platy habit of many and to perfect cleavage, as seen for example in larger hand specimens of micas.

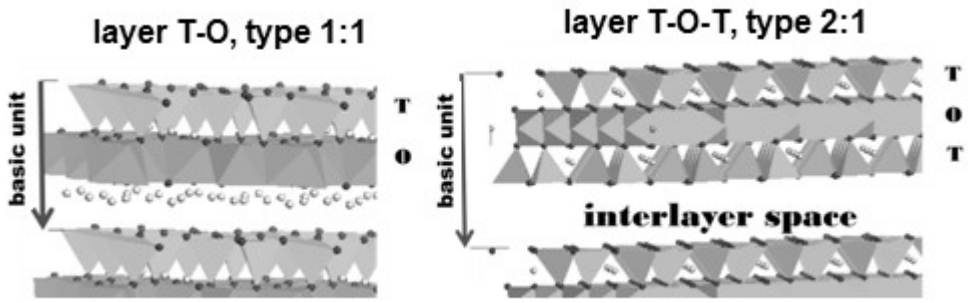

Figure 15. Models of layers T-O, type 1:1 and layer T-O-T, type 2:1.

The classification of the phyllosilicate clay minerals is based collectively, on the features of layer type (1:1 or 2:1), the dioctahedral or trioctahedral character of the octahedral sheets (i.e. 2 out of 3 or 3 out of 3 sites occupied), the magnitude of any net negative layer charge due to atomic substitutions, and the nature of the interlayer material.

The basis on which clay minerals are classified is shown below (see (Middleton et al., 2003) for a more detailed introduction to clay mineralogy).

Table 3. Classification of clay minerals.

LAYER TYPE	**Layer charge (q)**		**Group**	**Subgroup**	**Species (e.g.)**
1:1	q≈0		Kaolin-Serpentine	Kaolin	Kaolinite
				Serpentine	Berthierine
2:1	q≈0 q≈1	Increasing layer charge	Pyrophyllite-talc	Pyrophyllite	Pyrophyllite
				Talc	Talc
			Smectite (q≈0.2-0.6)	Di-smectite	Montmorillonite
				Tri-smectite	Saponite
			Vermiculite (q≈0.6-0.9)	Di-vermiculite	Di-vermiculite
				Tri-vermiculite	Tri-vermiculite

			Mica (q≈1.0)	Di-mica	Illite, Muscovite
				Tri-mica	Biotite
	q variable		Chlorite	Di-chlorite	Sudoite
				Tri-chlorite	Chamosite
			Sepiolite-Palygorskite	Sepiolite	Sepiolite
				Palygorskite	Palygorskite
Variable	q variable		Mixed-layer	Di-mica-di-smectite	Rectorite
				Tri-chlorite-tri-smectite	Corrensite

VERMICULITE

Vermiculite, 2:1 planar hydrous phyllosilicate, is the mineral with wide and unique application possibilities. Nowadays utilization of clays in nanocomposites is very in demand. Natural clay particles are hydrophilic and are sensitive to mechanical–chemical treatments. Their advantage is the nanobuilding units, the silicate layers, which can be obtained and used for applications in nanotechnology.

The group of 2:1 phyllosilicates is composed of two types of sheet, tetrahedral (T) and octahedral (O). According to the AIPEA Nomenclature Committee (Guggenheim et al., 2007), tetrahedral sheet is composed of continuous two-dimensional corner-sharing tetrahedra TO_4 involving three corners (basal oxygens) and the fourth corner (apical oxygen) pointing in any direction. The tetrahedral sheet has a composition of $[T_4O_{10}]_4$– (T_5Si_{41}, Al_{31}, Fe_{31},...) in which individual TO_4 are linked by sharing basal oxygens with TO_4 neighbors to form two-dimensional sheets where oxygens form an open hexagonal network. The apical oxygens form a corner of the octahedral coordination unit around larger octahedral cations. Tetrahedra are slightly distorted and the cavities bordered by six oxygens have ditrigonal symmetry (Radoslovich et al., 1962).

BENTONITE

Bentonite is absorbent aluminum phyllosilicate clay consisting mostly of montmorillonite. It was named by Wilbur C. Knight in 1898 after the Cretaceous Benton Shale near Rock River, Wyoming (Hosterman et al., 1992).

The different types of bentonite each are named after the respective dominant element, such as potassium (K), sodium (Na), calcium (Ca), and aluminum (Al). Experts debate a number of nomenclatorial problems with the classification of bentonite clays. Bentonite usually forms from

weathering of volcanic ash, most often in the presence of water. However, the term bentonite, as well as similar clay called tonstein, has been used to describe clay beds of uncertain origin.

For industrial purposes, two main classes of bentonite exist: sodium and calcium bentonite. In stratigraphy and tephrochronology, completely devitrified (weathered volcanic glass) ash-fall beds are commonly referred to as K-bentonites when the dominant clay species is illite. In addition to montmorillonite and illite another common clay species that is sometimes dominant is kaolinite. Kaolinite-dominated clays are commonly referred to as tonsteins and are typically associated with coal.

MONTMORILLONITE

Montmorillonite is a very soft phyllosilicate group of minerals that form when they precipitate from water solution as microscopic crystals, known as clay. It is named after Montmorillonite in France. Montmorillonite, a member of the smectite group, is 2:1 clay, meaning that it has two tetrahedral sheets of silica sandwiching a central octahedral sheet of alumina. The particles are plate-shaped with an average diameter around 1 μm and a thickness of 9.6 nm; magnification of about 25,000 times, using an electron microscope, is required to "see" individual clay particles.
Montmorillonite is a subclass of smectite, a 2:1 phyllosilicate mineral characterized as having greater than 50% octahedral charge; its cation exchange capacity is due to isomorphous substitution of Mg for Al in the central alumina plane. The substitution of lower valence cations in such instances leaves the nearby oxygen atoms with a net negative charge that can attract cations. In contrast, beidellite is smectite with greater than 50% tetrahedral charge originating from isomorphous substitution of Al for Si in the silica sheet.
The individual crystals of montmorillonite clay are not tightly bound hence water can intervene, causing the clay to swell. The water content of montmorillonite is variable and it increases greatly in volume when it absorbs water. Chemically, it is hydrated sodium calcium aluminium magnesium silicate hydroxide $(Na,Ca)_{0.33}(Al,Mg)_2(Si_4O_{10})(OH)_2 \bullet nH_2O$.

2.3.4 ANTIMICROBIAL AGENTS

"*The history of antimicrobials begins with the observations of Pasteur and Koch, who discovered that one type of bacteria could prevent the growth of another. They did not know at that time that the reason one bacterium failed to grow was that the other bacterium was producing an antibiotic. Technically, antibiotics are only those substances that are produced by one microorganism that kill, or prevent the growth, of another microorganism.*
The discovery of antimicrobials like penicillin by Alexander Fleming and tetracycline paved the way for better health for millions around the world. Before penicillin became a viable medical treatment in the early 1940s, no true cure for gonorrhea, strep throat, or pneumonia existed. Patients with infected wounds often had to have a wounded limb removed, or face death from infection. Now, most of these infections can be cured easily with a short course of antimicrobials" [1].

MECHANISMS OF ACTION OF ANTIMICROBIAL DRUGS

Selective Toxicity

Selective toxicity is the property of an ideal antimicrobial agent. Selective toxicity means that the drug is harmful to a parasite but not to the host. Usually the effect is relative rather absolute, i.e. a drug in a concentration tolerated by the host may damage an infecting microorganism. Selective toxicity may be a function of a specific receptor required for drug attachment, or it may depend on inhibition of biochemical events essential to the organism but not to the host. The mechanisms are discussed under four headings: (1) Inhibition of cell wall synthesis, (2) Inhibition of cell membrane function, (3) Inhibition of protein synthesis, and (4) Inhibition of nucleic acid synthesis.
Classification on mode of Action:
1. Inhibition of cell wall synthesis. Penicillins, cephalosporin, vancomycin, bacitracin, cycloserin are examples.
All (3-lactarn drugs like penicillins, cephalosporins are selective inhibitors of bacterial cell wall synthesis and therefore active against growing bacteria. Mechanism of action: Initial step is the binding of the drug to specific drug receptor PBPs (Penicillin- binding proteins) on bacteria. There are 3 to 6 PBPs having different effects. At least some of which are enzymes involved in transpeptidation (cross-linking) reactions.

After attachment, peptidoglycan synthesis is inhibited as final transpeptidation is blocked. Then there occurs inactivation of an inhibitor of autolytic enzyme in the cell wall. This activates the autolytic enzymes in the cell wall that results in lysis resulting in bacterial death.
Organisms with defective autolysin function are inhibited but not killed by l3dactam drugs, and they are said to be "tolerant".

The Gram-positive and Gram-negative bacteria differ in susceptibility to penicillins or cephalosporins on structural differences in their cell walls that decide binding, penetration, and activity of the drugs. The differences in cell wall are in the amount of peptidoglycan, presence of receptors and lipids, nature of cross-linking and activity of autolytic enzymes. Peptidoglycan layer of the cell wall is much thicker in Gram-positive than in Gram-negative bacteria.

Lack of toxicity of p-lactam drugs to animal cells is attributed to the absence of bacterial type cell wall with its peptidoglycan in animal cells.

Extended-spectrum P lactum (ESBLs) are enzymes that mediate resistance to extended-spectrum (third generation) cephalosporins (e.g., ceftazidime, cefotaxime, and ceftriaxone) and monobactams (e.g., aztreonam) but do not affect cephamycins (e.g., cefoxitin and cefotetan) or carbapenems (e.g., meropenem or imipenem). Production of ESBLs can be screened by broth microdilution and disk diffusion screening tests using selected antimicrobial agents.

2. Alteration of cell membrane function.
Polymyxin, amphotericin B, imidazole are examples.
These drugs act by disruption of the functional integrity of the cytoplasmic membrane. Macromolecules and ions escape from the cell causing cell damage or death. Selective

chemotherapy is possible as the cytoplasmic membrane of bacteria and fungi has a structure different from that of animal cells.
3. Inhibition of protein synthesis.
These drugs inhibit protein synthesis in bacteria. Bacteria have 70S ribosomes, whereas mammalian cells have 80S ribosomes. Subunits of each type of ribosome, their chemical composition, and functional specifies differ. Thus a drug can inhibit protein synthesis in bacterial ribosomes but not in mammalian ribosomes.
4. Inhibition of nucleic acid synthesis.
These drugs inhibit nucleic acid synthesis by different mechanisms.

The selected drugs for antimicrobial modification of silicate layers are listed in the following text.

CICLOPIROX OLAMINE

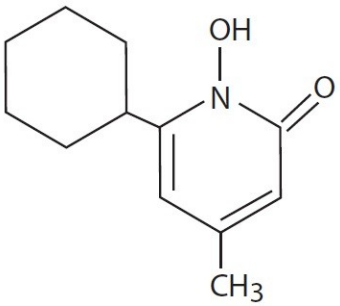

Figure 16. Ciclopirox olamine molecule.

In contrast to the azoles and other antimycotic drugs, the mechanism of action of ciclopirox (Fig.16) is poorly understood (Niewerth et al., 2003). However, loss of function of certain catalase and peroxidase enzymes has been implicated as the mechanism of action, as well as various other components of cellular metabolism.
In a study conducted to further elucidate ciclopirox's mechanism, several Saccharomyces cerevisiae mutants were screened and tested. Results from interpretation of the effects of both the drug treatment and mutation suggested that ciclopirox may exert its effect by disrupting DNA repair, cell division signals and structures (mitotic spindles) as well as some elements of intracellular transport (Leem et al., 2003). It acts by inhibiting the membrane transfer system by interrupting the Na+ K+ ATPase (Niewerth, 2003). It is currently being investigated as an alternative treatment to ketoconazole for seborrheic dermatitis as it suppresses growth of the yeast Malassezia furfur. Initial results show similar efficacy to ketoconazole with a relative increase in subjective symptom relief due to its inherent anti-inflammatory properties (Ratnavel et al., 2007).
Ciclopirox is considered a hydroxypyrimidine antifungal agent (Cappitelli et al., 2008).

IMIDAZOLE

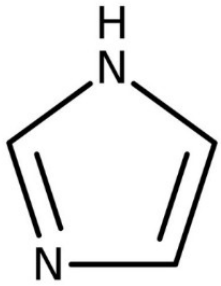

Figure 17. Imidazole molecule.

Imidazole is an organic compound with the formula $C_3N_2H_4$. It is a white or colorless solid that is soluble in water, producing a mildly alkaline solution. In chemistry it is an aromatic heterocycle classified as a diazole and having non-adjacent nitrogen atoms.
Many natural products, especially alkaloids, contain the imidazole ring. These imidazoles share the 1,3-C_3N_2 ring but feature varied substituents. This ring system is present in important biological building blocks, such as histidine and the related hormone histamine. Many drugs contain an imidazole ring (Fig.17), such as certain antifungal drugs, the metronidazole series of antibiotics, and the sedative midazolam.

TRIHEXYLTETRADECYLPHOSPHONIUM BROMIDE

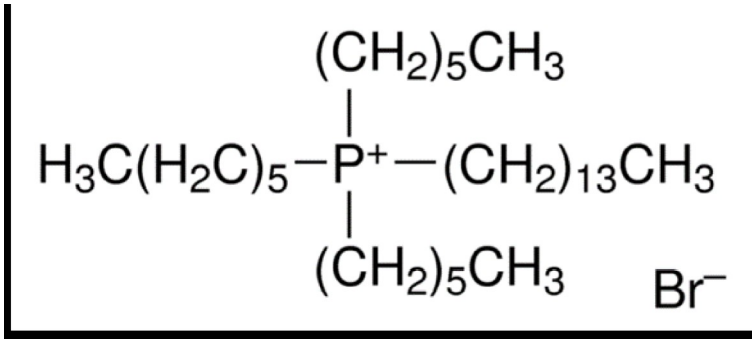

Figure 18. Trihexyltetradecylphosphonium bromide molecule.

Trihexyltetradecylphosphonium bromide (Fig.18) is a phosphonium-based ionic liquid that can be used as a recyclable reaction medium for Heck cross-coupling reactions. It can also be used to prepare supported liquid membranes (SLMs) for gas separation processes- The phosphonium salts are proven agent for antibacterial effect. They were studied when intercalated into montmorillonite interlayer gallery (Wu et al., 2011).

TROLAMINE

Trolamine or Triethanolamine (Fig.19) is a viscous organic compound that is both a tertiary amine and a triol. A triol is a molecule with three alcohol groups. It is a colourless compound although samples may appear yellow because of impurities.

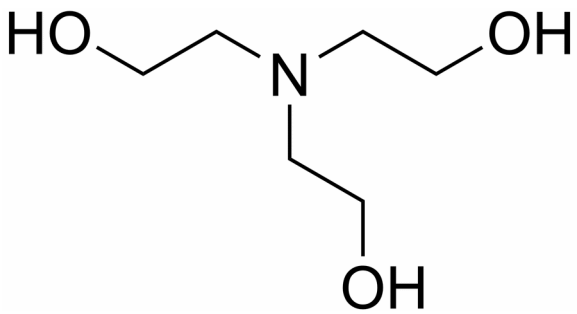

Figure 19. Trolamine molecule.

Triethanolamine is used primarily in making surfactants, such as for emulsifier. It is a common ingredient in formulations used for both industrial and consumer products. The triethanolamine neutralizes fatty acids, adjusts and buffers the pH, and solubilizes oils and other ingredients that are not completely soluble in water. Triethanolammonium salts in some cases are more soluble than salts of alkali metals that might be used otherwise, and results in less alkaline products than would from using alkali metal hydroxides to form the salt. Some common products in which triethanolamine is found are sunscreen lotions, liquid laundry detergents, dishwashing liquids, general cleaners, hand sanitizers, polishes, metalworking fluids, paints, shaving cream and printing inks (Ashford et al., 2011). Trolamine is also used in cosmetics and medicine for example to treat the ear diseases and infections.

CLOTRIMAZOLE

Clotrimazole is an antifungal medication used to treat vaginal yeast infections, oral thrush, diaper rash, pityriasis versicolor, and types of ringworm including athlete's foot and jock itch [2]. Ketoconazole is an imidazole antifungal used systemically to treat candidiasis. Clotrimazole. Clotrimazole is an imidazole antifungal used topically to treat candidiasis (Schaller, 1982).

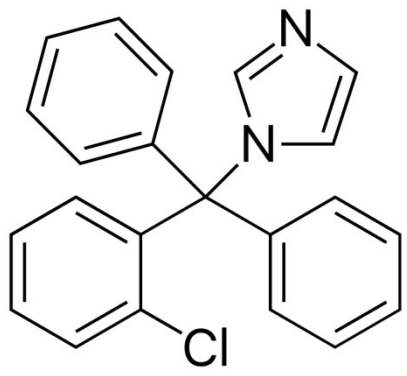

Figure 20. Clotrimazole molecule.

Clotrimazole was discovered in 1969 [2] and nowadays is on the World Health Organization's List of Essential Medicines, the most effective and safe medicines needed in a health system [3].

2.3.5 ANTITUMORAL DRUGS

There are numerous antitumorial drugs for gastroenterological cancer treatment. These drugs are used for specific cases in the system or other organs. Therefore the decision to include erlotinib to the study was for reason of wider applicability.

ERLOTINIB

In this research work EGFR inhibitor named Erlotinib (trade name “Tarceva”) was chosen.

Erlotinib (ERL) is a tyrosine kinase inhibitor. It works by helping to stop cancer cells from growing. This drug will be used in drug delivery system in study of nanocomposites with antibacterial and healing properties. Exact mechanism of antineoplastic activity is not fully elucidated. Appears to inhibit intracellular phosphorylation of tyrosine kinase associated with epidermal growth factor receptor (EGFR), which is expressed on the surface of normal and cancer cells. Specificity with regard to other tyrosine kinase receptors not fully characterized. Within this research work it is important to consider the interactions between Erlotinib antitumoral drug and organic antibacterial components, which will be used for biodegradable coatings inside the polymeric stents.

Erlotinib hydrochloride is approved to be used alone or with other drugs to treat: Non-small cell lung cancer (NSCLC) that is metastatic and has certain EGFR gene mutations. It may be used: As first-line therapy.

In patients on maintenance therapy or whose disease has gotten worse after treatment with chemotherapy.

The use of erlotinib hydrochloride to treat NSCLC that does not have the EGFR gene mutations is no longer FDA-approved.

Pancreatic cancer

It is used with gemcitabine hydrochloride in patients whose disease cannot be removed by surgery, is locally advanced, or has metastasized.

Erlotinib hydrochloride is also being studied for usage in the treatment of other types of cancer. In this study Erlotinib was used for molecular modeling, see chapter part 3.5.

In the experimental study I used Melphalan (Sigma Aldrich) and Chlorambucil (Sigma Aldrich) antitumoral drugs, which were recommended by MUDr. Oldřich Urban, Ph.D. specifically for the bile duct types of cancer. The experiment was about proper preparation of polymeric nanocomposite samples with above mentioned antitumoral drugs and testing it on drug release with HCT116 (Leeds) cancer cells resulting in obtaining the IC_{50} - the half maximal inhibitory

concentration (a measure of the potency of a substance in inhibiting a specific biological or biochemical function). At the moment of publication of this work the result is not obtained yet, but I recommend to continue in this research direction.

2.4. PROCESS OF BIOFILM ELIMINATION FROM SURFACE

Biofilm consists of:

- Microbes
- Extracellular polymers (EPS - polysaccarides, glycoproteins from microbes)
- Water (85-98%)
- Captured particles and other dissolved materials from the process stream

In the body, when biofilms form, they form a protective layer by which bacteria evade the immune system and antimicrobials.
At present, the most efficient treatment for biofilm infection is to mechanically remove the infected area or body part. This is sometimes possible if the focus is a catheter, an implant, or an infected organ that is eligible for transplantation (Bjarnsholt et al., 2015).

So far the two main strategies for preventing or suppressing bacterial biofilm infections are (1) early aggressive antibiotic treatment before the biofilm is formed or (2) chronic suppressive antibiotic treatment when the biofilm is established if it cannot be removed physically.

2.4.1 MECHANO/PHYSICAL PROCESSES

Removal of Microorganisms from Surfaces (Wirtanen, 2015).

Technique	Suitability	Limitations
Swab, sponge & Gauze	Open surfaces, large areas or irregular surfaces	Need suspension which will lower the sensitivity
Rinse	Enclosed areas or small items	Dilution of the contamination is inevitable decreasing the sensitivity
Direct contact	Critical spot areas with low contamination	Only small areas can be examined

Table 4. Different ways of biofilm physical removal.

2.4.2 Chemical processes

When bacteria form biofilms, they don't lump together by chance. In order to form biofilms, bacteria need to communicate with each other (Jakobsen et al., 2012).
One way to disrupt biofilm formation is to interrupt bacterial communication, also known as quorum sensing (QS) (Miller, 2001).

Quorum Sensing Inhibitors interrupt bacterial communication signals, which prevent them from aggregating.

For more information about natural biofilm disruptors see ANNEX.

2.5. CHARACTERIZATION TECHNIQUES AND MICROBIAL EFFECT TESTING

In order to study and characterize the prepared materials several analytical methods was selected. Each method provides important data which in the end shows the full picture about the material.
X-ray diffraction and FT Infrared spectroscopy methods were used for the structure evaluation and characterization of changes in the materials.
Several microscopy methods were employed to observe morphology of the nanofiller particles and the polymeric surface appearance.

2.5.1 X-Ray Diffraction technique

X-ray diffraction (XRD) methods help to explain the structural changes during layered silicates intercalation and after incorporation to the polymeric matrix.
XRD relies on the dual wave/particle nature of X-rays to obtain information about the structure of crystalline materials. A primary use of the technique is the identification and characterization of compounds based on their diffraction pattern.

The dominant effect that occurs when an incident beam of monochromatic X-rays interacts with a target material is scattering of those X-rays from atoms within the target material. In materials with regular structure (i.e. crystalline), the scattered X-rays undergo constructive and destructive interference. This is the process of diffraction. The diffraction of X-rays by crystals is described by *Bragg's Law*: $n\lambda=2d \sin \theta$,
where n is an integer, λ is the characteristic wavelength of the X-rays impinging on the crystallize sample, d is the interplanar spacing between rows of atoms, and θ is the angle of the X-ray beam with respect to these planes.

The directions of possible diffractions depend on the size and shape of the unit cell of the material. The intensities of the diffracted waves depend on the kind and arrangement of atoms in the crystal structure. However, most materials are not single crystals, but are composed of many tiny crystallites in all possible orientations called a polycrystalline aggregate or powder. When a powder

with randomly oriented crystallites is placed in an X-ray beam, the beam will see all possible interatomic planes. If the experimental angle is systematically changed, all possible diffraction peaks from the powder will be detected.

The parafocusing (or Bragg-Brentano) diffractometer is the most common geometry for diffraction instruments.

This geometry offers the advantages of high resolution and high beam intensity analysis at the cost of very precise alignment requirements and carefully prepared samples. Additionally, this geometry requires that the source-to-sample distance be constant and equal to the sample-to-detector distance. Alignment errors often lead to difficulties in phase identification and improper quantification. A mis-positioned sample can lead to unacceptable specimen displacement errors. Sample flatness, roughness, and positioning constraints preclude in-line sample measurement. Additionally, traditional XRD systems are often based on bulky equipment with high power requirements as well as employing high powered X-ray sources to increase X-ray flux on the sample, therefore increasing the detected diffraction signals from the sample. These sources also have large excitation areas, which are often disadvantageous for the diffraction analysis of small samples or small sample features.

X-ray diffraction method as a tool for characterizing materials has a long history. It is one of the methods that have been successfully used for the determination of the crystal structure of a material. Although the X-ray diffraction method is a well-known technique, the method should be used after fully recognizing the differences from other evaluation methods and the feature of the method. When comparing to the electron beam diffraction method, the merits of the X-ray diffraction method are as follows:

- Non-destructive and no special sample preparation is required.
- Possible to be preformed in atmosphere and under a special atmosphere such as a high-temperature or high-pressure condition.
- Possible to obtain information on the average structure in a relatively large area (mm to cm).
- Irradiation damages in organic materials are low.
- Possible to control the analysis depth by the incident angle onto the surface.
- Possible to characterize buried interface structure.

The last two points of merits are important for the evaluation of thin films (Inaba, 2008).

X-ray diffraction using X-ray optics has been applied to many different types of applications including thin film analysis, sample texture evaluation, monitoring of crystalline phase and structure, and investigation of sample stress and strain.

Measurement method	Scan axis	Obtainable information
Out-of-plane measurement	2θ/ω	Phase identification Crystal structure
Thin film method measurement	2θ	Phase identification Crystal structure
In-plane measurement	2θχ/φ φ	Phase identification Crystal structure
Pole figure measurement	χ(α), φ(β)	Preferred orientation
Rocking curve measurement	ω, χ, φ	Preferred orientation Crystallinity
Reciprocal space map	2θ/ω, ω 2θχ/φ, φ	Crystallinity Epitaxial Orientation Distortion/relaxation of the film
Reflectivity measurement	2θ/ω	Film thickness, density, roughness
Small angle scattering method	2θ/ω	Particle/pore size

*The Rigaku Journal, **24**(1), 2008*

Table 5. Characterization methods of thin film using X-ray diffractometer (Inaba, 2008).

2.5.2 FOURIER TRANSFORM INFRARED SPECTROSCOPY

Measurement techniques like attenuated total reflectance Fourier transform infrared spectroscopy (ATR) can for example be applied to characterize the composition of polymers.

FTIR Analysis or FTIR Spectroscopy is an analytical technique used to identify organic, polymeric, and, in some cases, inorganic materials. The FTIR analysis method uses infrared light to scan test samples and observe chemical properties.

A Fourier Transform InfraRed (FT-IR) Spectrometer is an instrument which acquires broadband Near InfraRed (NIR) to Far InfraRed (FIR) spectra. Unlike a dispersive instrument, i.e. a grating monochromator or spectrograph, FTIR spectrometers collect all wavelengths simultaneously. This feature is called the Multiplex or Felgett Advantage.
FT-IR Spectrometers are often simply referred to as FTIRs. But for the purists, an FT-IR is a method of obtaining infrared spectra by first collecting an interferogram of a sample signal using an interferometer, and then performing a Fourier Transform (FT) on the interferogram to obtain the spectrum. An FT-IR spectrometer collects and digitizes the interferogram, performs the FT function, and displays the spectrum.

Infrared (IR) spectroscopy, the study of the interaction of infrared light with matter, is one of the most important techniques available for materials analysis. This chapter, will provide an overview of the principles of IR and Fourier transform infrared (FTIR) spectroscopy and sample preparation. FTIR spectroscopy has been extensively used in both qualitative and quantitative analysis of

nanofillers and their nanocomposites. In qualitative analyses, the nanofillers such as metal oxide nanoparticles, carbonaceous nanostructure, clay, nanofiller synergy, and their polymer nanocomposites will be characterized by FTIR spectroscopy. In quantitative analyses, FTIR will be employed to show the influence of a nanofiller on the properties of nanocomposite films through changes in the band intensity of FTIR spectra. The effects of the nanofillers on the phase transformation of nanocomposite films is the topic to be researched (Jaleh et al., 2016). It is not always possible to unequivocally identify a compound by examining its IR spectrum alone. It is normal to use IR spectroscopy in conjunction with other techniques, such as chromatographic methods, mass spectrometry, nuclear magnetic resonance (NMR) spectroscopy, and various other spectroscopic techniques.

The IR spectroscopy method is accurate, faster than chemical analysis, and reduces exposure to irritating, toxic, and corrosive chemicals. The polymer nanocomposites are a mixture of polymers and fillers. If two components are immiscible, the IR spectrum should be the sum of the spectra of the two components. If the components are miscible, there is the possibility of chemical interactions between the individual polymer chains. Such interactions may lead to differences between the spectra of the polymers in the nanocomposite and the pure components. Generally, wave number shifts and band broadening are seen as evidence of chemical interactions between the components in a composite and are indicative of miscibility.

The IR spectra of clay minerals (which are not discussed in this chapter) show well defined absorption bands corresponding to fundamental stretching and bending vibrations of their structural units: for example, OH and Si-O groups. The stretching and bending vibrations of OH groups absorb in the 3700- 3500 and 950-650 cm^{-1} regions, respectively. The SiO stretching modes occur in the 1050-1000 cm^{-1}, while the most intense bending bands appear in the 550-400 cm^{-1} region.

2.5.3. Differential scanning calorimetry

Differential Scanning Calorimetry (DSC) is a technique used to investigate the response of polymers to heating. DSC can be used to study the melting of a crystalline polymer or the glass transition. The DSC set-up is composed of a measurement chamber and a computer. Two pans are heated in the measurement chamber. By measuring the heat change associated with the molecule's thermal denaturation when heated at a constant rate.

The higher the thermal transition midpoint (T_m), the more stable is the molecule. DSC measures the enthalpy (ΔH) of unfolding that results from heat-induced denaturation. It is also used to determine the change in heat capacity (ΔC_p) of denaturation. DSC can elucidate the factors that contribute to the folding and stability of native biomolecules. These include hydrophobic interactions, hydrogen bonding, conformational entropy and the physical environment.

Macromolecules and macromolecular assemblies (>5000 Daltons), such as polymers, proteins, sugars and lipids, can form well-defined structures that undergo thermally-induced conformational

changes. These structural rearrangements result in the absorption of heat caused by the redistribution of non-covalent bonds. Differential scanning calorimeters measure this heat uptake.

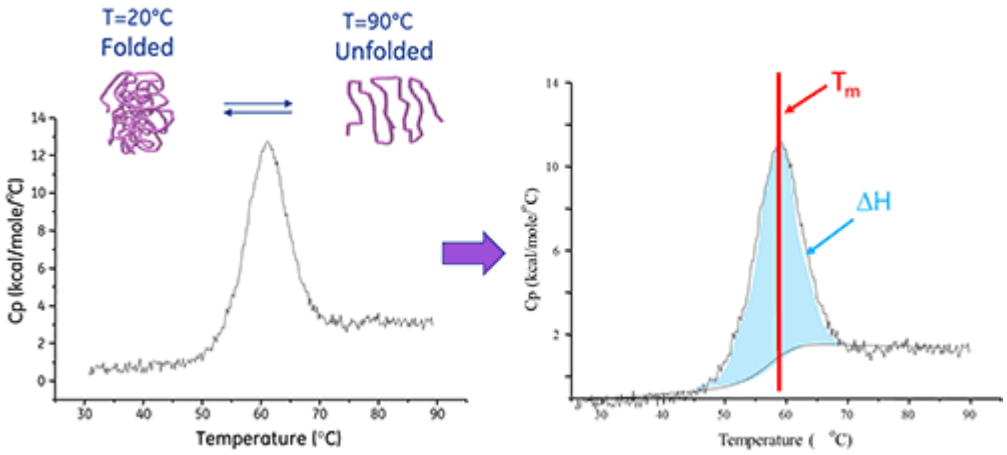

Figure 21. Demonstrative DSC measurement graph.

The enthalpy of protein unfolding is the area under the concentration-normalized DSC peak and has units of calories (or joules) per mole. In certain cases, thermodynamic models can be fitted to the data to obtain the Gibb's free energy (ΔG), the calorimetric enthalpy (ΔH_{cal}), the van't Hoff enthalpy (ΔH_{vH}), the entropy (ΔS) and the change in the heat capacity (ΔC_p) associated with the transition.

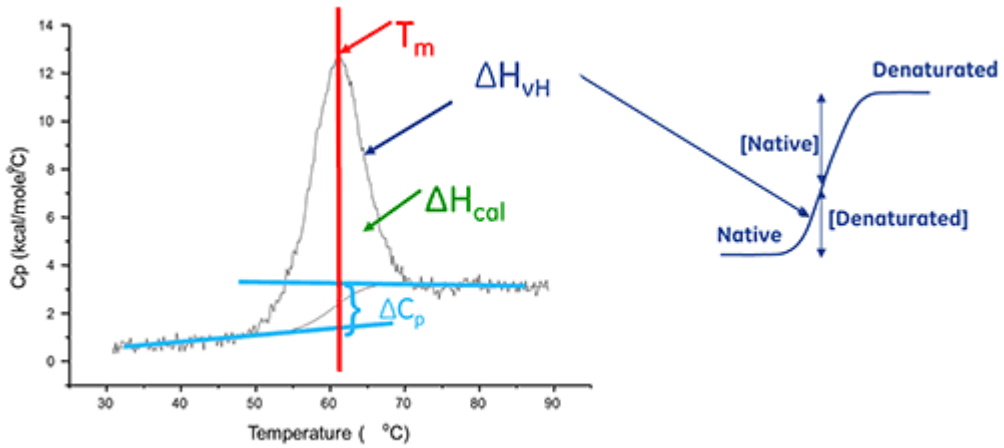

Figure 22. The meaning of DSC peaks.

Caloric effects observed in the DSC signal, e.g., the glass transition, crystallization and melting, as well as the pyrolytic decomposition and the combustion of the studied polymer samples, allow to see a detailed characterization. There are further advanced DSC tests like the determination of the oxidation induction time (OIT) which provides information about the thermal stability of polymers. It should be noted that in general two modes of DSC can be distinguished: heat flux versus power compensation; in this work, exclusively heat flux DSC was utilized which should not be put on a level with the simpler DTA (differential thermal analysis) method (Schindler et al., 2017).

2.5.4 Morphology and topography analysis by Scanning Electron and Atomic Force Microscopy

Different microscopic techniques ranging from optical microscopy to electron microscopy (EM) and scanning probe microscopy (SPM) play a vital role in the characterization of polymer nanocomposite morphology on different length scales. The unparalleled contribution of the microscopic techniques (especially of electron microscopy and scanning force microscopy, SFM) in the development of nanocomposite science and technology can be realized by the fact that almost all of the scientific literatures devoted to PNCs make a direct or an indirect reference to the use of these techniques. Thus, these techniques play a crucial role especially in the optimization of composite properties through structural characterization, which provide direct clues not only about the structure of the filler itself but also about the filler-matrix adhesion, filler distribution, and the impact of the filler on the morphology and properties of the embedding polymer matrix
Scanning Electron Microscopy (SEM) is a test process that scans a sample with an electron beam to produce a magnified image for analysis. The method is also known as SEM analysis and SEM microscopy, and is used very effectively in microanalysis and failure analysis of solid inorganic materials. Electron microscopy is performed at high magnifications, generates high-resolution images and precisely measures very small features and objects.

Applications
The signals generated during SEM analysis produce a two-dimensional image and reveal information about the sample, including external morphology (texture), chemical composition, when used with the energy dispersive spectroscopy (EDS) feature, and orientation of materials making up the sample.

The EDS component of the system is applied in conjunction with SEM analysis to determine elements in or on the surface of the sample for qualitative information. It also measures elemental composition for semi-quantitative results and identifies foreign substances that are not organic in nature and coatings on metal.

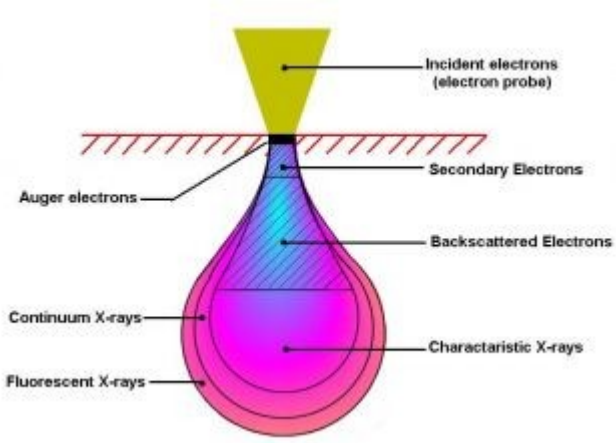

Figure 23. Electron beam interaction diagram.

Scanning Electron Microscopy uses a focused beam of high-energy electrons to generate a variety of signals at the surface of solid specimens (Fig. 23). In most SEM microscopy applications, data is

collected over a selected area of the surface of the sample and a two-dimensional image is generated that displays spatial variations in properties including chemical characterization, texture and orientation of materials. The SEM is also capable of performing analyses of selected point locations on the sample. This approach is especially useful in qualitatively or semi-quantitatively determining chemical compositions, crystalline structure and crystal orientations.

The EDS detector separates the characteristic X-rays of different elements into an energy spectrum and EDS system software is used to analyze the energy spectrum in order to determine the abundance of specific elements. A typical EDS spectrum is portrayed as a plot of X-ray counts vs. energy (in keV). Energy peaks correspond to the various elements in the sample. Energy Dispersive X-ray Spectroscopy can be used to find the chemical composition of materials down to a spot size of a few microns and to create element composition maps over a much broader raster area. Together, these capabilities provide fundamental compositional information for a wide variety of materials, including polymers and metals.
Electron microscopy, complemented by other techniques, has played important role in the elucidation of morphology and structure-property correlations of polymers including homopolymers, copolymers, blends, and composite materials. When employed vigilantly by an experienced microscopist with proper care during sample preparation, electron microscopy most reliably characterizes every detail concerned with the morphology of polymers on various length scales. EM identifies the structure and properties of specific locations of polymers and the information is not restricted to the average values (Adhikari et al., 2009).

Since the introduction of the Nobel Prize-winning scanning tunneling microscope (STM) and then the invention of the atomic force microscopy (AFM) from the landmark publication by Binnig, Quate, and Gerber, the field of scanning probe microscopy has exploded well beyond using interatomic forces to image topography on the nanometer scale. The ability to measure intermolecular forces and see atoms is scientifically tantalizing.

Topography imaging alone does not always provide the answers that researchers need and the surface topology often does not correlate to the material properties. For these reasons, advanced imaging modes have been developed to provide quantitative data on a variety of surfaces. Now, many material properties can be determined with AFM techniques (Fig. 24), including friction, electrical forces, capacitance, magnetic forces, conductivity, viscoelasticity, surface potential, and resistance.

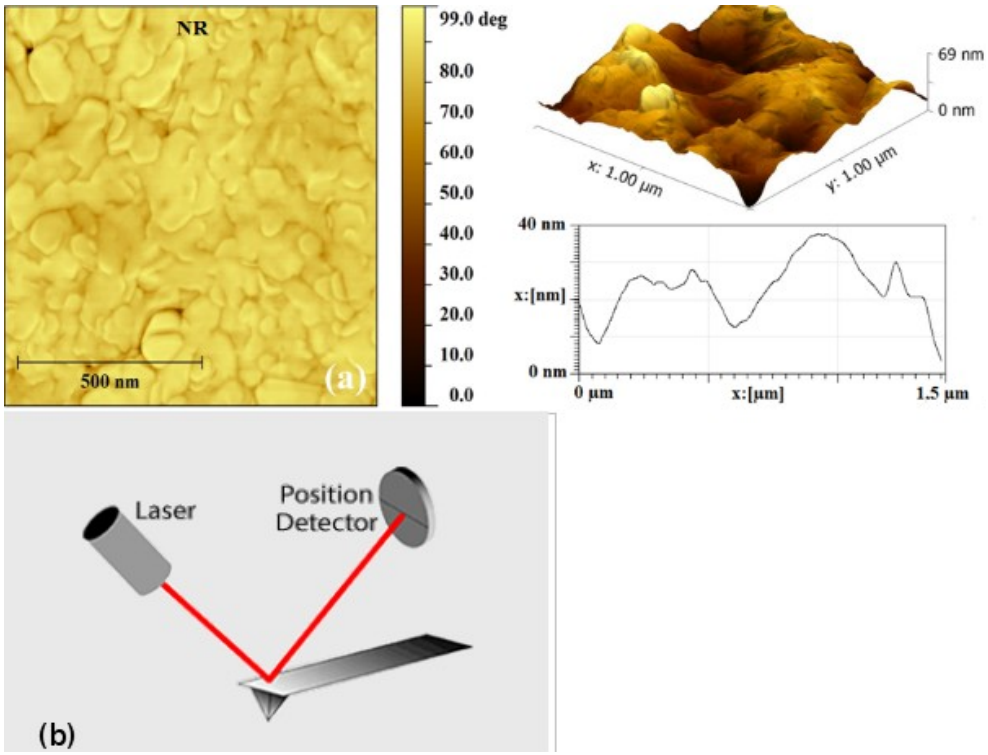

Figure 24. a) Example of AFM image including 3D profile and measurement of profile height, (b) Laser beam deflection on AFM cantilever when detected with position detector.

Analogous to how a Scanning Tunneling Microscope works, a sharp tip is raster-scanned over a surface using a feedback loop to adjust parameters needed to image a surface. Unlike Scanning Tunneling Microscopes, the Atomic Force Microscope does not need a conducting sample. Instead of using the quantum mechanical effect of tunneling, atomic forces are used to map the tip-sample interaction.

Often referred to as scanning probe microscopy (SPM), there are Atomic Force Microscopy techniques for almost any measurable force interaction – van der Waals, electrical, magnetic, thermal. For some of the more specialized techniques, modified tips and software adjustments are needed.

In addition to Angstrom-level positioning and feedback loop control, there are 2 components typically included in Atomic Force Microscopy: Deflection and Force Measurement.
Because the Atomic Force Microscope relies on the forces between the tip and sample, these forces impact AFM imaging. The force is not measured directly, but calculated by measuring the deflection of the lever, knowing the stiffness of the cantilever (Bandyopadhyay et al., 2008).

2.5.5 MICROBIOLOGICAL TECHNIQUES.

MICROBIOLOGICAL MEDIA

Bacteria will grow on practically any source of organic food which provides carbon compounds to be respired for energy, and nitrogen compounds to be incorporated into proteins for growth. These substances are normally provided dissolved in water. However, in nature, bacteria can break down solid and insoluble substances by releasing enzymes into the substrate in which they are growing. These substances are thus broken down or digested to simpler substances and the process is called extracellular digestion because it takes place outside the bacterial cells.

The two normal media used in bacteriology are a clear soup-like liquid nutrient broth, usually in tubes, and nutrient agar, which is set into a jelly by the addition of a seaweed extract called agar, and when melted poured into glass or plastic Petri dishes - also known as "plates".

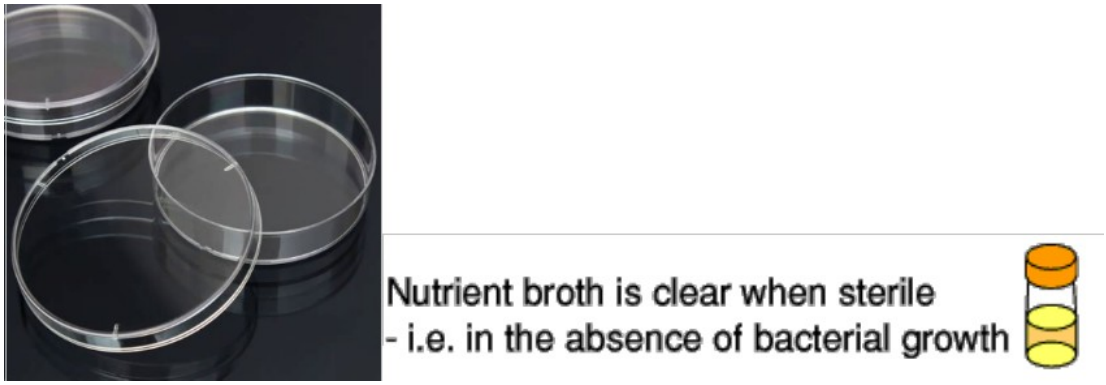

Figure 25. Disposable Petri dishes used for antimicrobial testing.

A standard carbon source is glucose, and nitrogen is often provided by peptones (partially digested proteins), or inorganic salts. Minerals and vitamins may also be provided, according to the growth requirements of the bacteria. Combinations of chemicals (buffers) may be used to keep the pH stable. Measured amounts of the concentrates are added to water, and dissolved to reconstitute the media.

Sometimes, substances are mixed into media, in order to suppress growth of other types of bacteria. There are many such selective media.

These media must then be sterilised by heating in an autoclave (like a pressure cooker) at 121°C (pressure 1 bar or 15 lb/sq. in.) for 15 minutes, which kills all living organisms, including spores.

All apparatus used from this point onwards must be sterilised by heat (glassware - 160 °C for 2 hrs) or exposure to radiation.

Aseptic techniques must be used to reduce the likelihood of bacterial contamination. This usually involves disinfection of working areas, minimising possible access by bacteria from the air to exposed media, and use of flames to kill bacteria which might enter vessels as they are opened.

Bacteria may be introduced to the media (inoculated) by various means. Usually the bacteria e.g. from a drop in a heat-sterilised loop are spread on the surface of (ready set) agar. A similar technique is used with broth cultures.

Sometimes bacteria in a liquid are introduced using a sterile pipette to the Petri dish before the (fairly cool) agar medium is poured on top ("pour plates").

Then the Petri dishes containing agar or tubes containing broth are incubated, i.e. put in a special apparatus at a fixed temperature (usually 37°C - human body temperature, for possible pathogens - or 25°C for bacteria from the environment). In schools, lower incubation temperatures are used in order to discourage the growth of potential pathogens.

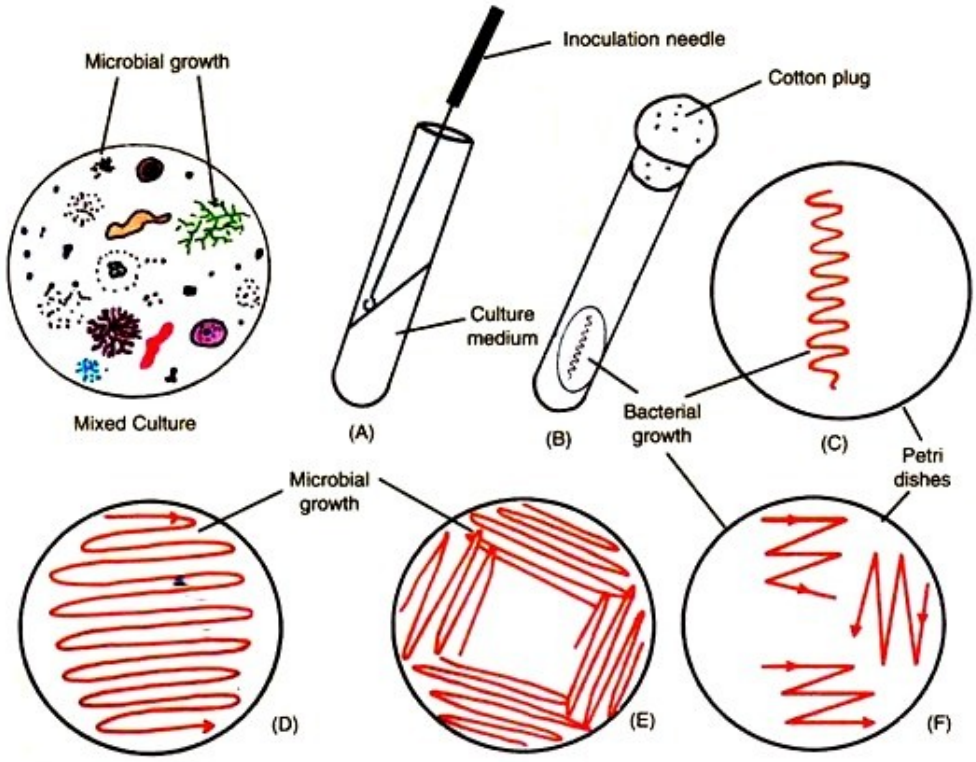

Figure 26. Isolation of bacteria from a mixed culture. (A) isolation of pure culture and inoculation

needle containing a loop, (B) pure culture, (C)(D)(E) and (F) streaking of bacterial culture by different methods.

When growing bacteria, it is usual to invert the Petri dishes (Fig.26), so as to prevent condensation droplets from falling onto the surface of the agar. Petri dishes are often "sealed" at this stage to prevent people who handle them from contamination by bacteria, which will multiply greatly. It is normal to use 2 strips of adhesive tape from base to lid rather than attempt seal the circular edge of the Petri dish. This is to guard against the possibility of anaerobic organisms growing due to lack of air. However, it must be borne in mind that any drips from a partially sealed Petri dish are potential sources of infection.

Cultures are usually examined after 24 hrs incubation.

Liquid media such as broth become cloudy if bacteria are present. This could be the result of only one bacterial cell originally entering the medium, then dividing repeatedly to produce millions!

Bacteria on agar "plates" become visible as distinct circular colonies; each colony should represent an individual bacterial cell (or group) which has divided repeatedly but, being kept in one place, the resulting cells have accumulated to form a visible patch.

By an extension of this method using serial dilutions in sterilised liquids, the number of bacteria in a given amount of sample, e.g. food, can be calculated.

After use, bacterial cultures, etc. must be sterilised by the use of heat, before disposal.

AGAR AND BROTH DILUTION METHODS

Agar dilution and broth dilution are the most commonly used techniques to determine the minimal concentration of antimicrobial agents that kill (bactericidal activity, MBC) or inhibit the growth (bacteriostatic activity, MIC) of microorganisms (Getzin et al., 2008).
In the agar dilution method, different concentrations of antimicrobial agent, either by direct addition, or by incorporation of the film forming solution or of finely divided active film sample, are added to non-selective agar medium before solidification. The test microorganisms are diluted to around log 7.0 CFU/mL and 1 to 2 are added to the plates in different spots (ca. 4.0 CFU per spot).
There are several advantages of the agar dilution method including capacity to test different strains at once, easy detection of contamination and capacity to test opaque materials.

In the broth dilution assay, an antimicrobial is added to a culture tube of non-selective broth medium at different concentrations. This method can be carried out by using glass test tube dilution (broth macrodilution) or microtiter plastic plates containing 96 wells (broth microdilution). Tubes are inoculated to contain approximately log 5.7 CFU/mL of the test microorganism.

After incubation at 35 ± 2 ℃, the tests are examined and the MIC is determined generally by spectrophotometry. Turbidity of the medium increases with microbial growth, therefore, it is necessary to build a calibration curve relating turbidity with microbial growth. The success of this method depends on the sensitivity of the device and the correct interpretation of results. Spectrophotometers generally require log 6.0–7.0 CFU/mL for detection (Piddock, 1990)
Below these concentrations, the lack of sensitivity should not be confused with absence of microbial growth and, therefore, sampling for direct seeding is recommended.

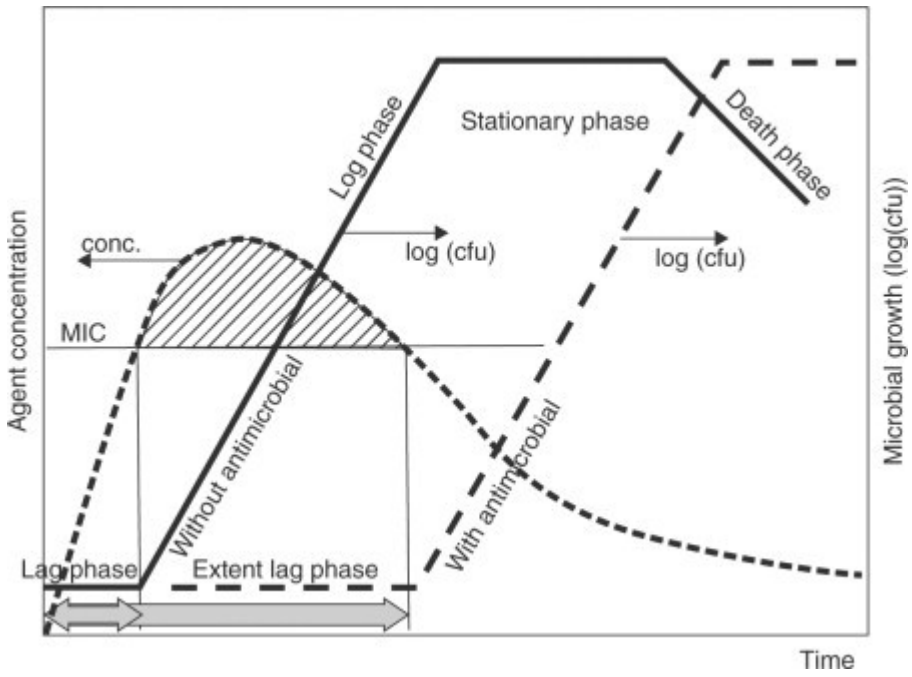

Figure 27. Effect of an antimicrobial agent on the bacterial growth curve.

In order to study antimicrobial capacity of packaging films, they are immersed in 10 mL of Mueller Hinton broth prior to the inoculation of microorganism in exponential phase (when bacteria are more sensitive). Tubes are incubated under optimum conditions for the test microorganism from 16 to 24 hours. Antimicrobial effect could be determined by spectro-photometry or by plating and counting.

Total inhibition of a pathogen or spoilage microorganism is not always required. An increased lag phase, especially under conditions of severe abuse, is often sufficient to protect the consumer. A description of the effect of an antimicrobial compound on the growth (or death) kinetics of a microorganism can be obtained through a growing curve such as the one shown in Fig.27. The release of the antimicrobial agent from the active package results in an increase in the concentration to which the microorganisms are exposed. The agent concentration reaches a maximum and decreases continuously due to the loss of the agent out of the package or by dispersion in the food product, with a profile similar to that shown in Fig.27. The presence of an antimicrobial agent at concentrations above the MIC results in a delay in the log phase and

lengthening of the lag phase, with the subsequent increase in the shelf life of the product. Once the agent concentration decreases below the MIC, microorganisms resume their growth.

This method is similar to the broth dilution assay but, in this case, the medium is sampled at appropriate times (e.g., 0, 2, 4, 8, 12, 24 and 48 hours) and the mber of viable microorganisms is determined by plating. Several responses of the test microorganism may be encountered in this type of analysis, including stationary phase growth level suppression, lag phase increase, decrease in the growth rate during log phase and lethality (Davidson et al., 1989). The disadvantage of these methods is that they are more tedious and longer than the agar diffusion one.

3. EXPERIMENTAL PART

3.1. PREPARATION OF POLYMERIC NANOCOMPOSITE

This part is divided into 2 basic parts and so preparation of clay functional nanofillers and preparation polymeric nanocomposite films with nanofillers.

3.1.1. MATERIALS

Three clay minerals were selected as carriers of antimicrobial/medicinal properties. Two of them are smectites (bentonite and montmorillonite); one is vermiculite so we could compare the effect of antimicrobial action and compounding efficiency such filler with polymeric matrix.

Composition and crystalochemical formula are from literature (Valášková et al. 2008).

Five antimicrobial agents and different chemical compositions are shown in Table 6.

Following group of precursors are matrices for polymeric nanocomposite films. One of them is a monomer (vinyl acetate) and two of them are polymers (polyvinyl alcohol and polyethylen oxide).

Table 6. Chemicals and clays used during the experiment.

Component (abbreviation)	**Origin**	**Formula**	**Properties**
Vermiculite (VMT)	Brazil	$(Mg,Fe,Al)_3(Al,Si)_4O_{10}(OH)_2 \cdot 4(H_2O)$	Fraction ≤40 μm
Bentonite (BEN)	CZ	$(Ca, Na)(Al, Mg, Fe, Zn)_2(Si, Al)_4O10(OH)_2$ - xH_2O	Fraction ≤40 μm
Montmorillonite (MMT)	Ivančice	$Ca_{0.24}K_{0.06}Na_{0.09}Mg_{0.10}(Al_{2.25}2Fe^{3+}{}_{0.54}Mg_{0.90}Ti_{0.04})(Si_{0.79}6Al_{0.04})\ O_{20}(OH)_4$	Fraction ≤40 μm

Imidazole (imi)	Sigma Aldrich	$C_3H_4N_2$	M =68.077 g/ mol
Trihexyltetradecylphosphonium bromide (bro)	Sigma Aldrich	$[CH_3(CH_2)_5]3P(Br)(CH_2)13CH_3$	M = 563.76 g/ mol
Ciclopirox olamine (ciclo)	Sigma Aldrich	$C_{12}H_{17}NO_2 \cdot C_2H_7NO$	M = 268.35 g/ mol
Vinyl acetate (VA)	Sigma Aldrich	$CH_3CO_2CH=CH_2$	M = 86.09 g/mol
Benzoyl peroxide (BP)	Sigma Aldrich	$(C_6H_5CO)_2O_2$	M = 242.23 g/ mol
Trolamine (trol)	Sigma Aldrich	$C_6H_{15}NO_3$	M = 149.190 g/mol
Clotrimazole (clo)	Sigma Aldrich	$C_{22}H_{17}ClN_2$	M = 344.837 g/mol
Polyethylene oxide (PEO)	Sigma Aldrich	$C_{2n}H_{4n+2}O_{n+1}$	M = 18.02 + 44.05n g/mol
Polyvinyl alcohol (PVAL)	Sigma Aldrich	$(C_2H_4O)_x$	D = 1.19-1.31 g/cm^3

3.1.2. TECHNIQUES AND DEVICES

Based on the state of a sample several methods were selected in order to characterize and observe the properties of materials.

Structural analysis was performed using X-ray powder diffraction (XRD) analysis using the X-ray powder diffractometer Ultima IV Rigaku (Japan), operated at 40 kV and 40 mA (CuKα radiation). The XRD patterns of samples were measured at Bragg-Brentano arrangement, range 2-60°2θ, scan speed 2°/min.

The infrared spectra (FTIR) were measured using single reflection ATR technique with a diamond crystal on infrared spectrometer with Fourier transformation Specifications of the Nicolet iS50 Infrared Spectrometer, Spectral range 7.800 - 350 cm^{-1};Ge / KBr beam splitter for the mid-infrared region; Software switchable 3 positions for detectors in the basic spectrometer; 0.09 cm^{-1} spectral resolution; Integrated ATR diamond attachment to allow free sample space; Module for transmission measurement in KBr tablets;

Nicolet iN10 FTIR microscope, Thermo Scientific, USA, The IR spectra were measured in the form of spectral maps using a single reflection ATR adapter with germanium crystal (16 scans, 8 cm^{-1}

resolution) in the middle region of IR radiation (4000-600 cm $^{-1}$) on an iN 10 FTIR microscope.

DSC131 evo - Differential Compensation Calorimetry DSC (-170 to 700°C), Temperature range from room temperature to 700°C; Cryothermostat for cooling -70°C to 400°C; Liquid Nitrogen Accessories -170°C to 500 °C; Scanning rate 0.01 to 100°C / min; Ar atmosphere (N2, O2, He);

Al cups 30,100 µl, Al2O3, (Pt) is set for both solid and liquid samples can be tested over a wide range of temperatures; is widely used to determine melting temperatures, glass transitions, crystallization and degradation.

Light microscope Olympus BX51 equipped with bright field and dark field observation mode , reflection and transmission mode, nosepiece 4x-40x , polarization filter. ¨

Scanning electron microscope FEI QUANTA 450 FEG, EDS Oxford elemental analysis (SED, BSED, GSED, vCD, SS-BSED, STEM detectors.

Atomic Force Microscope (AFM) Solver-Next, NT-MDT, possible to operate in contact, semi-contact and non-contact modes; contact mode (topography, friction force mode, modular force mode, force spectroscopy); non-contact mode (percussion topography, phase image measurement, electrostatic force microscopy, magnetic force measurement, Kelvin probe microscopy, scanning capacitance microscopy); x-y-range: 100 x 100 micrometers, z-axis 10 micrometers; z-axis noise - 0.04 nm, x, y-axis - 0.2 nm with capacitive sensors (i.e. with active linearization) switched on, 0.02 nm in case of capacitive sensors off; both solid and powder samples can be analyzed.

3.1.3. Methods for organoclays preparation

The techniques for preparation of organoclays are based on wet intercalation with presumable cation exchange modification.

Firstly, clay minerals were mixed together with antimicrobial organic compound. The solutions of individual agent were prepared as following:

Solution of 1.0 M Imidazole 1.5 g soluble in 20 ml distilled water and additional of 5 ml non-aqueous ethanol; for 0.025 M Trihexyltetradecylphosphonium bromide 0.35 g soluble in 20 ml distilled water and addition of 5 ml non-aqueous ethanol; for 1.0 M ciclopirox olamine is 1.5 g ciclopirox in 20 ml water with addition of 5 ml non-aqueous ethanol.

Dry clays in amount of 4 g were mixed with 100 ml of solution. Then placing the suspension to 200 ml flask magnetic stirring on magnet hotplate (80°C, 200 rpm) for 2 hours was done. After 2 hours mixture was centrifuged at 3500 rpm for 20 minutes and solid part – organoclay – was placed on

Petri dish, and then placed to the furnace on 80°C for 24 hours. After complete drying samples were grind in agate mortar to fine powder.

3.1.4. METHODS FOR NANOCOMPOSITE PREPARATION

Experimental work related to preparation of self-standing film divides into two parts. First, the functional filler must be prepared and in second step compounded to monomer via *in situ* polymerization.

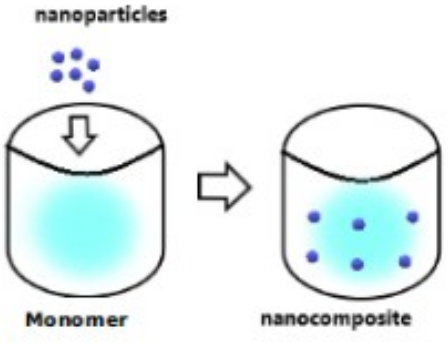

Figure 28. Polymerization *in situ* – from monomer: nanofiller is with monomer in one reactor.

POLYMERIZATION OF VINYL ACETATE

Next step is polymerization *in situ* with help of an initiator. The polymerization of matrix was carried out in a simple reaction setting: hot plate, lockable container. The mixture of monomer vinyl acetate and modified clay was in 10:1 weight ratio. The clay nanofiller was placed into a glass jar with a tight lid and mixed with vinyl acetate adding an initiator - benzoyl peroxide. The jar containing the mixture of monomer, initiator and nanoclay was ultrasonicated for 2 minutes or till no visible agglomerates of clay powder were observed. Further, the jar is heated on the hotplate to 150°C (depending on the type of hotplate, the set temperatures may vary). The lid shouldn't be closed too tight so it would be possible to open it after polymerization.

The polymerization process takes approximately 15 minutes in case of vinyl acetate and chosen initiator, but the time may vary according to the settings and equipment. It may also depend on the type of used nanofiller. The samples with ciclopirox olamine polymerize longer than 15 minutes (from 25 to 50 minutes).

PREPARATION OF THE THIN FILM FROM POLYMERIZED VINYL ACETATE

During the observation of the heating jar the appearance of “bubbles” can be noticed as well as the increased viscosity of the liquid mixture, this means the polymerization started. Right after the starting of polymerization the liquid mixture in the jar rapidly becomes more and more viscous and needs to be removed from the heating plate as soon as possible. For preparation of thin films it is needed to have a neat smooth surface, therefore the Teflon material was chosen. Teflon was cut to 10-12 cm^2 pieces and fixed on the rotating plate. While it was slowly rotated, the polymerized mixture from the jar was poured to a Teflon piece forming a thin polymeric film on the surface. Teflon with the thin film was left overnight in the dry dark clean place without dust. Then the thin film was easily peeled from the Teflon.

PREPARATION OF THE THIN FILMS FROM POLYMERIC POWDERS

Both polymers (PEO and PVAL) have been used as polymeric powders with molecular weight suitable for solution in water (Fig.29). The process included dissolving of polymers in destilled water and compounding with filler nanoparticles.

Figure 29. Polymeric water solutions of PEO and PVAl.

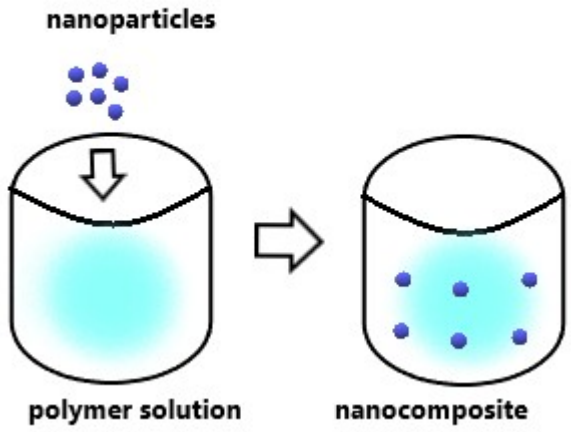

Figure 30. Re-polymerization– from polymer solution: nanofiller is mixed with diluted polymer.

The mixture of polymer and nanofiller was applied to a piece of Teflon or glass. After complete drying out it was peeled off from the material.

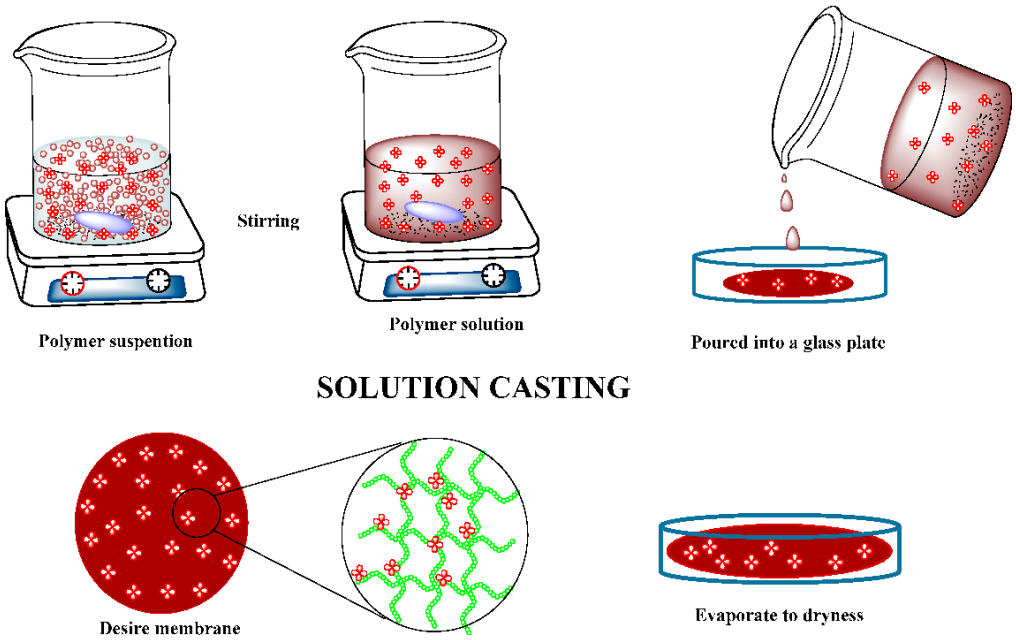

Figure 31. The visualization of the polymer solution preparation steps (Roy et al., 2017).

As the polymerization process is over the flask with polymer should be taken away from the hotplate and a thin layer slowly applied on the piece of Teflon. The piece of Teflon should be attached to the rotating device and slowly rotated while the thin layer of polymer is applying on it. After the preparation place the Teflon with polymer to a dry dark space without dust for 24 hours. After 24 hours the obtained dry polymeric thin film removes from the Teflon piece. The films were analyzed on XRD, AFM and FT IR to find out if the films are suitable for medical treatment usage. As a result the polymeric thin films are presented on Fig.32 and Fig.33.

Figure 32. PEO + MMT/Imidazole macro photo.

Figure 33. PVA + MMT macro photo.

EXTRUSION METHOD OF THIN FILM PREPARATION

For the comparison to the melt techniques several samples were prepared using extrusion methods.

Polyethylene oxide nanocomposite was prepared using melt extrusion methods in UTB Zlin [4]. The percentage of modified clay powder in the polymer was 1%. The amount of 8-9 grams of polymer was taken for one sample, so 0.08-0.09 grams of clays respectively. The process was performed on the laboratory Extruder (Fig.34). The settings were on 200-210°C and 100 rpm in N_2 inert atmosphere. Filling the extruder with a sample powder takes approximately 5 minutes and then the extrusion process takes 4 minutes. If we consider the cleaning of the equipment as part of the process, we may say that preparation of one sample on laboratory extruder takes 45 minutes.

Figure 34. Laboratory extruder UTB Zlin.

After extrusion the samples were pressed under the hydraulic press to create a thin film (Fig.35).

Figure 35. Melting hydraulic press UTB Zlin.

First, 2.7-3 grams of the sample from extruder should be placed to the special form (2mm) (Fig.36) and melted under a first type of hydraulic press on 200°C for 2 minutes.

Figure 36. The form for creating thin films.

After melting the form is replaced to the second type of hydraulic press which provides cooling of sample during 10-15 minutes (Fig.37).

Figure 37. Cooling hydraulic press UTB Zlin.

After all the manipulations such thin film was obtained (Fig.38)

Figure 38. PEO thin film prepared via extrusion method in UTB Zlin.

The preparation by extrusion method takes much longer time, is much more energy-consuming and more dangerous regarding to the equipment using conditions if we compare it to the Re-polymerization technique (in case of PEO).
To obtain such a film (Fig.38) you will need 1,5-2 hours of time and three complex machines.

3.2. STRUCTURE CHARACTERIZATION AND DISCUSSION

3.2.1. X-RAY DIFFRACTION METHODS FOR STRUCTURAL CHANGES

Organomodification of silicate layers is important for better compatibility with polymeric matrix. After the organoclay has swollen in the solvent, the polymer is added to the solution and intercalates between the clay layers. The simple organic modification of the clay through ion-exchange reactions is not always enough to achieve nanocomposite formation. This is because an ideal compatibilization agent between two intrinsically incompatible components should have (combined in one molecule) parts which mix thermodynamically stable and easily with both components.

In our case the modification is multifunctional, the modified with organic matter silicate layer is simultaneously the active substance for antimicrobial activity.
XRD methods are important for evaluation of changes during intercalation process.
For observation of changes several patterns of intercalated class and polymeric nanocomposites were selected.

Since the molecules of selected active agent are relatively large, the intercalation is not always happening in the sense of inserted molecule / cation to the interlayer space of silicates.

In case of vermiculite (Fig. 39) we are not observing big changes in position of the vermiculite basal peak. From original 1.419 nm organoform shifts to 1.291 nm indicating that interlayer water was removed and large ciclopyroxolamine molecule was not intercalated, but adhered to the silicate layer. Later on the interlayer space of the polymeric nanocomposite remains slightly changed.

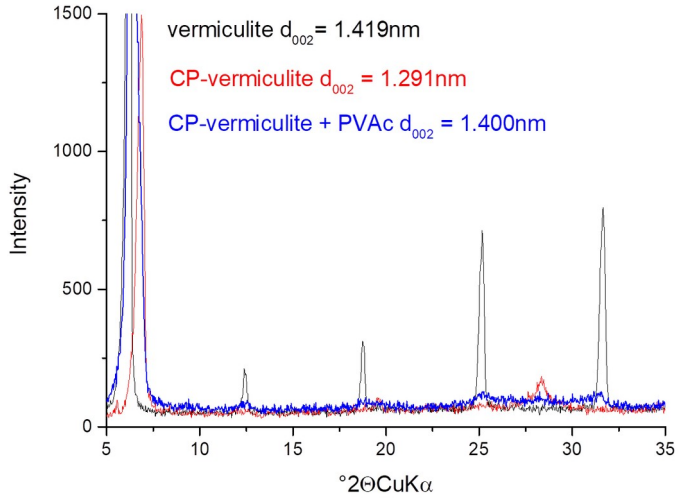

Figure 39. XRD patterns of VMT changes, original vermiculite, organovermiculite with ciclopyroxolamine CP- vermiculite and polymeric nanocomposite - CP-vermiculite + PVAc

Similar situation is repeating in case of bentonite (Figure 40 and 41). Original peak of bentonite (d = 1.21 nm) is similar to the one of organically modified with clotrimalzole (clo) and phosphonium cation (bro).

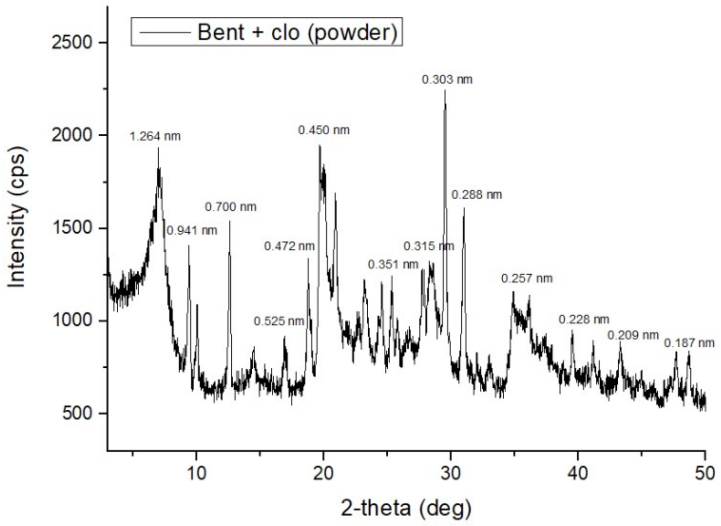

Figure 40. XRD patterns of BEN + clo sample (powder) with indicated interlayer spaces d.

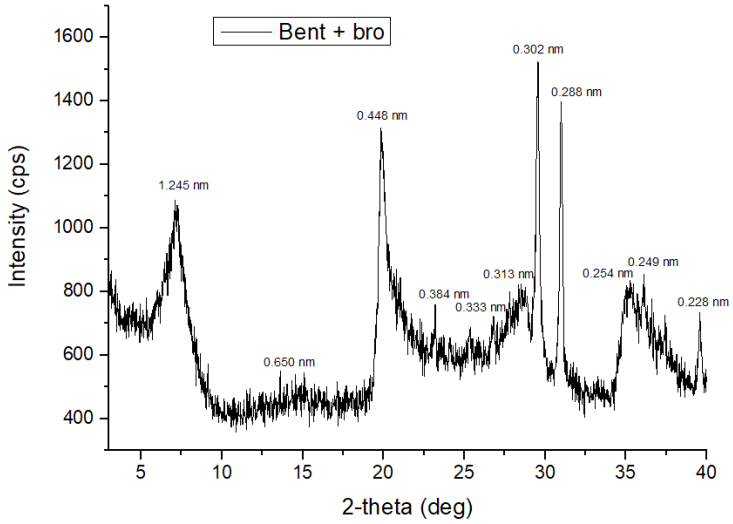

Figure 41. XRD patterns of BEN + bro sample (powder) with indicated interlayer spaces d.

Next diffraction patterns (Fig. 42) compares two smectites – montmorillonite and bentonite – and their interaction with imidazole molecule. We can observe slightly more modified structure of the montmorillonite sample compared to bentonite where the interlayer space has changed from the indicating monolayer intercalation to the interlayer space.

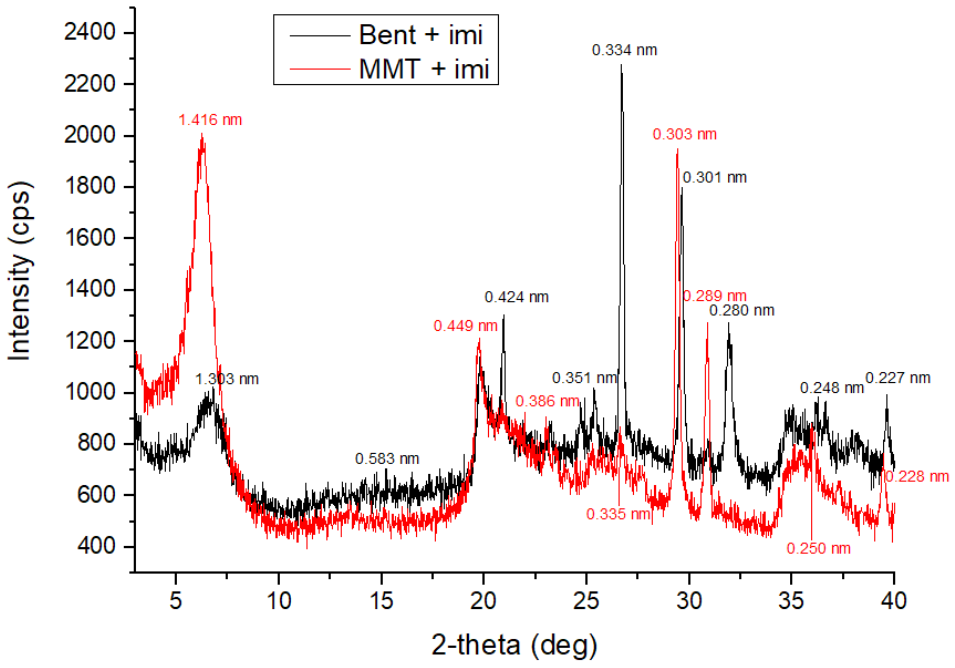

Figure 42. X-ray diffraction patterns of clay particles modified with antimicrobial agent imidazole.

Comparing further (Fig. 43) the imidazole organoMMT and pure MMT embedded in PVAl, there is a clear disappearance of basal diffraction of the organoMMT. Therefore better incorporation of the filler can be presumed.

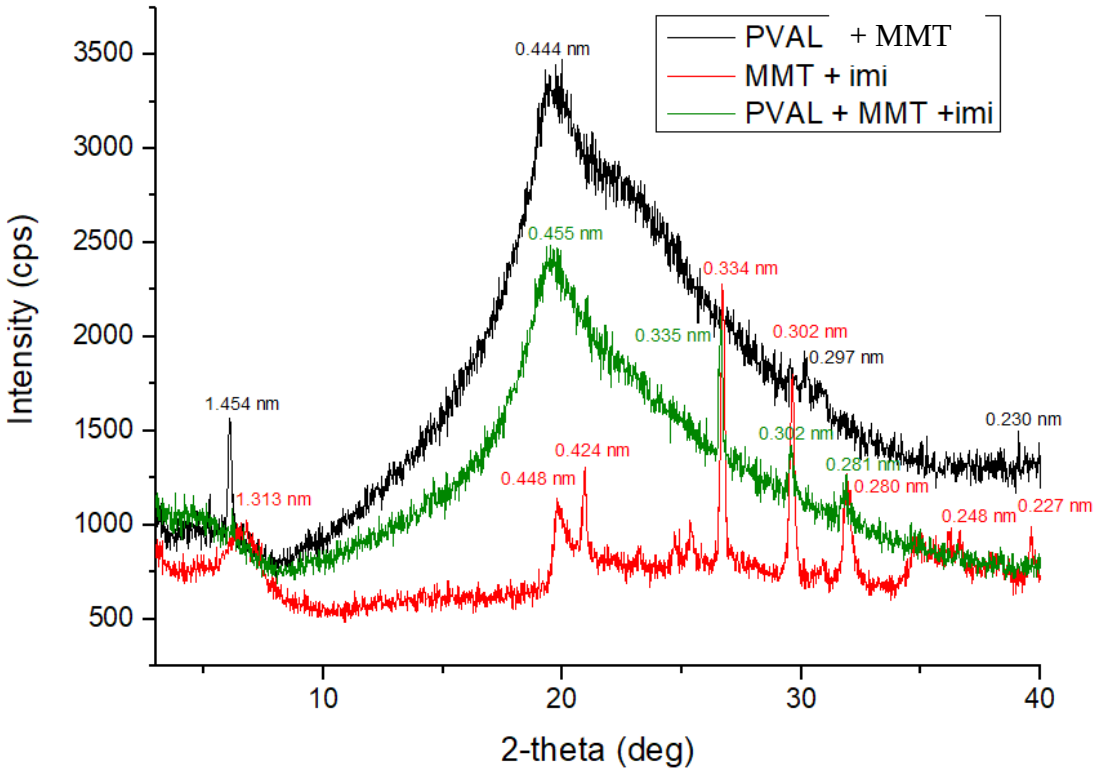

Figure 43. X-ray diffraction patterns of polymeric nanofilm PVAL + MMT + imi, modified clay

particles MMT + imi and pure polymeric film PVAL.

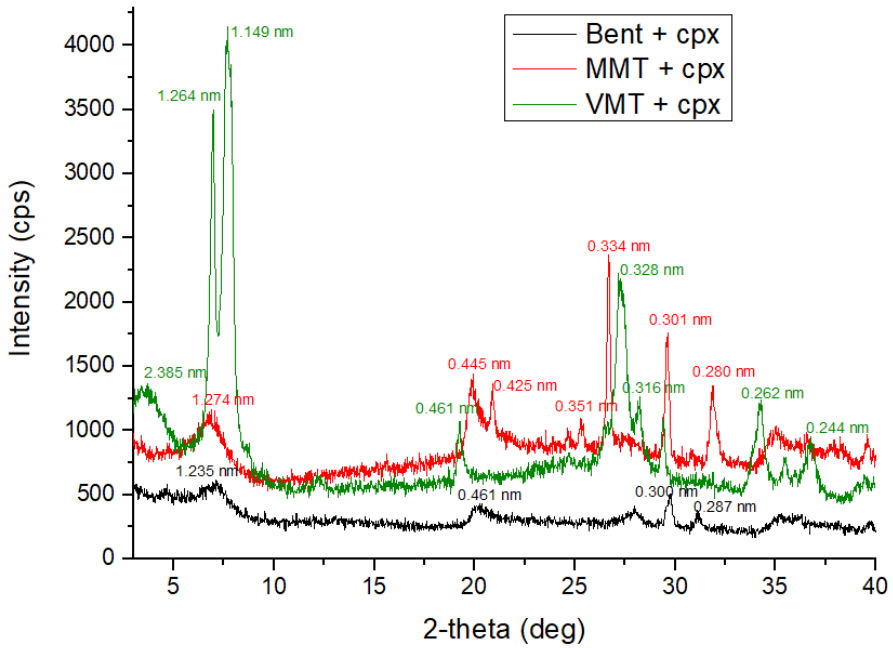

Figure 44. X-ray diffraction patterns of 3 types of clay particles modified with antimicrobial agent ciclopirox olamine.

The changes observable after modification of all 3 clays with ciclopyroxolamine (Fig. 44) are rather small. Only in case of VMT we can see the peak at small angles, which can be partly intercalated VMT with large molecule of CPX.

Further comparison of organovermiculite VMT + cpx and after incorporation to the polymers prepared via solution of polymers (Fig.45), we can see the decrease of crystalline matter in case of PVAl. Surprisingly the same method of preparation in case of PEO is not much affecting the filler.

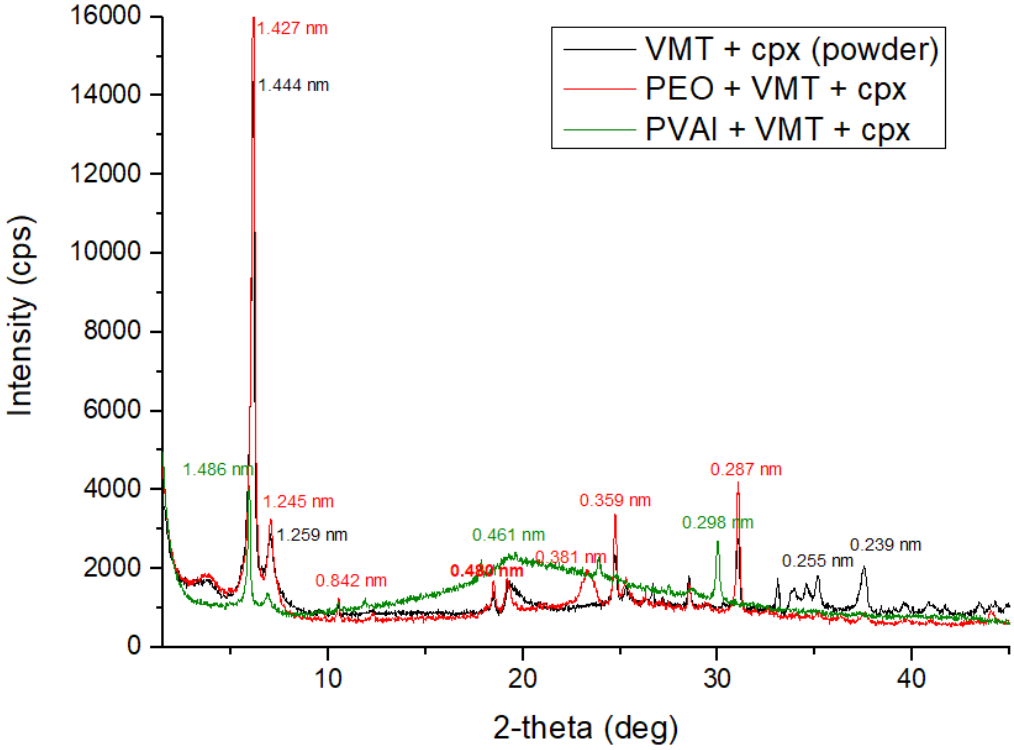

Figure 45. X-ray diffraction patterns of polymeric nanofilm PVAL + VMT + cpx, polymeric nanofilm PEO + VMT + cpx and clay particles modified with antimicrobial agent VMT + cpx (powder).

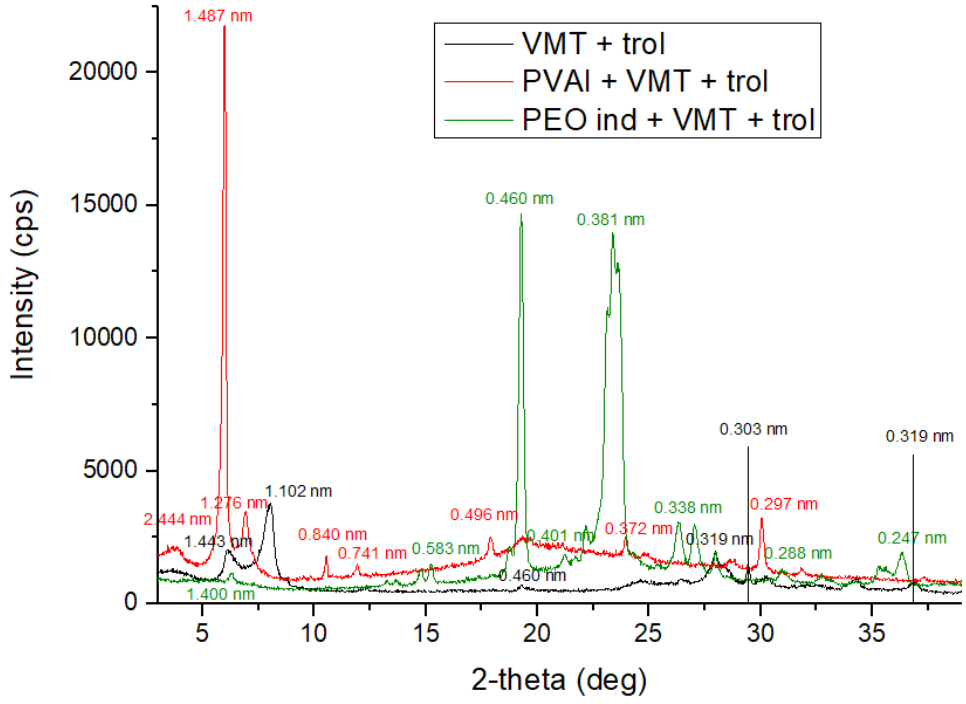

Figure 46. X-ray diffraction patterns of polymeric nanofilm PEO ind + VMT + trol, polymeric nanofilm PVAL + VMT + trol and clay particles modified with antimicrobial agent VMT + trol.

The molecule of trolamine was selected for similar application as ciclopyroxolamine, it is smaller and therefore smoother and more predictable in interaction with other components of the nanocomposite. On Fig.46 a slight change in vermiculite structure is visible, the basal peak is divided to the non-intercalated part (1.102 nm) and an intercalated one (1.443 nm). After adding to the PVAl both peaks shift to higher numbers. In case of PEO (here the one from extruder is used – industrial –ind) the crystalline character of polymer is eliminating possibility to observe low quantity content of VMT.

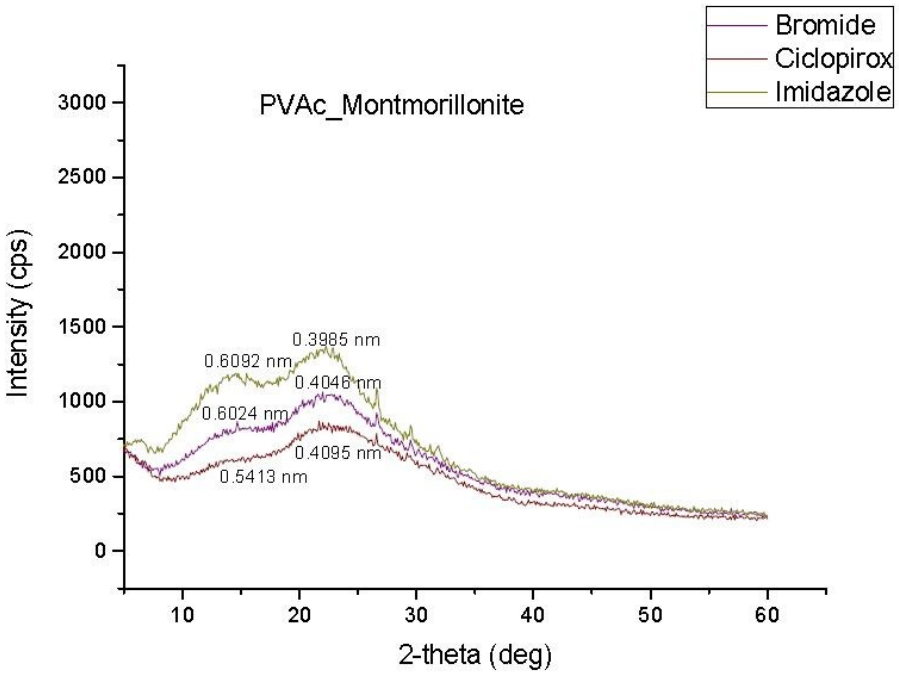

Figure 47. X-ray diffraction patterns of polymeric nanofilm containing 3 types of modifying antimicrobial agents.

Following example of PVAc (Fig.47) is showing well incorporated MMT nanofiller into the matrix. All 3 patterns are showing negligible peaks of remaining silicate basal diffraction. This should be caused by *in situ* polymerization where the filler was sufficiently dispersed in the conditions of polymerization.

A slightly different situation is in case of vermiculite (Fig.48), where the basal peak is still identifiable and the exfoliation of silicate layers is not as good as in case of montmorillonite.

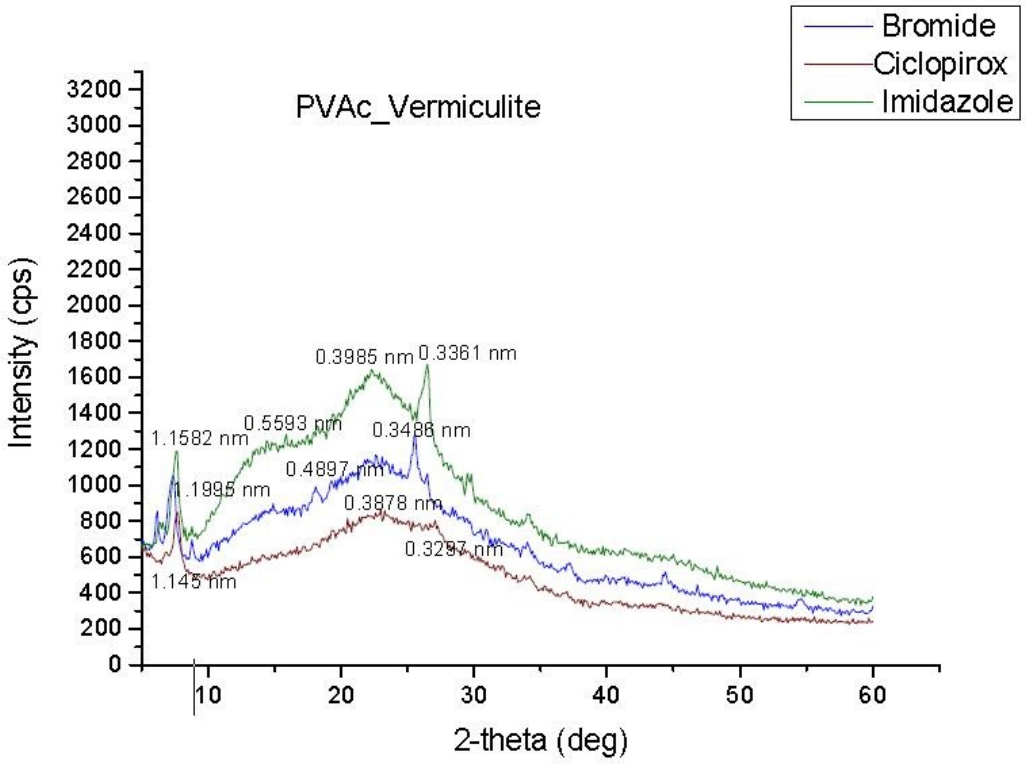

Figure 48. X-ray diffraction patterns of polymeric nanofilm containing 3 types of modifying antimicrobial agents.

3.2.2. FT INFRARED SPECTROSCOPY INTERACTION STUDY

Infrared spectroscopy was used for observation possible creation or destruction bonds in polymeric nanocomposite. The submitted samples are showing the comparison of pure polymeric nanocomposite and the nanocomposite after stability testing.

The IR spectra of clay minerals (which are not discussed in this chapter) show well defined absorption bands corresponding to fundamental stretching and bending vibrations of their structural units: for example, OH and Si-O groups. The stretching and bending vibrations of OH groups absorb in the 3700-3500 and 950-650 cm^{-1} regions, respectively. The Si-O stretching modes occur in the 1050-1000 cm^{-1}, while the most intense bending bands appear in the 550-400 cm^{-1} region.

Infrared spectroscopy was used for observation possible creation or destruction bonds in polymeric nanocomposite. The submitted samples are showing the comparison of pure polymeric nanocomposite and the nanocomposite after stability testing. The stability testing was performed

for PVAc samples because the other two types of nanocomposites are partially water soluble and relevancy for these tests would be not confrontable to PVAc polymer.

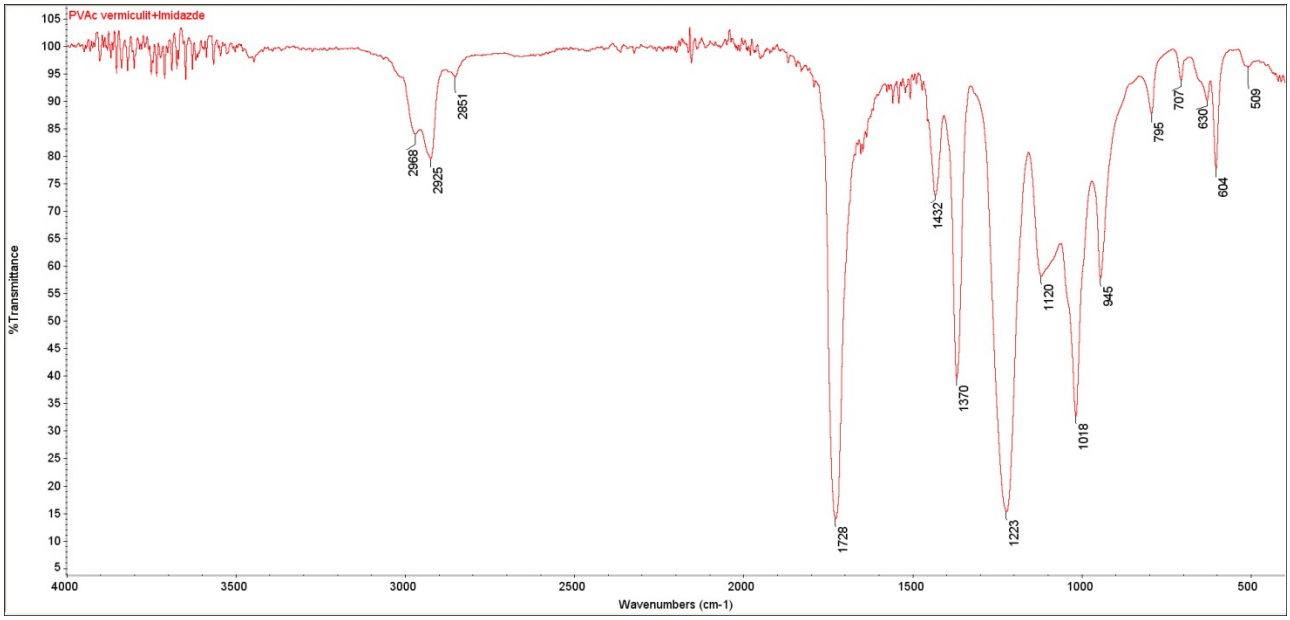

Figure 49. FTIR spectrum of PVAc + vermiculite + imidazole sample

Characteristics bands of PVAc: C-H vibrations 2974 (asymmetric $-CH_3$), 2926 (asymmetric $-CH_2$), and 2852 cm^{-1}(symmetric $-CH_2$), esters C=O at 1728 cm^{-1}, 1222 and 1121 cm^{-1} C-O-C stretching vibrations and 1018 cm^{-1} CH-O vibrations, C-H deformation vibration at 1428 ($-CH_3$), 1370 ($-CH_3$), 945 ($C-CH_3$), and 706 cm^{-1}.

The band at 1560 cm^{-1} could be caused by degradation of PVAc and may correspond to the aromatic C-H vibrations. Very intensive band at 3379 cm^{-1} corresponds to the O-H vibrations. It's visible from the graphs that after the stability testing water is appearing on the 3500-3000 cm^{-1}, the peaks on the right became slightly shorter because of crystalline degradation and on 1638 cm^{-1} the water presence is visible. (Fig. 49)

STABILITY TESTING

Next step of experiment was to simulate the human liquids and their influence at polymeric film. For the first simple simulation it was decided to use Acetic acid (CH_3COOH) with different pH (5.1; 6.1; 7.0; 8.5; 9.8). The polymeric film was cut into small pieces and placed to the acetic acid

solutions. After couple of hours, it was dried out on 125℃. Some films had deformation but after repeating the experiment the film stayed holistic. After all, 45 unstrained samples were obtained. To make the analysis faster only higher pH samples were analysed on FT IR.

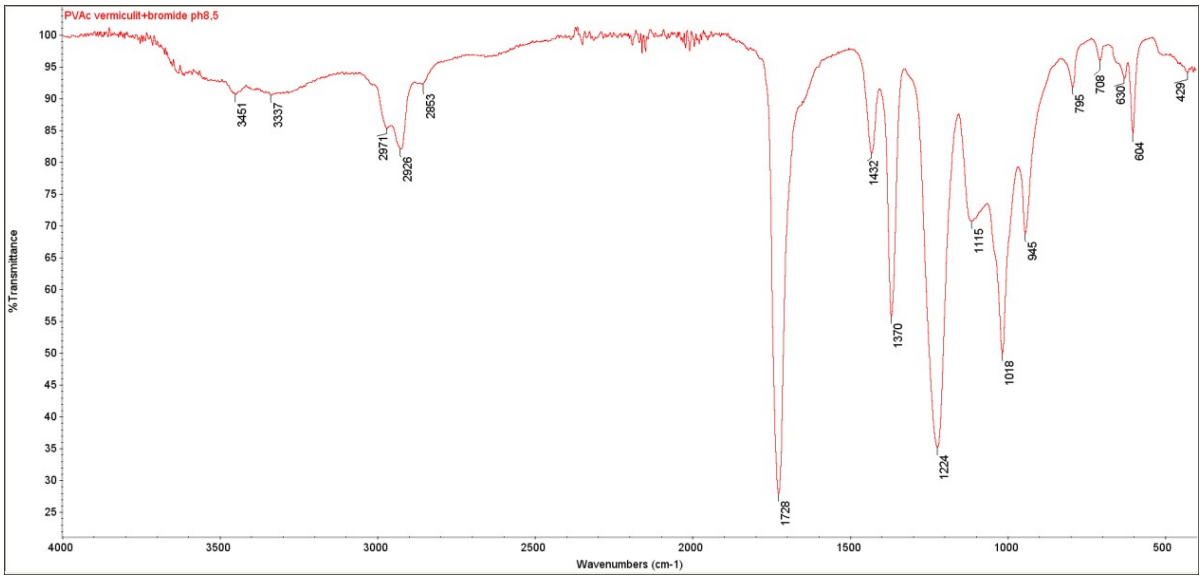

Figure 50. FTIR spectrum of PVAc + VMT + bro after stability testing at pH8.5.

Stability testing and changes observation had two levels. One was observation of changes in clay part of nanocomposite and second was the organic modification.
From the Fig. 50 and 51 we can observe slight changes in case of water content, which might be related to higher hydrophilicity of vermiculite regarding to modifying organic matter for the individual cases.
We can state here that PVAc nanocomposite will be more stable at pH 8.5 and modified with VMT + phosphonium cation.

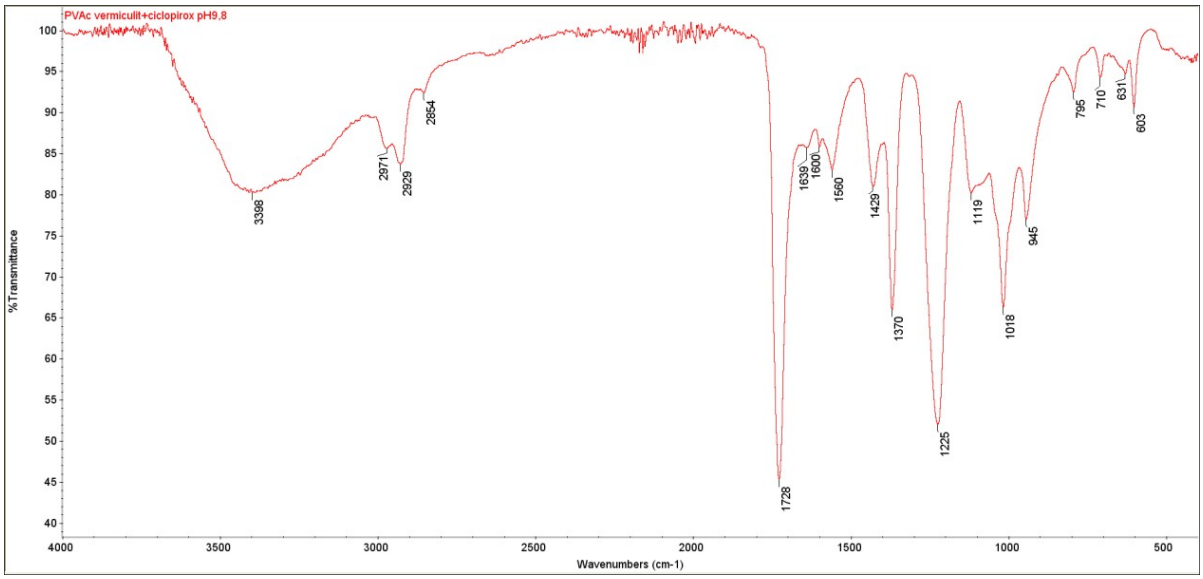

Figure 51. FTIR spectrum of PVAc + VMT + ciclo after stability testing at pH9.8.

Following comparison of PVAc with MMT and bentonite modified with ciclopyrox olamine (Fig. 52 and 53) is showing the difference in water content (band 3400 cm $^{-1}$) and small deviations in organic matter (band 842 and 646 cm^{-1}). Both changes are happening in case of bentonite, therefore we can presume lower stability of PVAc nanocomposite.

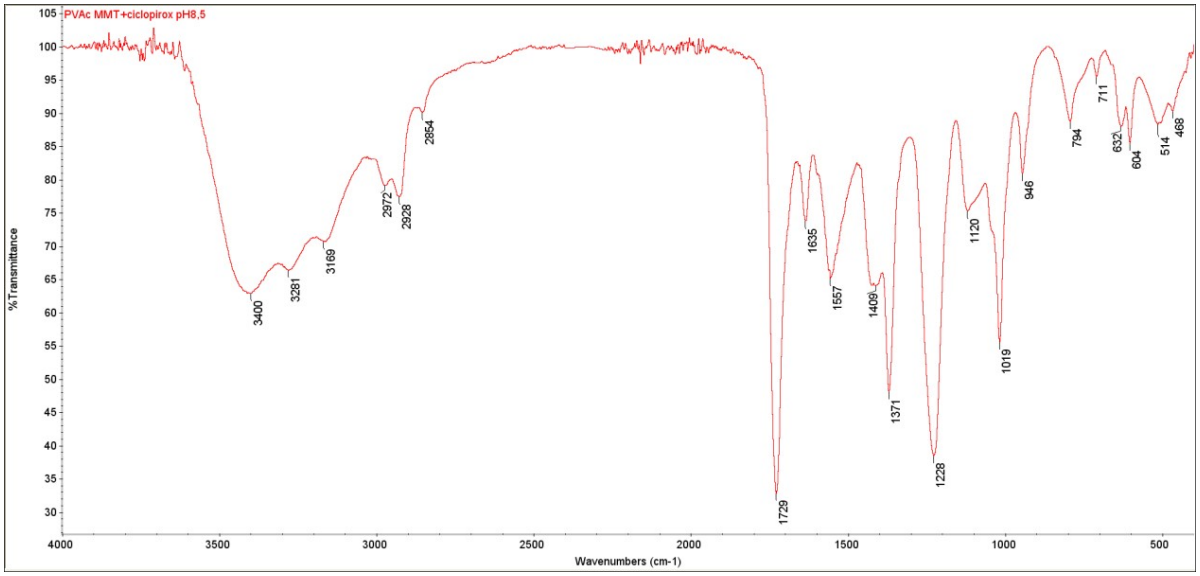

Figure 52. FTIR spectrum of PVAc + MMT + ciclo, after stability testing at pH8.5.

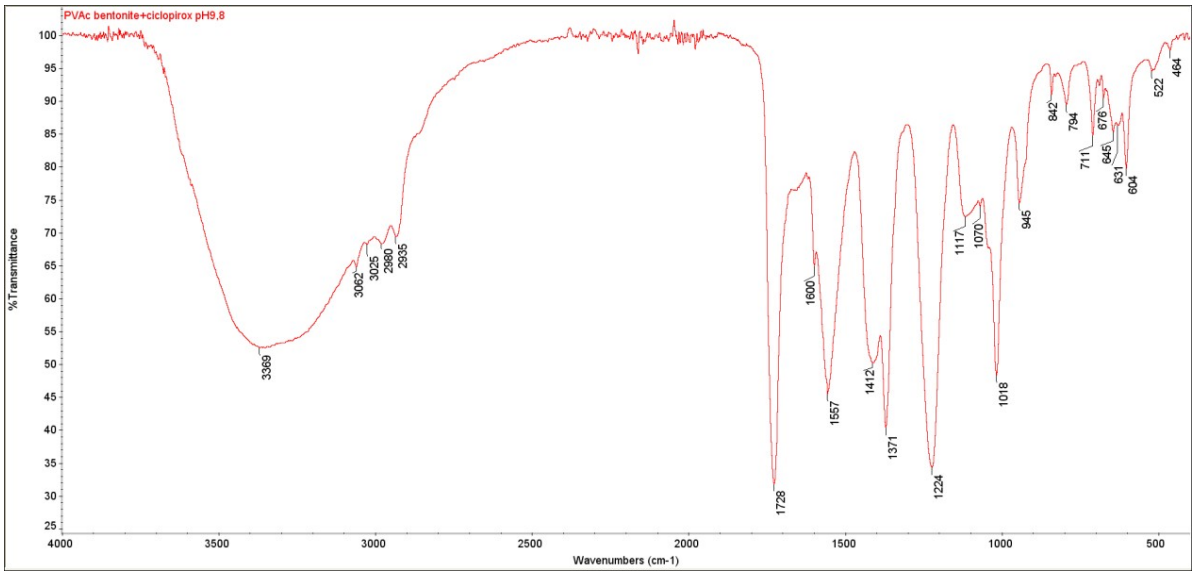

Figure 53. FTIR spectrum of PVAc + BEN + ciclo, after stability testing at pH9.8.

Last selected comparison is the most important, because it compares the sample before and after stability testing. The example was chosen so the highly water sensitive sample with

montmorillonite for the reason to observe the most visible changes during FTIR measurement. The spectrum on the Fig. 54 look different, the way how the sample after testing is broadened predicts the disruption of integrity of the nanocomposite. The broad band of water 3401 cm $^{-1}$, that was not observable in original sample before testing is causing the lower intensities of other bands of the clay and organic matter as well. The organic matter bands are not changing the positions much but they are becoming less intensive.

Generally we found that stability testing for PVAc based nanocomposites provides information about small changes in the structure and bonding interactions evaluated using FTIR spectroscopy methods. From this point of view we can consider the polymeric nanocomposite films stable.

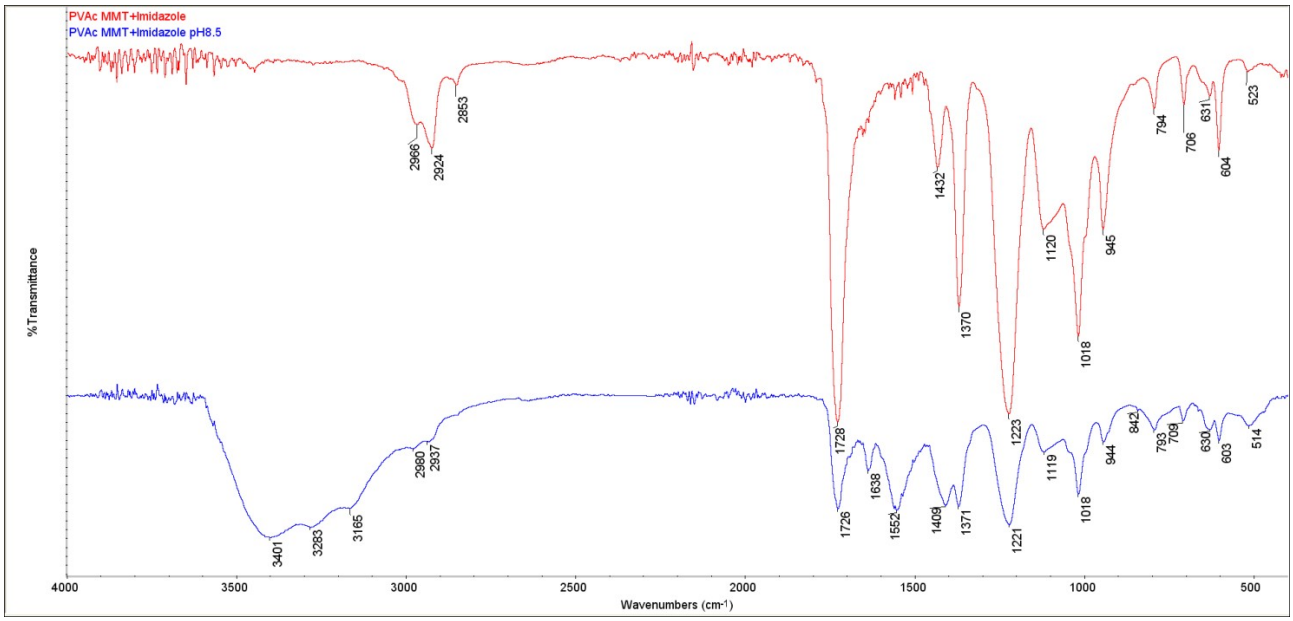

Figure 54 . Comparison of spectra PVAc + Montmorillonite + Imidazole and PVAc + Montmorillonite + Imidazole (pH 8.5).

As a special technique for observation of individual phases dispergation FTIR microscopy was selected (Fig. 55), with possibility to observe an area of sample in size of 500 x 500 microns of obtained spectra from selected points. Different colours in the map are showing related information regarding the spectrum below the map. The rule is: the more red in the scale, the better fitting phase.

Polyvinyl acetate the red spectrum was selected as a phase for comparison, therefore the areas appearing red are the best fit to the reference spectrum. The areas in yellow are still partially

fitting the polymer but vary in certain bands. The least fitting areas are blue..
The presumption is that purely red areas are only PVAc and purely blue areas are inorganic, therefore related to clay particles. The other areas are their interfaces.
The measured map is showing well organized nanocomposite where individual phases are not mixed and are identifiable as individual, then there is some interfacial matter connecting the components of nanocomposite. The components distribution is good and the nanocomposite then can be considered as homogenous.

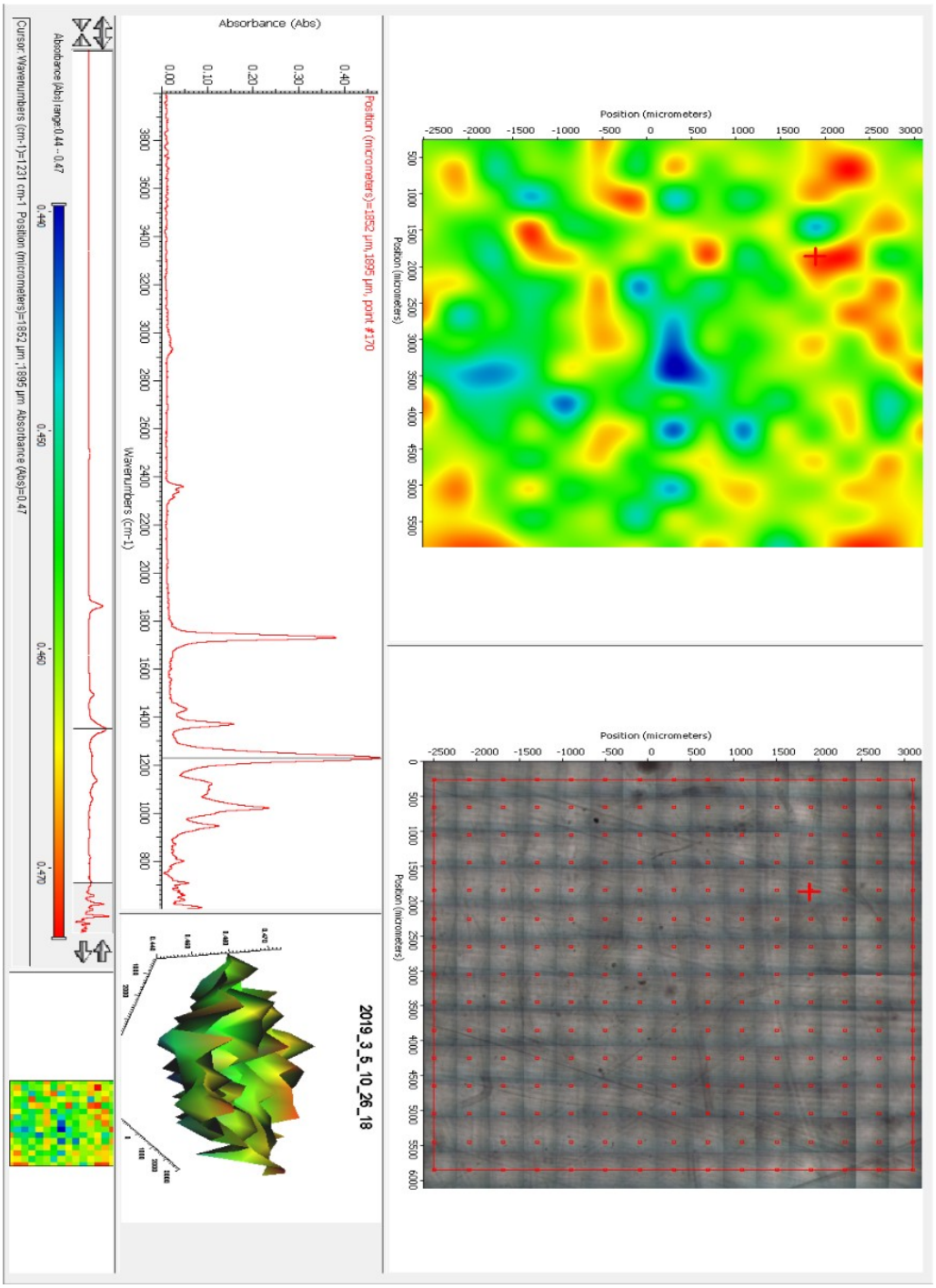

Figure 55. FTIR microscopy mapping of PVAc + VMT-ciclo sample.

3.2.3. THERMAL BEHAVIOUR

Thermal behaviour of prepared polymeric nanofilms was studied using DSC methods.

These methods allow to understand the gentle changes in the selected range of temperatures.

For the purpose of human medicine application the range from -20°C to 400°C was selected.

As first for observation we selected PEO based nanocomposites sample to see the effect of nanofiller in low temperature up to 50° C. We found that the highest number of changes is taking place in range from 10 to 40°C. Each modifying agent had different effect e.g. bentonite with imidazole was reacting soon at about 23°C while pure montmorillonite only at 32° C. Generally non-modified fillers have changes around 30°C, but modified clays are starting thermal changes sooner. These changes are related to the decomposition of PEO.

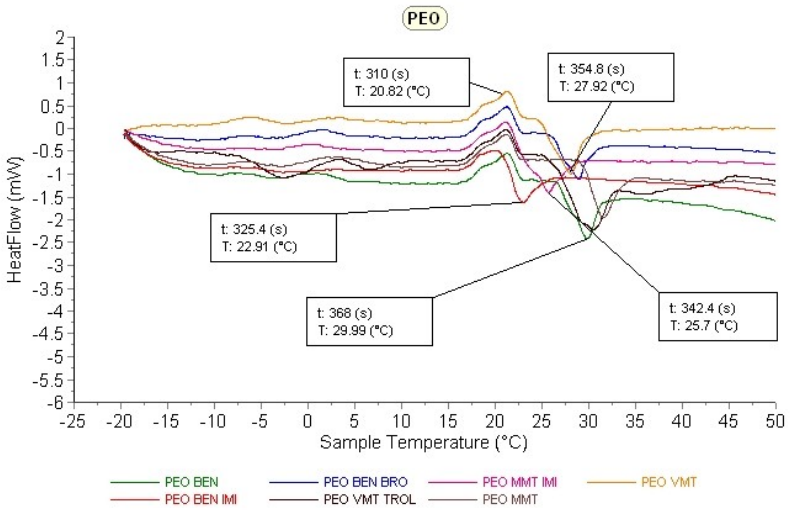

Figure 56. DSC spectra of samples PEO nanocomposites , range -20 to 50°C.

Second part of the analysed spectra is showing uniform changes (Fig. 57) regarding to temperature. There are differences in power of endothermic decomposition, pure vermiculite filler is the least active.

The higher temperature changes are not mentioned because there was no reaction observed.

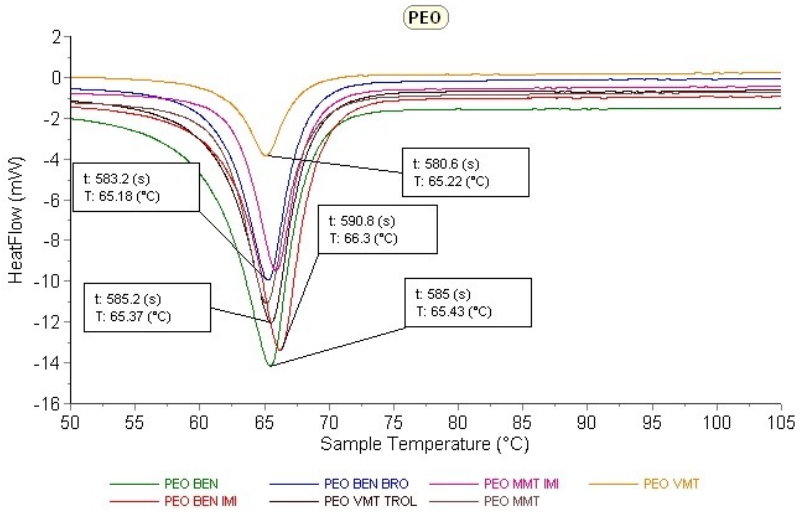

Figure 57. DSC spectra of samples PEO nanocomposites, range 50 to 100°C.

Next analysed polymer was PVAc (Fig. 58) where the changes are taking place up to 350 °C. Most variable are samples up to 75°C and later at 135°C melting peak is appearing. Decomposition temperature is starting from 320°C intensively for sample with VMT ciclo and least performing for bentonite with imidazole.

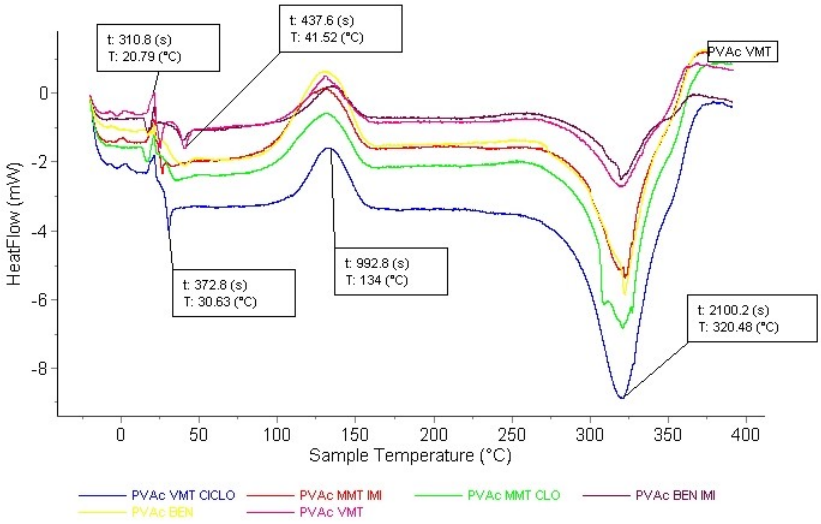

Figure 58. DSC spectra of samples PVAc nanocomposites, range -20 to 400°C.

Observing detail of the DSC spectra in range from -20 – 100°C (Fig. 59), we can see exo- and endothermal changes of evaporation at 20°C and oxidation starting at 25°C. Mild reaction is performing in MMT with clotrimazole while the most intensive changes are reported in VMT + ciclo nanofiller.

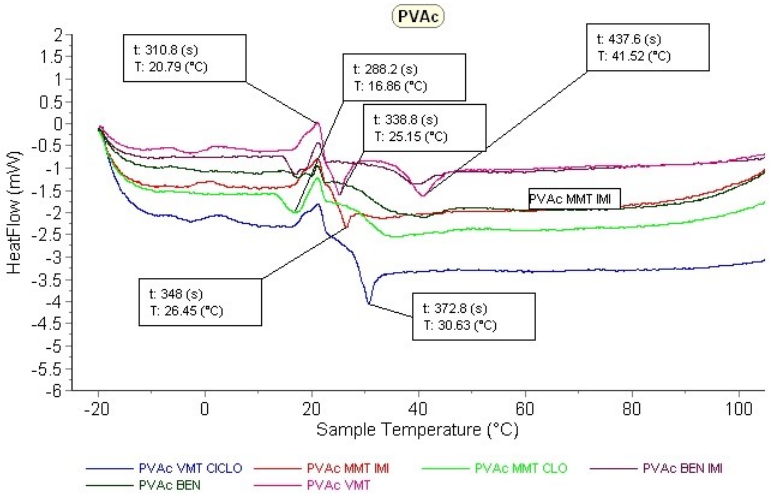

Figure 59. DSC spectra of samples PVAc nanocomposites, range -20 to 400°C.

Last analysed polymeric nanocomposite films were those based on polyvinyl alcohol.

The range of observable changes was selected from -20 to 100°C where the changes are evaluable. First exothermal changes are observable at 20°C when the endothermal effect of oxidation starts to reach the maximum for some samples at the 25°C (pure non-modified clays) to temperature 31°C (MMT-IMI, BEN-IMI). The endothermal decomposition takes place place at around 51°C, where the least observable is pure VMT and most visible is pure bentonite.

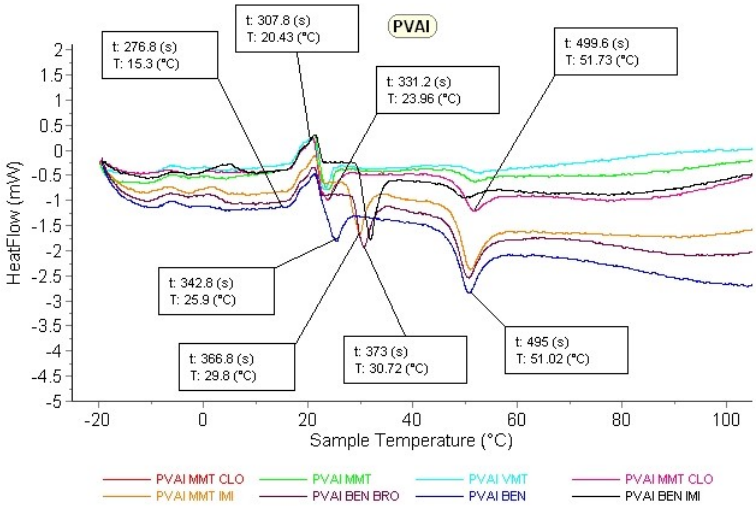

Figure 60. DSC spectra of samples PVAl nanocomposites, range -20 to 100°C.

Generally the DSC analysis exposed the fact that organic modification changes the thermal properties of polymeric nanocomposite along with the oxidation and decomposition temperature,

which is very important for further applications.

3.3. MORPHOLOGY CHARACTERIZATION AND DISCUSSION

3.3.1. LIGHT MICROSCOPY OBSERVATION

The light microscopy techniques are used here in two modes. First, the reflection mode, is to provide information about the surface conditions and to observe artefacts or anomalies of the process. Second mode is transmission mode, when the source light is going through the sample and the image shows the objects in the bulk of the sample if the matrix is transparent for the light. For our purpose transmission mode was applied to explore distribution of filler in matrix.

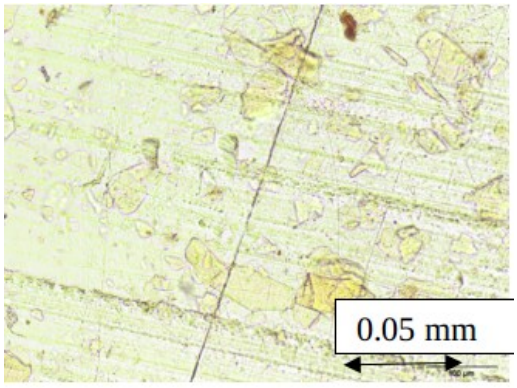

Figure 61. LM image PVAc + Vermiculite + Ciclopirox olamine Bright Field, transmission mode.

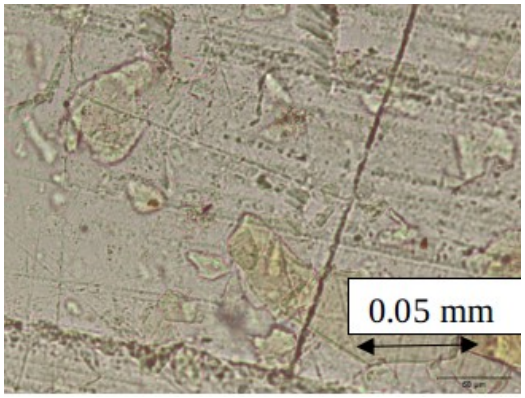

Figure 62. LM image PVAc + Vermiculte + Cicloprox olamine Dark Field, transmission mode.

Two representative samples are given (Fig.61 and 62) to show that particles are distributed over the matrix but size and thickness is various. For the purpose of substrate as drug and antibacterial carrier such condition of filler distribution is sufficient.

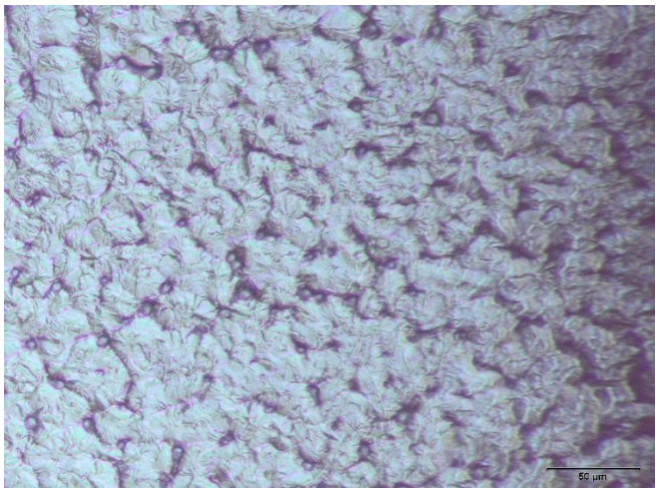

Figure 63. LM image of PEO + MMT + IMI in dark field, reflection mode

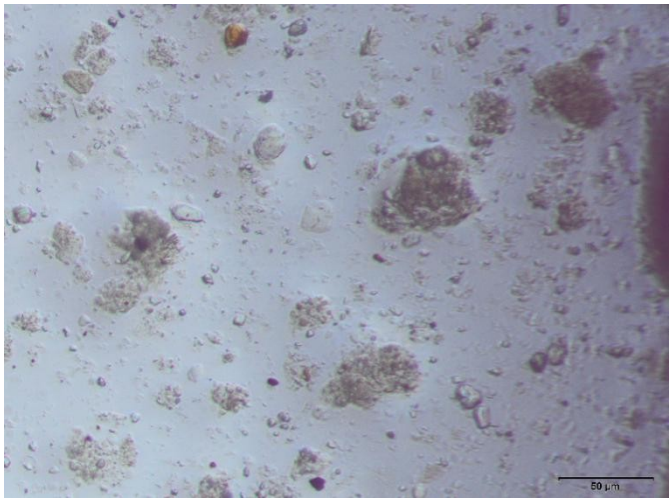

Figure 64. LM image of PVAc + MMT + imi , dark field , reflection mode

In the figures 63 and 64 we used reflection mode to observe condition of the surface. We found that sample of nanocomposites based on PEO and PVAc are very different. It is caused by the methods of preparation but also the type of the polymer. We can see 3D effect of the surface , where the PEO surface is much rougher than PVAc one. Both samples have very uniform distribution of visible nanofiller particles.

3.3.2. Atomic Force Microscopy

The atomic force microscopy is suitable tool to provide information from surface such as way of nano filler distribution in matrix or submicroscopic destruction of polymeric film. Selected samples of film were scanned for morphology of the surface. There was found rather regular distribution of clay particles along the film and no disruption of continuity of film after stability testing (Fig.65 and Fig.66).

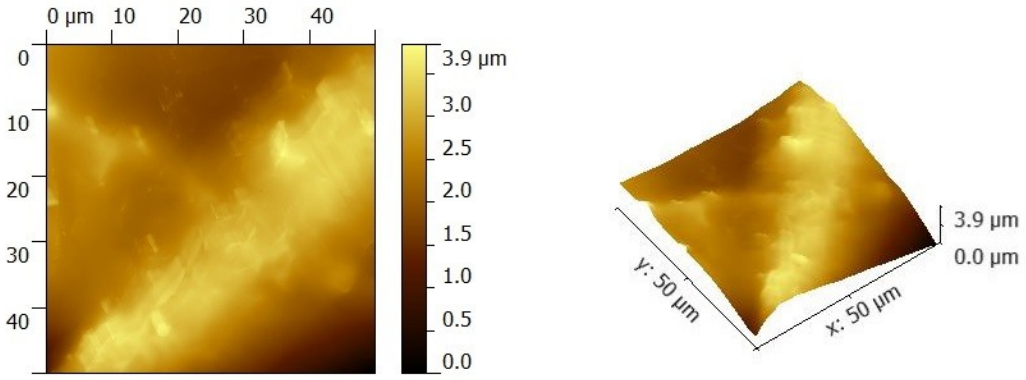

PVAc+VERM_ciclo_pure

Figure 65. PVAc + Vermiculite/Ciclopirox olamine.

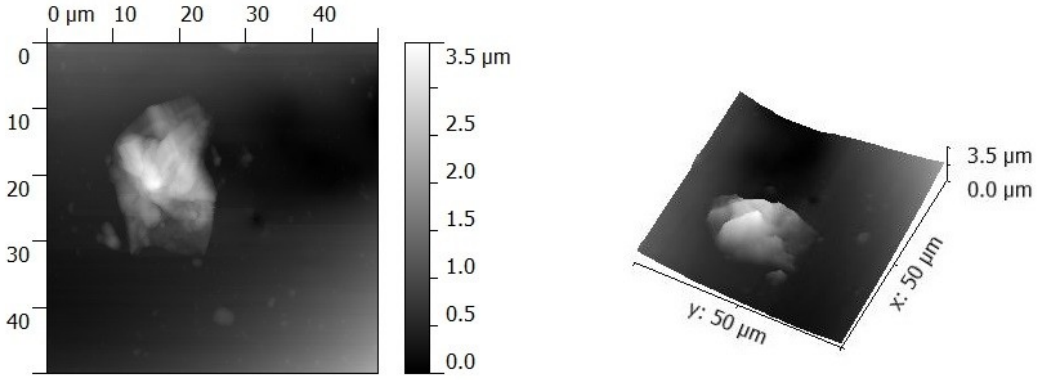

PVAc+VERM_imid_pure

Figure 66. PVAc + Vermiculite/Imidazole.

3.3.3. Scanning Electron Microscopy (SEM)

SEM methods were used to observe nanofiller morphology and size of the particles.
The organoclays prepared from vermiculites are exposing the exfoliated particles with visible layered structure (Fig. 67-68). The nanoparticles were observed using 2 detectors and the back scattered detectors -BSE- the particles being compact without extra matter (e.g. organic matter) on the surface.

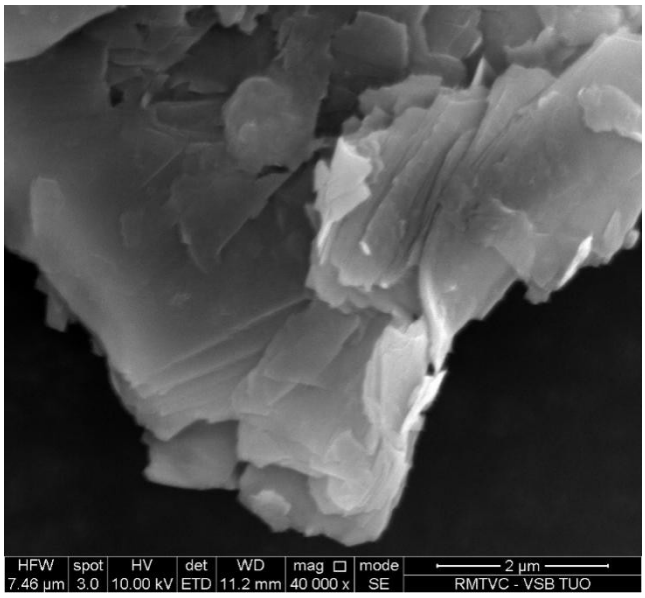

Figure 67. SEM image of organovermiculite VMT + ciclo acquired with SE detector.

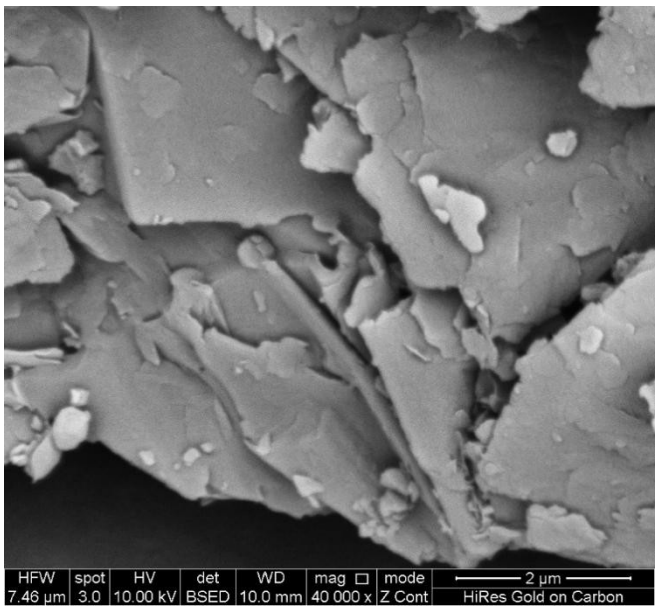

Figure 68. SEM image of organovermiculite VMT + ciclo acquired with BSE detector.

Comparing bentonite particles (Fig. 69) to the vermiculite particles we can see a very different morphology. Particles are compact without layered character. They appear to be covered with smaller particles or other matter and they look agglomerated and larger.

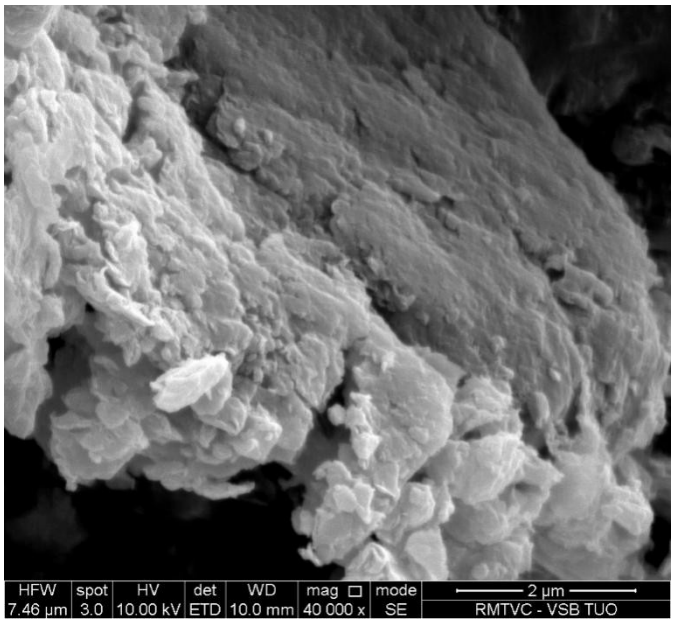

Figure 69. SEM image of organobentonite ben ciclo acquired with SE detector.

Similar situation seems to be in case of montmorillonite with imidazole. Particles are less agglomerated than in case of bentonite but still hardly visible layered character presents large particle more then 5 microns.

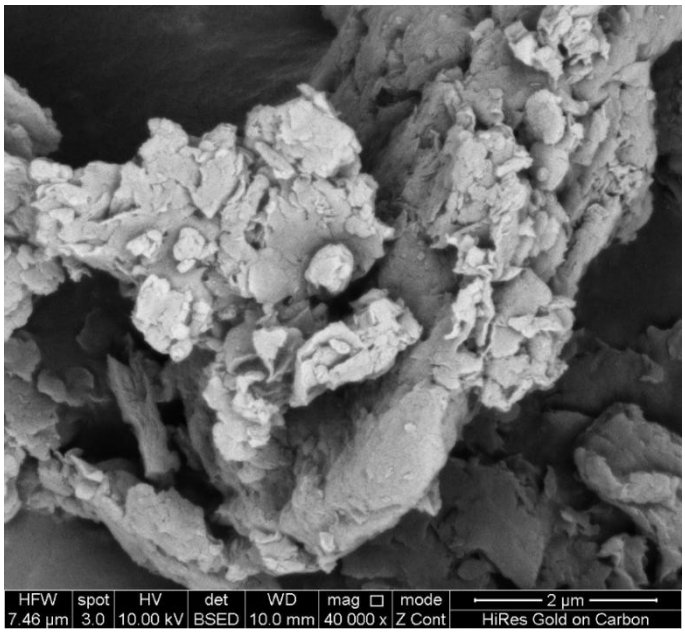

Figure 70. SEM image of MMT -imidazole particle acquired with SE detector.

To evaluate morphology of the film SEM was used. It was found that particles of clays are generally embedded into polymeric matrix and they have various micrometric sizes. The elemental analysis is also presented according to chosen point on the SEM image. It shows the presence of organoclay nanoparticles in the polymeric matrix. Some of polymeric films are partially disrupted due to preparation technique, where small grows are visible on surface (Fig.71). Disruption also took

place while the beam was intense on a not enough stable sample, it left small holes in some of polymeric samples. (Fig. 72).

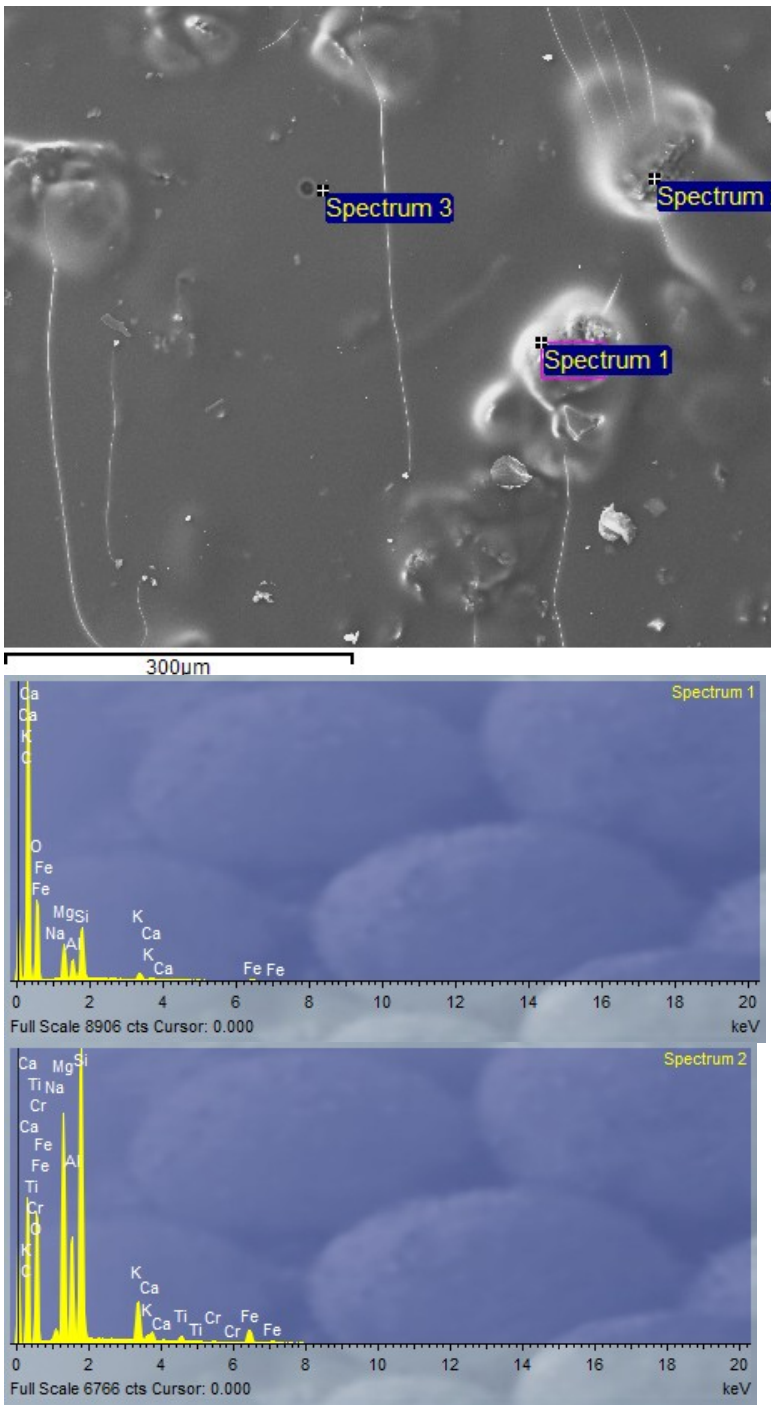

Figure 71. SEM of PVAc VMT trol sample with elemental analysis.

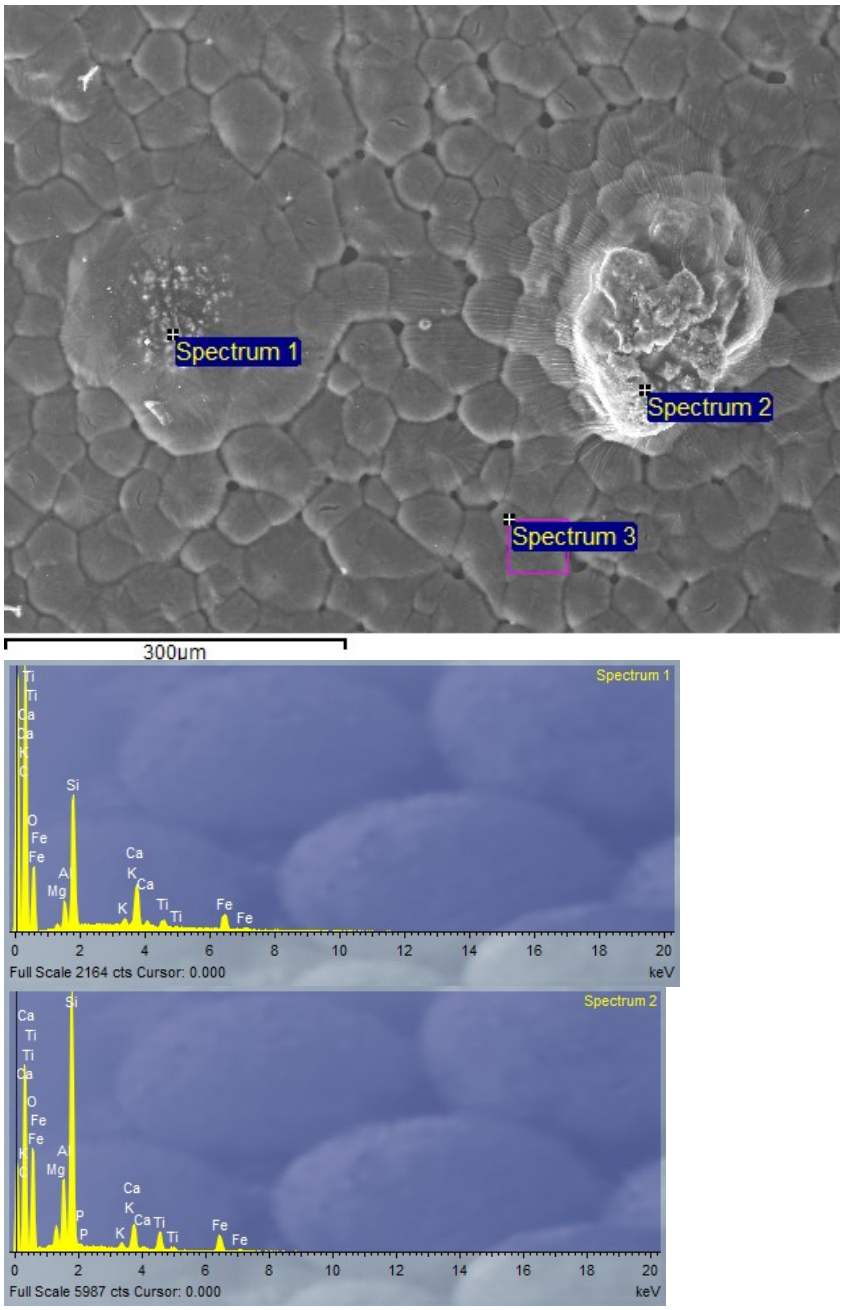

Figure 72. SEM of PEO MMT ciclo sample with elemental analysis.

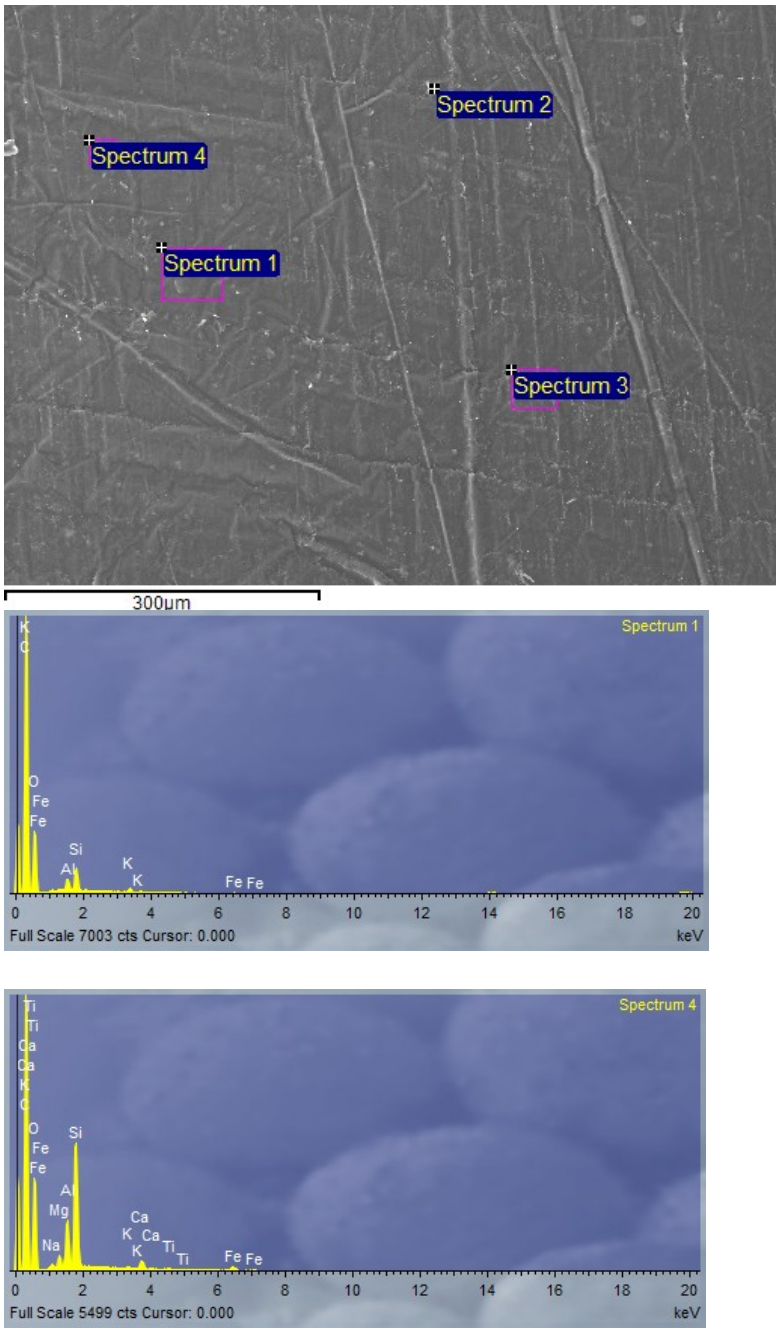

Figure 73. SEM of PVAc bent ciclo sample with elemental analysis.

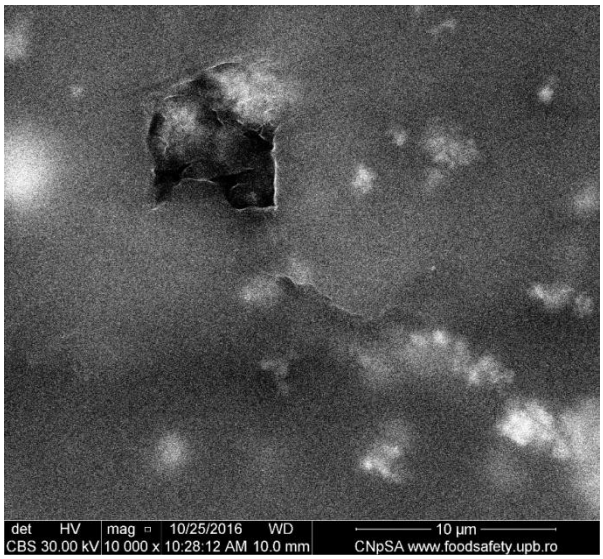

Figure 74. Detail of polymeric surface with VMT particle using SEM.

In the detailed image of polymeric surface (Fig.74) we can observe the various types of incorporation of the nanofillers to the matrix. Not all particles are inside the polymer and some of them are not covered with it. This might be beneficial for antimicrobial activity and further application since the exposed surface of particles is most active and gradual uncovering immersed particles will provide long term functional surface

In the Fig.75 we can observe relatively rough and lamellar surface of PVAc nanocomposite. This could be cause by casting method of preparation of such polymeric nanocomposite. The nanofiller particles are also visible as lighter below the lamellas. Such surface provides nanostructured morphology – individual lamellas can be estimated as submicron wide, and can play a role in antimicrobial activity as patterned surface.

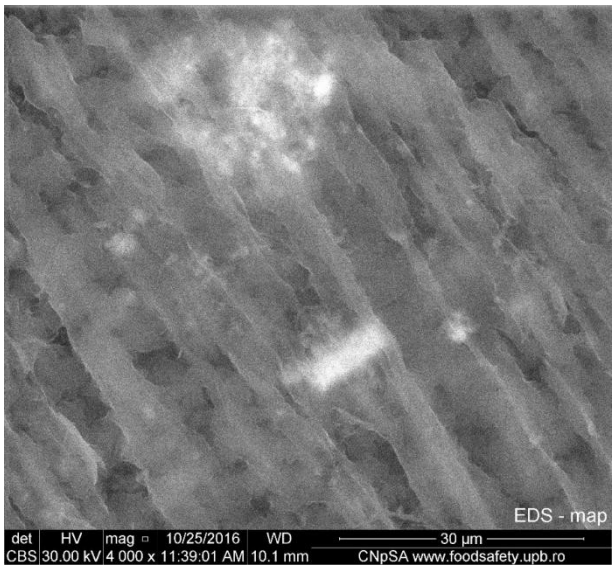

Figure 75. Detail of PVAc nanocomposite surface – the morphology after casting method.

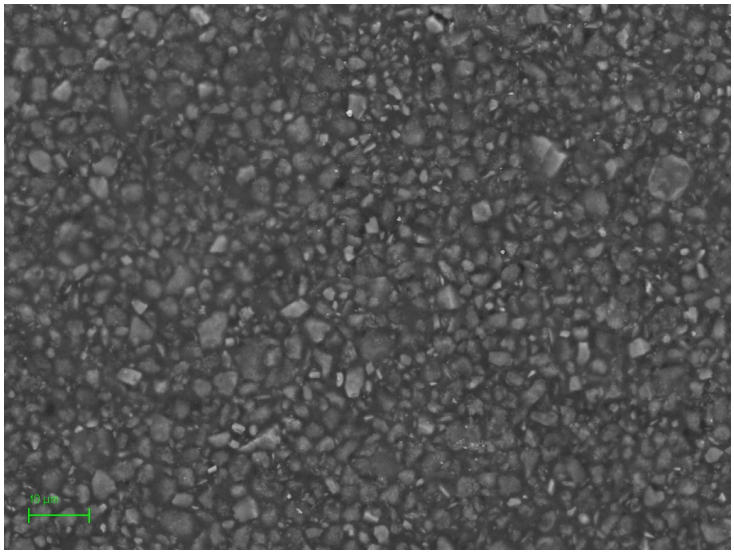

Figure 76. Image of SEM of PVAl + MMT + ciclo 2.5Kx surface.

This image can be compared to the one of LM (Fig.63), where uneven surface was observed. SEM revealed the granular-like morphology.

3.4. ANTIMICROBIAL TESTING

Further analysis was about proving the antimicrobial properties of obtained polymeric nanocomposites. For that purpose several microbiological procedures with the bacteria related to bile duct microflora were done.

Commercial solid Műller-Hinton and Schaedler agar plates for the cultivation of bacteria without any additional modifications were used.

Staphylococcus aureus 3953, *Enterococcus faecalis* 4224 and *Pseudomonas aeruginosa* 1960 were acquired from the Czech Collection of Microorganisms (Czech Republic). *Clostridium difficilae* was isolated from an incognito patient at the hospital in Ostrava.

Incubation of bacteria was conducted in Biological thermostat BT 120M at 37°C. Incubation of *C. difficilae* was conducted in Whitley A35 anaerobic workstation (Don Whitley Scientific) at 37°C under anaerobic conditions.

Agar plates were inoculated with bacterial strains. Squares of samples (approx. 1 cm^2) were placed on the inoculated plates and incubated. After 24 hours visual evaluation was performed. This experimental setup is based on disc diffusion test which is commonly used for test with antibiotics. In this case diffusion of active substance (nanocomposite filler) was not occurred and therefore zones of inhibition are not as evident as in case of disc diffusion test and thus cannot be measured. Antibacterial effect of tested materials it is thus limited to the immediate surroundings.

	Bact.strain / Sample	S.aureus	E.faecalis	E.coli	P.auruginosa	C.difficilae
1	MMT + bro	++	+	-	-	+
2	MMT + imi	++	+	-	-	+
3	MMT + ciclo	++	+	-	-	+
4	BEN + bro	++	+	-	-	++
5	BEN + imi	++	+	-	-	+
6	BEN + ciclo	++	+	-	-	+
7	VMT+ bro	++	-	-	-	+
8	VMT + imi	++	-	-	-	+
9	VMT + ciclo	++	-	-	-	+

Table 7. ++ - “strong” antibacterial activity, + - antibacterial activity, - no-antibacterial activity.

3.4.1 Antimicrobial testing of 36 polymeric nanocomposites.

36 different nanocomposites were prepared, see Table 8.

Polyvinyl acetate	**Polyvinyl alcohol**	**Polyethylene oxide**
BEN + imi	BEN + imi	BEN + imi
BEN + ciclo	BEN + ciclo	BEN + ciclo
BEN + bro	BEN + bro	BEN + bro
VMT + ciclo	VMT + ciclo	VMT + ciclo
VMT + trol	VMT + trol	VMT + trol
VMT + clo	VMT + clo	VMT + clo
MMT + clo	MMT + clo	MMT + clo
MMT + imi	MMT + imi	MMT + imi
MMT + ciclo	MMT + ciclo	MMT + ciclo
MMT	MMT	MMT
VMT	VMT	VMT
BEN	BEN	BEN

Table 8. Prepared samples, see the abbreviations in Table 7.

Preparation of media:
“Sobrecapa” (overlayer)

Destilled water	250 ml
Dibasic phosphate	2.5 g
Monobasic phosphate	1 g
Agar	2 g
Brain heart infusion (BHI)	3.75 g

BHAT

Destilled water	250 ml
Dibasic phosphate	2.5 g
Monobasic phosphate	1.075 g
Agar	4.25 g
BHI	9.25 g

Two solutions were prepared, the overlayer solution was put to a microwave until boiling. After microwave the solution had to be moved to glass test-tubes, 6 ml each tube, closed with test-tube caps and moved to autoclave for 15 minutes on 121°C together with the BHAT solution.
After autoclave BHAT was moved to water bath to cool down to 55°C and then the liquid was rapidly poured to Petri dishes, which were closed overnight on 37°C.

The overlayer method showed following results (Table 9):

Polyvinyl alcohol	*Staphylococcus aureus*	*Enterococcus (S47)*	*Escherichia coli*
MMT + clo	++	-	-
MMT + imi	++	-	-
MMT + ciclo	++	-	+
MMT	-	-	-

Polyvinyl acetate	*Staphylococcus aureus*	*Enterococcus (S47)*	*Escherichia coli*
MMT + clo	+	-	+
MMT + imi	+	-	-
MMT + ciclo	-	-	-
MMT	+	-	-

Polyethylene oxide	*Staphylococcus aureus*	*Enterococcus (S47)*	*Escherichia coli*
MMT + clo	+++	-	-
MMT + imi	-	-	-
MMT + ciclo	+++	++	++
MMT	-	-	-

Table 9. Overlayer method antimicrobial ativity on different samples.
+++ - high inhibition
++ - good inhibition
+ - small inhibition
- - no inhibition

The streaking method:

Polyvinyl acetate	*Staphylococcus aureus*	*Enterococcus (S47)*	*Escherichia coli*
Bent + ciclo	+	-	-
VMT + ciclo	+	-	-
MMT + ciclo	+-	-	-
MMT	+	-	-

Table 10. The inhibition of various polymeric nanocomposite samples via streaking method.

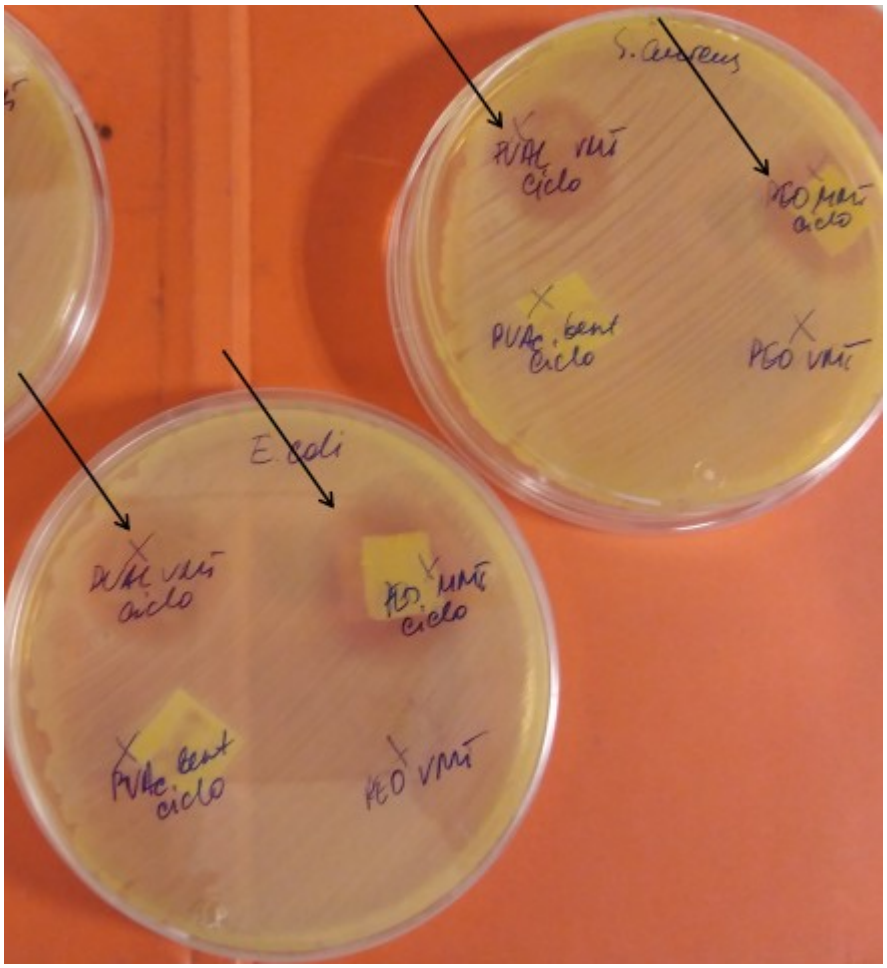

Figure 77. The visible inhibition on a Petri dish.

3.4.2 Bile salts simulation

In parallel we tried to perform bile salts based medium to try to grow the bacteria in human-like gastrointestinal conditions.

To obtain the pH 3.0 and pH 2.0 in 150ml BHI we used Chlorhydric acid (37% HCl). The agar did not

solidify.
So we decided to replace HCl with citric buffer. For 200ml 6.02 g of Sodium Citrate and 0.867 g of citric acid. We used this buffer instead of destilled water for the medium (BHbroth 3.7 g, agar 1.8 g, 100ml pH 2 buffer; BHbroth 3.7 g, agar 1.8 g, 100ml pH 3 buffer).

To see if bacteria will grow on such medium we prepared 4 Petri dishes - 2 with 1.8% BHI bile salts and 2 with 3.6% bile salts. Next day all 4 plates were with grown bacteria on it.

Bact. strain Sample	*Staphylococcus aureus*		*Enterococcus* (S47)		*Escherichia coli*	
PEO VMT ciclo	+++	+++	+++	++	+++	+++
PVAc MMT ciclo	+-	+-	-	-	-	-
PVAl bent ciclo	+++	+++	+++	++	+++	+++
PVAl bent	-	-	-	-	-	-
The concentration of bile salts in the BHI	1.8% bile salts	3.6% bile salts	1.8% bile salts	3.6% bile salts	1.8% bile salts	3.6% bile salts

Bact. strain Sample	*Staphylococcus aureus*		*Enterococcus* (S47)		*Escherichia coli*	
PVAl VMT ciclo	+++	+++	+++	+	+++	+
PEO MMT ciclo	+++	+++	+++	+++	+++	+++
PVAc bent ciclo	+-	+-	-	-	-	+-
PEO VMT	-	-	-	-	-	-
The concentration of bile salts in the BHI	1.8% bile salts	3.6% bile salts	1.8% bile salts	3.6% bile salts	1.8% bile salts	3.6% bile salts

Bact. strain Sample	*Staphylococcus aureus*		*Enterococcus* (S47)		*Escherichia coli*	
PVAc VMT ciclo	+-	+-	-	-	-	-
PVAl MMT ciclo	+++	+++	+++	++	+++	++
PEO bent ciclo	+++	+++	+++	+++	+++	+++
PVAc MMT	+-	+-	-	-	-	-
The concentration of bile salts in the BHI	1.8% bile salts	3.6% bile salts	1.8% bile salts	3.6% bile salts	1.8% bile salts	3.6% bile salts

Table 11. Antimicrobial activity in the bile salts experiment.

3.4.3. BIOFILM FORMATION

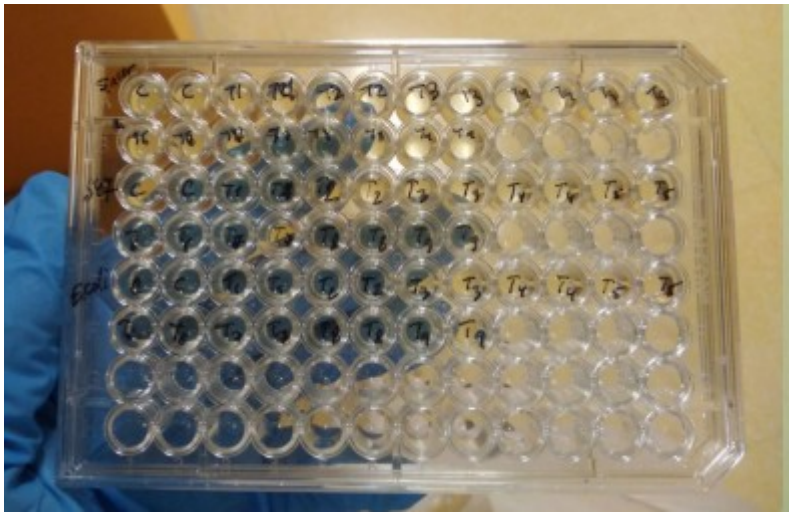

Figure 78. The microtiter well plate for growing biofilms. C - control (no sample, only biofilm), T1 - PEO VMT ciclo, T2 - PEO MMT ciclo, T3 - PEO BEN ciclo, T4 - PVAc VMT ciclo, T5 - PVAc MMT ciclo, T6 - PVAc BEN ciclo, T7 - PVAl VMT ciclo, T8 - PVAl MMT ciclo, T9 - PVAL BEN ciclo. *Note*: the wells duplicate.

For growing of biofilms the microtiter well plates were used (Fig.78). 4.9 mcL of TSB with bacteria and without bacteria were put to the wells and left overnight.

After overnight the liquid from wells was removed without disturbing of biofilm. Then it was washed with 200 mcL NaCl (0.85%) and the liquid was again removed. Then 200 mcL of Milli-Q water was poured and after that the polymeric nanocomposite thin film samples were placed to the wells. The microtiter plates went to incubate on 37°C for 1 hour.

After an hour the polymers and water are removed from wells. Wash with 200 mcL NaCl, remove. Next step is dilution. The diluted solution drops put to Petri dishes (Fig.79)

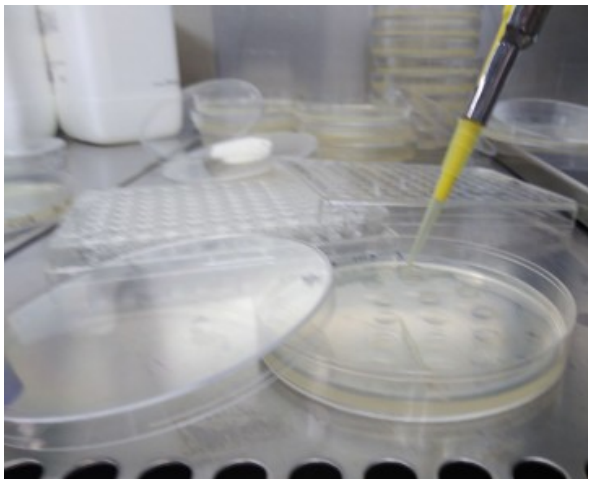

Figure 79. The dilution technique.

As visible on Fig.78. the wells duplicate, C, C, T1, T1 etc.

We used both (1) and (2) on separate plates for clear results in order to exclude the mistakes.
T1 – PEO + VMT + ciclo
T2 – PEO + MMT + ciclo
T3 – PEO + BEN + ciclo
T4 – PVAc + VMT + ciclo
T5 – PVAc + MMT + ciclo
T6 – PVAc + MMT + ciclo
T7 – PVAl + VMT + ciclo
T8 – PVAl + MMT + ciclo
T9 – PVAl + BEN + ciclo

(1) 1 hour	*S. aureus*	*S47*	*E.coli*
control	8/11/7 (-5)	1/1/3 (-5)	7/8/10 (-5)
T1	11/14/13 (-5)	20/14/7 (-4)	1/2/2 (-5)
T2	5/3/10 (-5)	12/4/7 (-5)	1/5/5 (-5)
T3	4/2/5 (-5)	2/14/8 (-4)	4/6/9 (-5)
T4	4/6/5 (-5)	10/7/6 (-5)	11/8/6 (-5)
T5	8/5/3 (-5)	10/5/7 (-5)	9/7/7 (-5)
T6	7/8/12 (-5)	4/2/2 (-4)	6/6/3 (-5)
T7	3/5/4 (-5)	4/9/1 (-4)	4/4/2 (-5)
T8	2/3/3 (-5)	8/6/5 (-4)	9/8/1 (-5)
T9	5/2/4 (-3)	14/21/16 (-4)	9/9/10 (-5)

(2) 1 hour	*S. aureus*	*S47*	*E.coli*
control	9/9/6 (-5)	4/4/5 (-5)	6/7/7 (-5)
T1	8/13/12 (-5)	4/9/9 (-5)	3/4/3 (-5)
T2	7/5/3 (-5)	8/6/10 (-4)	15/6/27 (-4)
T3	6/6/5 (-5)	7/4/5 (-5)	6/4/7 (-5)
T4	1/6/5 (-5)	17/16/13 (-4)	3/5/3 (-5)
T5	4/4/3 (-5)	7/12/8 (-4)	5/6/1 (-5)
T6	10/10/9 (-5)	6/13/10 (-4)	5/6/5 (-5)
T7	13/12/8 (-5)	17/23/17 (-4)	3/6/8 (-5)
T8	6/8/3 (-5)	10/11/13 (-4)	11/9/10 (-5)
T9	3/4/2 (-5)	19/15/18 (-4)	3/2/3 (-5)

Table 12. Dilution test results after 1 hour.

Now the same test but after 24 hours of incubation:

(1) 24 hours	*S. aureus*	*S47*	*E.coli*
control	15/17/15 (-5)	25/20/18 (-5)	9/14/12 (-5)
T1	15/15/11 (-5)	15/13/11 (-5)	24/31/27 (-4)
T2	11/17/14 (-5)	8/9/5 (-5)	12/26/19 (-4)
T3	31/40/31 (-5)	5/11/11 (-5)	10/9/13 (-5)
T4	10/17/10 (-5)	19/16/18 (-5)	18/22/25 (-5)
T5	12/8/14 (-5)	8/9/8 (-5)	17/24/17 (-5)
T6	10/12/9 (-5)	17/13/17 (-5)	9/8/4 (-5)
T7	15/19/19 (-5)	28/25/31 (-5)	14/14/19 (-5)
T8	33/27/23 (-5)	6/6/6 (-6)	24/16/23 (-5)
T9	23/31/32 (-5)	24/19/20 (-5)	14/14/8 (-5)

(2) 24 hours	*S. aureus*	*S47*	*E.coli*
control	9/17/11 (-5)	15/12/14 (-5)	13/15/8 (-5)
T1	5/5/11 (-4)	6/4/7 (-5)	4/5/5 (-4)
T2	21/33/33 (-4)	9/13/12 (-5)	4/8/5 (-4)
T3	33/47/43 (-4)	16/16/20 (-5)	11/13/14 (-5)

T4	5/11/14 (-5)	21/18/21 (-5)	15/21/15 (-5)
T5	14/13/12 (-5)	9/16/11 (-5)	8/15/15 (-5)
T6	19/22/21 (-5)	10/19/19 (-5)	30/30/27 (-5)
T7	29/27/26 (-4)	32/24/28 (-5)	4/7/4 (-6)
T8	9/11/9 (-5)	15/20/17 (-5)	19/21/25 (-5)
T9	20/24/17 (-5)	31/23/38 (-5)	7/8/6 (-5)

Table 13. Dilution test results after 24 hours.

Obtained results allow to count CFU/ml and to view it by time (Fig.80).
Colony-Forming Unit (CFU) is a unit used to estimate the number of viable bacteria or fungal cells in a sample. Viable is defined as the ability to multiply via binary fission under the controlled conditions. Counting with colony-forming units requires culturing the microbes and counts only viable cells, in contrast with microscopic examination which counts all cells, living or dead. The visual appearance of a colony in a cell culture requires significant growth, and when counting colonies it is uncertain if the colony arose from one cell or a group of cells. Expressing results as colony-forming units reflects this uncertainty.

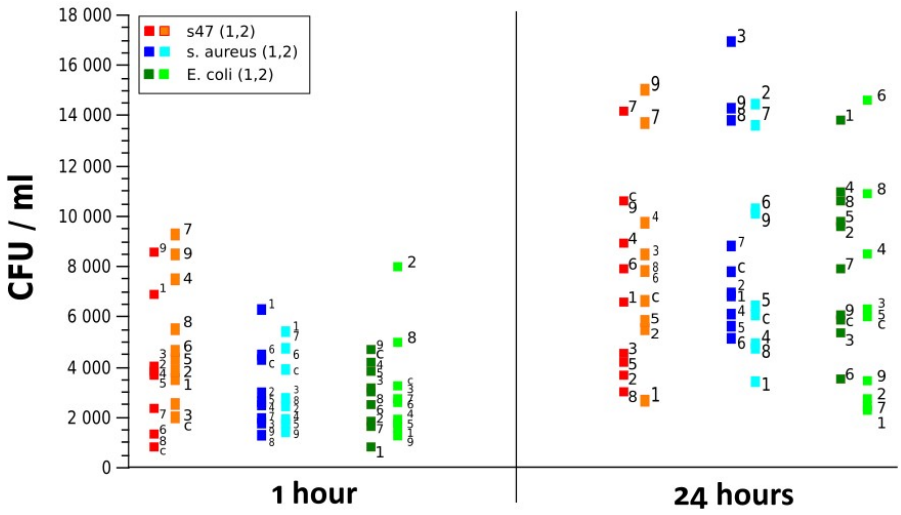

Figure 80. CFU/ml by time. Red – *S47*, blue – *S.aureus*, green – *E.coli*.

It shows how 3 different biofilms react on 9 types of samples in 1 hour and in 24 hours of inhibition. There is no visible difference between (1) and (2) duplicates, which means that the conditions were similar. As I performed this test only once, further tests are recommended to obtain full picture. Next attempt was to grow biofilm in an improved way with the liquid flow simulation to imitate the flow of bile liquids.

VIEWING OF BIOFILM GROWTH

Another way of biofilm growing simulation was performed on a non-standard equipment, which was self-assembled by Dr. Ben Johnson (Leeds). The description of the experiment and the scheme of the system (Fig.81-82) is shown below.

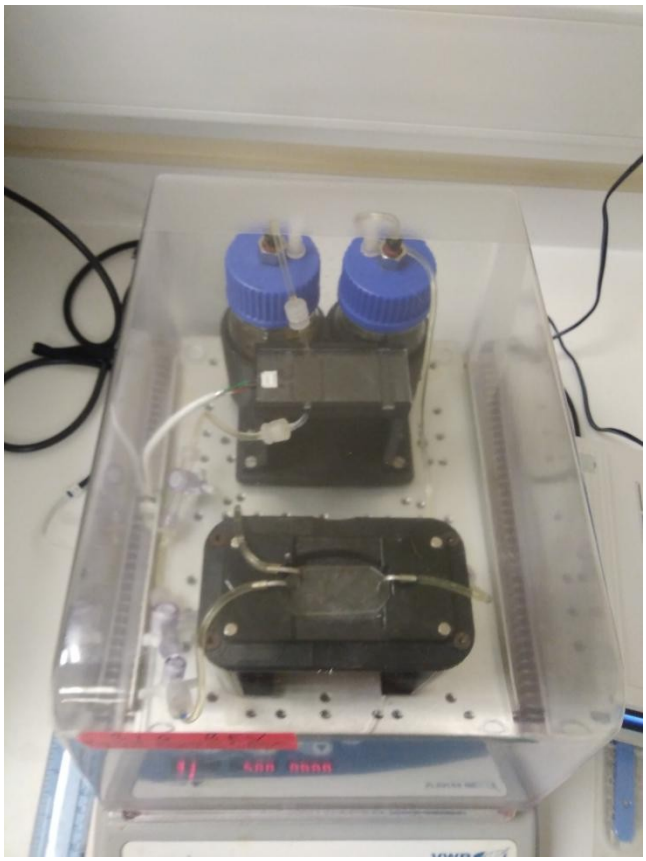

Figure 81. The improvised self-assembled by Dr. Ben Johnson biofilm growing system.

Microfluidic chip:
All microfluidic devices used are initially produced using photolithography techniques. A usable device is then produced by PDMS casting on the silicon master. The devices are then cut, hole punched, and bound to 50 × 22 mm 0.13 – 0.17 mm glass cover slips via oxygen plasma bonding.
Bacterial growth system
The full system (shown below) comprises of 2 100mL Duran bottle reservoirs, one for media and another for the effluent / waste. Each bottle is fitted with a 0.22 µm filter to allow pressure equalisation and flow through the system. Flow through the system is supplied by a single MP6 piezo pump which is controlled via an external controller, a flow rate of 50 µL / min is used to mimic *in vivo* flow rates.

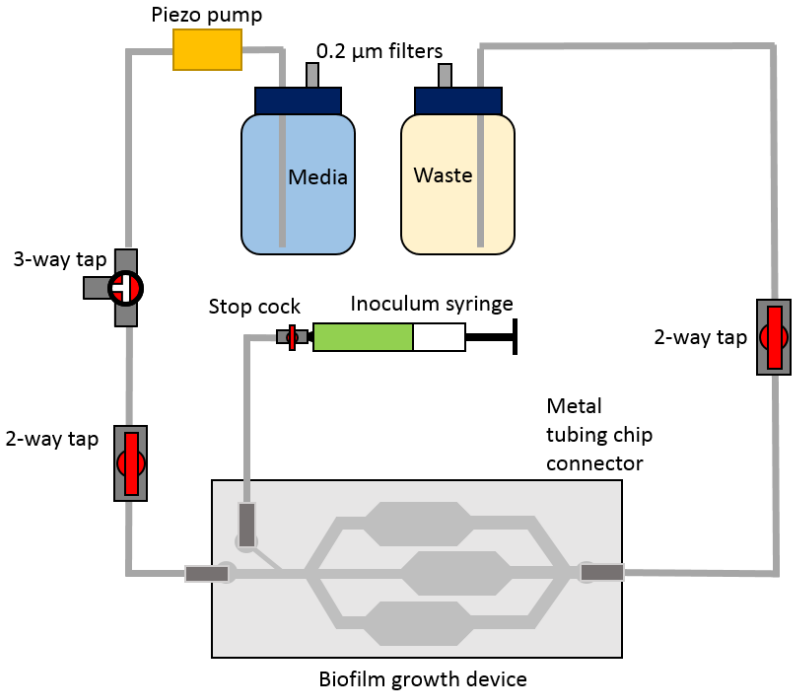

Figure 82. Biofilm growth system scheme.

The tubing directly into and out of the pump has an internal diameter of 1.3 mm, with all other tubing sections measuring 1.6 mm ID, luer lock male / female fittings are used throughout to connect parts. Inoculation is performed using a 1 mL syringe via a stop cock which automatically shuts off to avoid back-flow or leakages.

Standard Operating Procedure

1. Stock culture preparation
    a. Autoclave (250 - 500 mL) of BHI broth and allow to cool to room temperature.
    b. Check growth on primary plate culture is pure based on colony morphology
    c. If no evidence of contamination exists on the primary culture plate, touch three separate colonies of test bacteria a sterile disposable loop and inoculate 100mL of BHI broth, incubate this at 37°C overnight, simultaneously inoculate an LB-agar plate to check sterility of the broth culture.
    d. Using bacterial broth, produce 100 x 1mL aliquots, flash freeze, and store at -80°C freezer for future use.

2. Leak check and sterilisation
    a. All apparatus is autoclaved, movable parts (2- and 3-way valves, stop cocks) are soaked in 70% ethanol.
    b. All autoclaved apparatus is transported to a category II safety cabinet and irradiated with UV light for 30 minutes.
    c. Within the safety cabinet, the whole system is assembled, all valves are opened and the whole system is flushed with 70% ethanol followed by air (*Note*: this could flush also the polymeric sample), this can be done using syringes by hand or the micro pump, though these must first be primed.

d. The system is then primed with sterilised MilliQ water.
e. Arrange all valves in the way media flow path is unimpeded, check the inoculation stop cock is closed.
f. Fill the media reservoir with autoclaved BHI broth.
g. Transport the system to the incubator set to 37°C and set the pump to flow overnight at 300 Hz and 30-40 V_{pp} – configure beforehand for 50 µL min^{-1} flow rate.
h. Once complete, move system to safety cabinet and check for leaks. A sample of the media can be taken to inoculate a horse-blood agar and sabouraud agar plate using sterile plastic loop (Fig.83). Immediately replace the waste media reservoir lid after this step.
i.

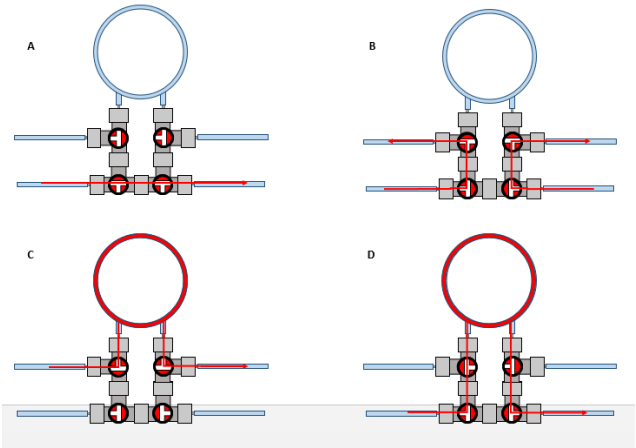

Figure 83. The loops diagram.

3. System inoculation with *S.aureus*
    a. 5 mL of *S.aureus* UAMS-1 cell culture is drawn into a 5 mL syringe, then connected to the system via the bacterial inlet tubing stop cock.
    b. The 2-way valve prior to the device's media channel connection is closed to prevent back-flow.
    c. The bacterial stop cock is opened and the inoculum is carefully injected slowly to flow the bacteria towards the waste media outlet.
    d. Once inoculated, transfer the system back to the incubator set at 37°C for one hour to allow the bacteria to settle and properly adhere to the surfaces within the chamber, **do not** remove the syringe at this point.
4. Media flow and overnight growth
    a. Open the 2-way valve prior to the chip media connection and set the micro pump to flow fresh media overnight at a flow rate of 50 µL min^{-1}
    b. Check the system in the morning next day to ensure no leaks have occurred.
5. Staining and use of reagent loop
    a. Prepare a solution of live/dead stain (DMAO and EthD-III in 0.85% NaCl solution).
    b. Reagent loop can be primed with 0.85% NaCl buffer as the diagram below shows (Fig.82), removal of bubbles and air pockets is essential to maintain biofilm integrity.
    c. Once the loop is primed with the live/dead stain, introduce using a micro pump set to 50 µL min^{-1} ensuring the 3-way valve connecting to the system blocks back-flow of stain up the media tubing.

d. Once the system has been stained, stop the pump flow and leave the system in the dark for 20 minutes.
e. Give the system one final flush through at the same flow rate with buffer only to remove unused dye, prepare for transport to confocal microscope.

Figure 84. Sample of media on horse blood agar result.

Transporting the system to the confocal microscope requires placement of the system into a sealed container to avoid spills and an accidental disconnections during transit.

The confocal microscope Leica DMi8 viewing.

Top chamber - polymer+clay
Central chamber - control w/o sample
Bottom chamber - polymer+clay+antimicrobial agent (Fig.85)

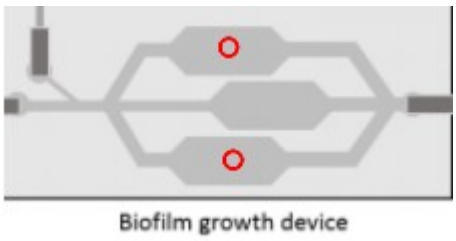

Figure 85. Biofilm growth device scheme, the samples are shown in red color.

Magnification 2.5x of the device is shown on Fig.86-88:

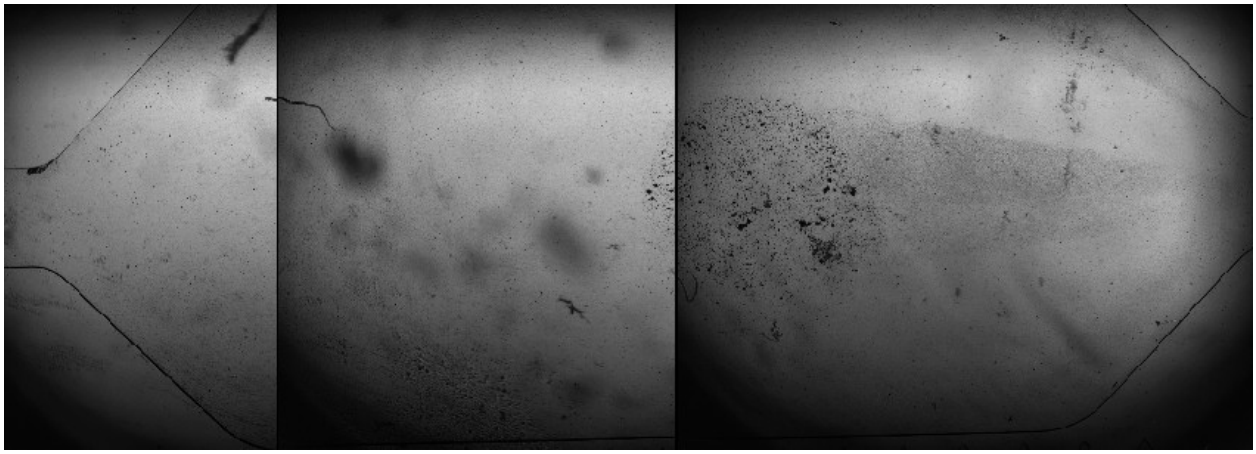

Figure 86. Top chamber 2.5x.

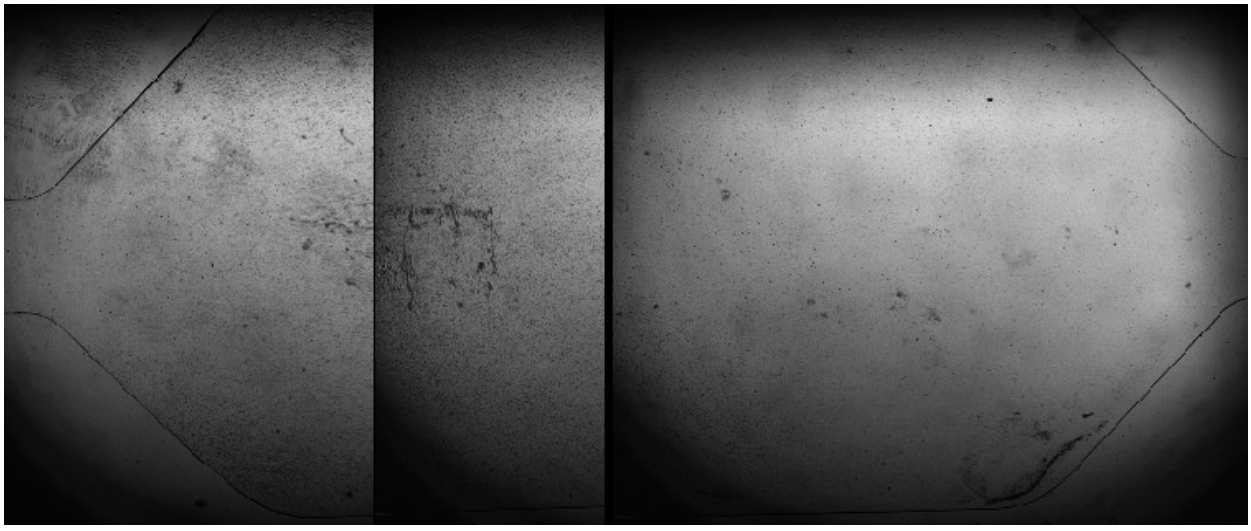

Figure 87. Central chamber 2.5x.

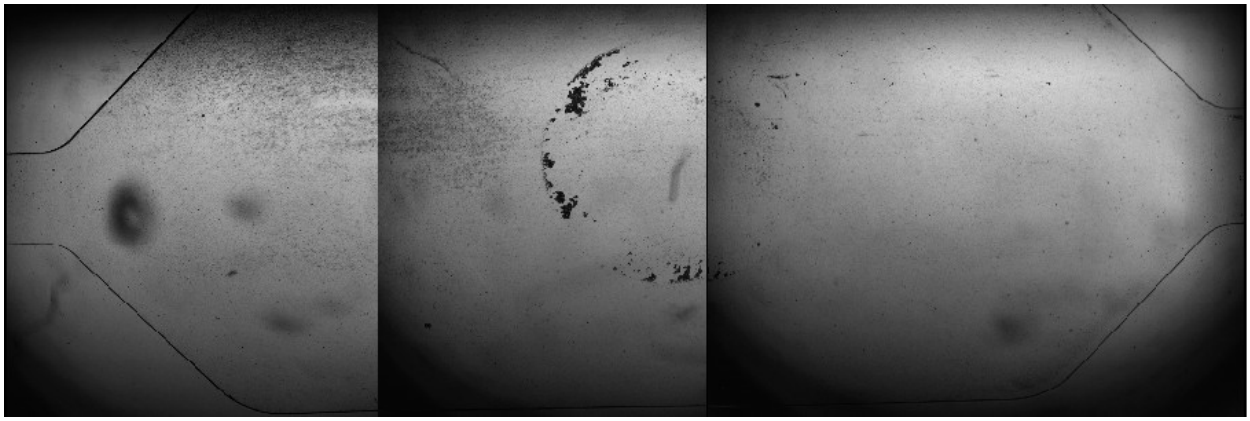

Figure 88. Bottom chamber 2.5x.

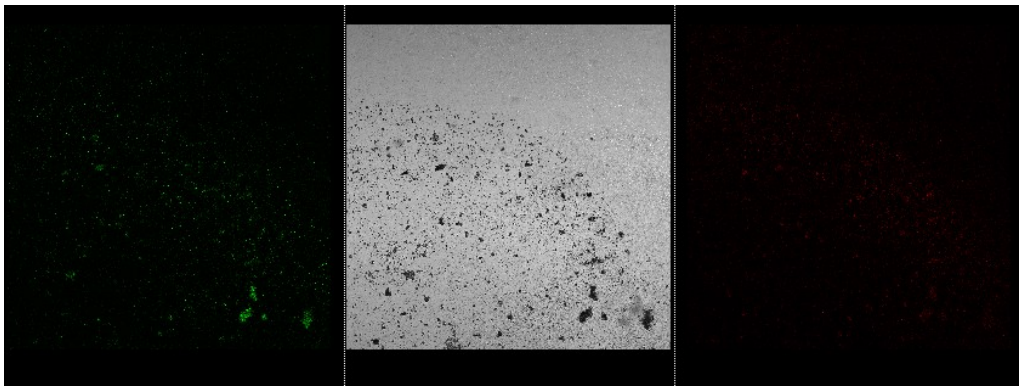

Figure 89. Top part 10x magnification. Green (left) - live cells, red (right) - dead cells.

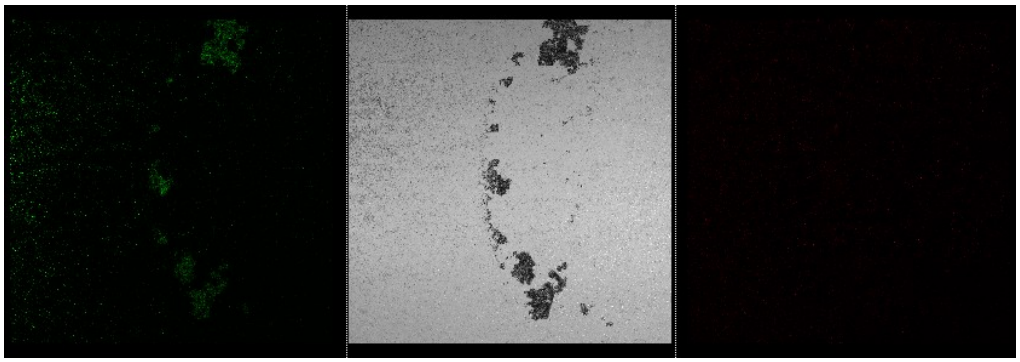

Figure 90. Bottom part 10x magnification. Green (left) - live cells, red (right) - dead cells.

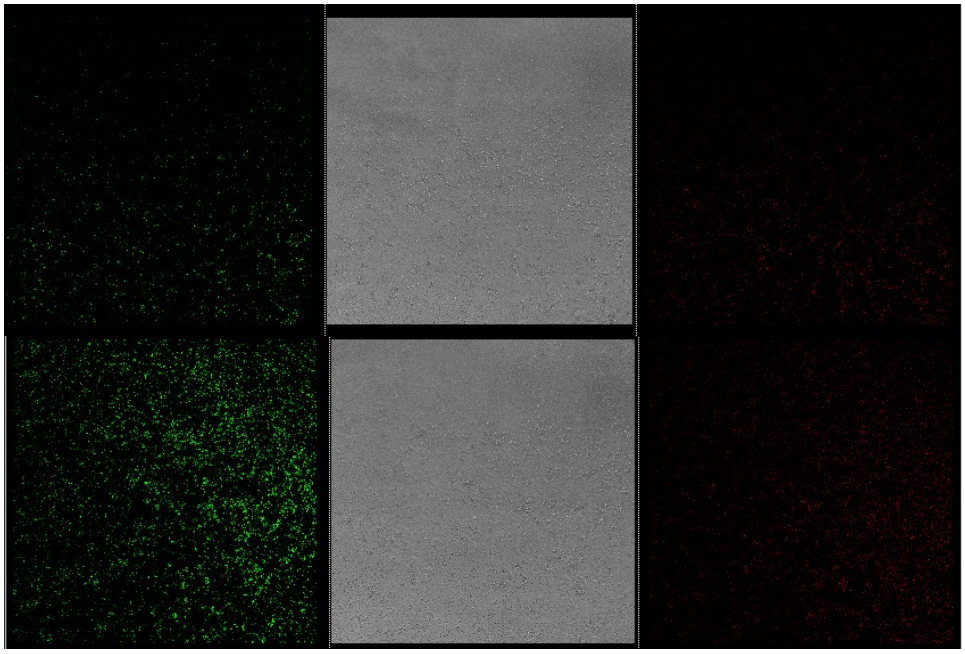

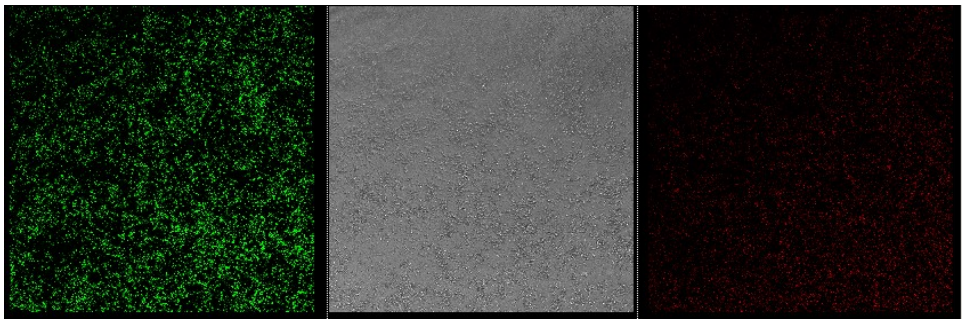

Figure 91. Top, Central and Bottom parts with 40x magnification. The location: in the middle of a chamber. Green (left) - live cells, red (right) - dead cells.

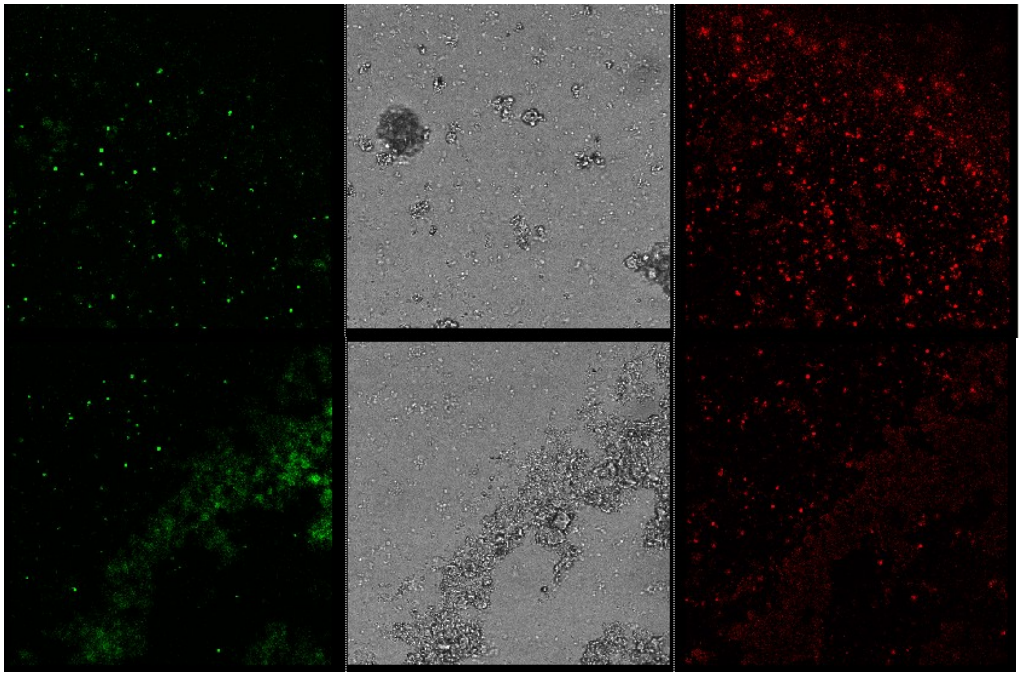

Figure 92. Top and Bottom parts 100x magnification. The sample residuals. Green (left) - live cells, red (right) - dead cells.

The experiment was done only once and only one sample was tested. For the next experiment like this in case of water soluble polymeric matrices I would recommend to pay attention about flushing the system with liquids like media or ethanol as it may affect the presence of polymeric matrix, dissolve it to some extent and flush out some of antimicrobial agent, too.

This experiment showed that the samples are affecting the *S.aureus* biofilm growth by lowering it (Fig.93-95), more data is needed for deeper understanding. I would recommend to try out other polymers and other antimicrobials as well as different bacterial strain biofilm simulation or even a simulation of a multimicrobial biofilm which is more likely to meet in the human gastrointestinal conditions.

The green filter is supposed to show us the living cells and the red filter - dead cells.

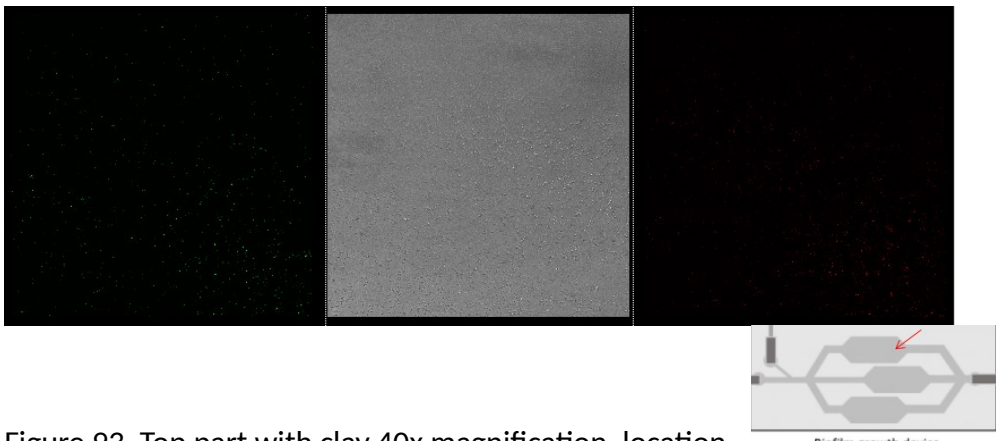

Figure 93. Top part with clay 40x magnification, location - . Green (left) - live cells, red (right) - dead cells.

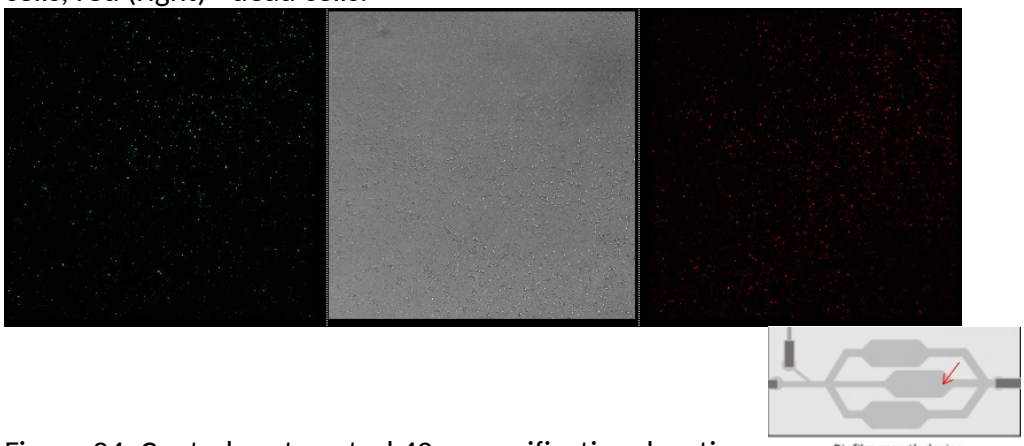

Figure 94. Central part control 40x magnification, location - . Green (left) - live cells, red (right) - dead cells.

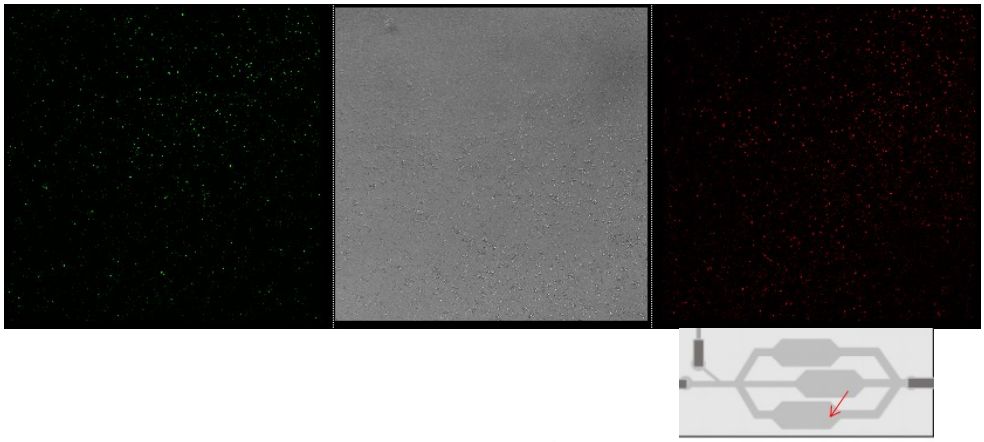

Figure 95. Bottom part 40x magnification, location - . Green (left) - live cells, red (right) - dead cells.

It is well visible that there is significantly more bacteria, as it is without any sample, so based on that we can presume that the sample is functional against given biofilm in these improvised “in-body conditions”.

3.5. MOLECULAR MODELING

The selected for the molecular modeling study biodegradable triblock copolymers are polycaprolactone polyethylene glycol polycaprolactone (PCL-PEG-PCL) and polycaprolactone polyglycolic acid polycaprolactone (PCL-PGA-PCL) and as an antitumoral drug, Erlotinib was chosen. By means of molecular modeling, it was found out that for both matrices the bigger amount of drug is a reason of growing of cohesive energy density (CED). It means that the system is more stable when there is a greater amount of drug. In the case of polyethylene glycol (PEG) and polyglycolic acid (PGA) the data was obtained, that together with generally lower values of CED for PCL-PEG-PCL matrix the findings may indicate stronger interaction between Erlotinib and PGA than with PEG. This work was a first step for understanding the advantages and disadvantages of various materials for medical using. See the full study (Hlaváč et al., 2018).

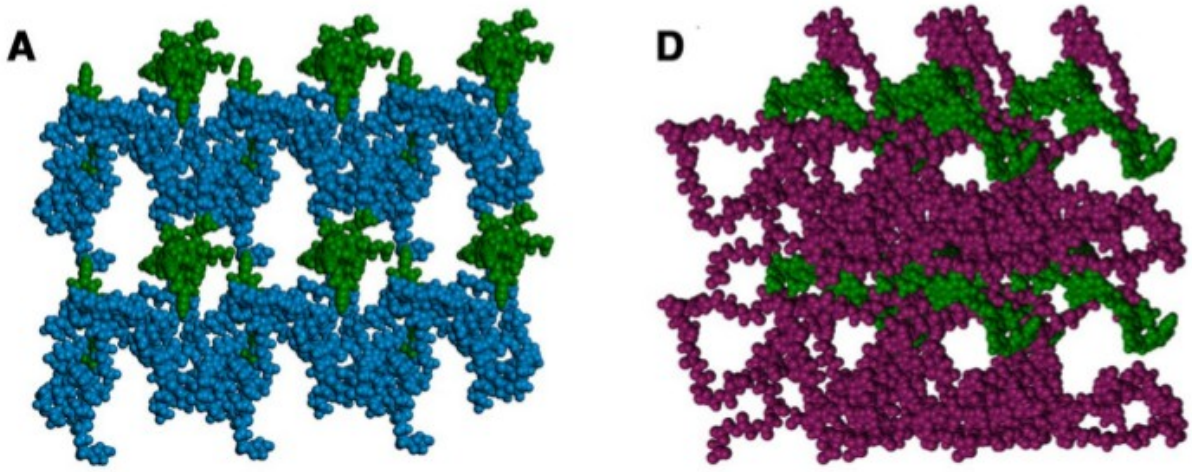

Figure 96. Mutual positions of ERL and hydrophilic parts of copolymers at the end of MD simulation performed under periodic boundary conditions. a PCL/PEG_1; d PCL/PGA_1. ERL molecules are displayed in green, PEG blue and PGA violet colors. PCL parts of chains are omitted for clarity.

4. CONCLUSION

The presented work is focused on materials suitable for medical applications, where rapidly growing microbial biofilm is one of the serious dangers for life and health of a human being. Since the range of the materials and applications in the field of prosthetics inserted in the body is large, this work specializes only on one type of medical devices like gastroenterological stents applied in case of the extracted or damaged bile duct.

The goal of this research was to develop a functional antimicrobial polymer coating, which might be used afterwards for medical applications such as biliary stents. The research in this field focuses on study and optimization of polymeric stent material in accordance with the conditions in the body.

A number of materials was prepared experimentally, characterized by various techniques, viewed by molecular modeling and tested in “in-body conditions”. In my opinion, based on multiple experiments, the purpose to find the most effective combinations of nanocomposite contents is achieved.

- Modified natural clay minerals were proved to be functional antimicrobial agents when embedded to polymeric matrix.

- Modification of the clay doesn’t have to reach the intercalated level. Partly-intercalated montmorillonite layers and surface-modified vermiculites had positive impact on incorporation of nanofiller to the polymeric matrix and antimicrobial properties.

- Selection of the 3 polymeric matrices was done based on the known clinical facts and literature recherche. Based on experimental knowledge modifying compounds – imidazole, clotrimazole and ciclopyroxol amine - were selected for natural clay minerals.

- At the time of elaboration of the dissertation work unique technique for preparation and casting thin polymeric films was established. Tailoring the conditions of the nanocomposite preparation a well dispersed nanocomposite with self-standing properties was possible to fabricate.

- To prove the functionality in the application for inner coating of polymeric bile duct stent several testing methods were proposed. Nanocomposite testing for stability was performed in base pH conditions, as known for bile fluid. The stability was proved for PVAc nanocomposites.

- Functionality of the polymeric nanocomposite is synergic and the individual’s properties are multiplied with strength of other component. The best combinations of the researched materials are vermiculite and montmorillonite particles modified with ciclopirox olamine, imidazole and clotrimazole. Regarding polymeric matrices all 3 selected matrices showed

their applicability for medical purposes.

In further research I recommend to focus on above mentioned combinations of components in nanocomposite and continue to develop an antitumoral polymeric nanocomposite with antimicrobial properties.

5. REFERENCES

Internet Sources

[1]https://courses.lumenlearning.com/boundless-microbiology/chapter/overview-of-antimicrobial-therapy/
[2]https://www.drugs.com/monograph/clotrimazole.html
[3]http://www.who.int/medicines/publications/essentialmedicines/EML_2015_FINAL_amended_NOV2015.pdf?ua=1
[4]http://cps.utb.cz/en/science-research/equipment

Bibliography

Adhikari R, Michler GH. Polymer nanocomposites characterization by microscopy. Polymer Reviews. 2009; 49 (3): 141–80.

Alves FRF, Silva MG, Rôças IN, Siqueira Jr JF. Biofilm biomass disruption by natural substances with potential for endodontic use. Brazilian Oral Research. 2013; 27 (1): 20–25.

Ammons MC, Copié V. Mini-review: Lactoferrin: a bioinspired, anti-biofilm therapeutic. Biofouling. 2013; 29 (4): 443–55.

An YH, Friedman RJ. Concise review of mechanisms of bacterial adhesion to biomaterial surfaces. Journal of Biomedical Materials Research. 1998; 43 (3): 338–48.

Artifon ELA, Coelho F, Frazao M, Marques S, Paione JB, Takada J, et al. A prospective randomized study comparing partially covered metal stent versus plastic multistent in the endoscopic management of patients with postoperative benign bile duct strictures: a follow-up above 5 years. Revista de gastroenterología del Perú : órgano oficial de la Sociedad de Gastroenterología del Perú. 2012; 32 (1): 26–31.

Ashford RD. Ashford's Dictionary of Industrial Chemicals (3rd ed.). Saltash, Cornwall: Wavelength Publications 2011, p. 9252

Bandyopadhyay S, Samudrala SK, Bhowmick AK, Gupta SK. Applications of Atomic Force Microscope (AFM) in the Field of Nanomaterials and Nanocomposites. 2008 p. 504–68.

Banin E, Brady KM, Greenberg EP. Chelator-Induced Dispersal and Killing of Pseudomonas aeruginosa Cells in a Biofilm. Applied and Environmental Microbiology. 2006; 72 (3): 2064–69.

Barkay O, Mosler P, Schmitt CM, Lehman GA, Frakes JT, Johanson JF, et al. Effect of Endoscopic Stenting of Malignant Bile Duct Obstruction on Quality of Life. Journal of Clinical Gastroenterology. 2013; 47 (6): 526–31.

Barret KE, Barman SM, Boitano S, Brooks HL. Ganong's Review of Medical Physiology 24th Edition's Review of Medical Physiology. Ganong's Review of Medical Physiology 24th Edition's Review of Medical Physiology. 2012.

Bitinis N, Hernandez M, Verdejo R, Kenny JM, Lopez-Manchado MA. Recent Advances in Clay/Polymer Nanocomposites. Advanced Materials. 2011; 23 (44): 5229–36.

Bjarnsholt T, Alhede M, Jensen PØ, Nielsen AK, Johansen HK, Homøe P, et al. Antibiofilm Properties of Acetic Acid. Advances in Wound Care. 2015; 4 (7): 363–72.

Bosma JW, Siegert CEH, Peerbooms PGH, Weijmer MC. Reduction of biofilm formation with trisodium citrate in haemodialysis catheters: a randomized controlled trial. Nephrology Dialysis Transplantation. 2010; 25 (4): 1213–17.

Böttcher T, Kolodkin-Gal I, Kolter R, Losick R, Clardy J. Synthesis and Activity of Biomimetic Biofilm Disruptors. Journal of the American Chemical Society. 2013; 135 (8): 2927–30.

Caballero-George C, Marin, Briceño. Critical evaluation of biodegradable polymers used in nanodrugs. International Journal of Nanomedicine. 2013; 8: 3071–91

Cappitelli F, Sorlini C. Microorganisms Attack Synthetic Polymers in Items Representing Our Cultural Heritage. Applied and Environmental Microbiology. 2008; 74 (3): 564–69.

Cavaliere R, Ball JL, Turnbull L, Whitchurch CB. The biofilm matrix destabilizers, EDTA and DNaseI, enhance the susceptibility of nontypeable Hemophilus influenzae biofilms to treatment with ampicillin and ciprofloxacin. MicrobiologyOpen. 2014; 3 (4): 557–67

Chaieb K, Kouidhi B, Jrah H, Mahdouani K, Bakhrouf A. Antibacterial activity of Thymoquinone, an active principle of Nigella sativa and its potency to prevent bacterial biofilm formation. BMC Complementary and Alternative Medicine. 2011; 11 (1): 29

Chaignon P, Sadovskaya I, Ragunah C, Ramasubbu N, Kaplan JB, Jabbouri S. Susceptibility of staphylococcal biofilms to enzymatic treatments depends on their chemical composition. Applied Microbiology and Biotechnology. 2007; 75 (1): 125–32

Choudalakis GA, Gotsis AD. Permeability of Polymer/Clay Nanocomposites. MRS Proceedings. 2011; 1312: mrsf10-1312-ii13-04

Cohen NR, Lobritz MA, Collins JJ. Microbial Persistence and the Road to Drug Resistance. Cell Host & Microbe. 2013; 13 (6): 632–42

Coté GA, Slivka A, Tarnasky P, Mullady DK, Elmunzer BJ, Elta G, et al. Effect of Covered Metallic Stents Compared With Plastic Stents on Benign Biliary Stricture Resolution. JAMA. 2016; 315 (12): 1250

Cyphert EL, von Recum HA. Emerging technologies for long-term antimicrobial device coatings: advantages and limitations. Experimental Biology and Medicine. 2017; 242 (8): 788–98

Davidson PM, Parish ME. Methods for testing the efficacy of food antimicrobials. Food technology (USA). 1989; (January): 148–55

Davies D. Understanding biofilm resistance to antibacterial agents. Nature Reviews Drug Discovery. 2003; 2 (2): 114–22

Dinicola S, De Grazia S, Carlomagno G, Pintucci JP. N-acetylcysteine as powerful molecule to destroy bacterial biofilms. A systematic review. European review for medical and pharmacological sciences. 2014; 18: 2942–48

Donelli G, Guaglianone E, Di Rosa R, Fiocca F, Basoli A. Plastic Biliary Stent Occlusion: Factors Involved and Possible Preventive Approaches. Clinical Medicine & Research. 2007; 5 (1): 53–60

Donlan R. Biofilms and Device-Associated Infections. Emerging Infectious Diseases. 2001; 7 (2): 277–81

Donlan RM. Biofilm Formation: A Clinically Relevant Microbiological Process. Clinical Infectious Diseases. 2001; 33 (8): 1387–92

Dumonceau J-M, Heresbach D, Devière J, Costamagna G, Beilenhoff U, Riphaus A. Biliary stents: models and methods for endoscopic stenting. Endoscopy. 2011; 43 (07): 617–26

England RE. A prospective randomised multicentre trial comparing 10 Fr Teflon Tannenbaum stents with 10 Fr polyethylene Cotton-Leung stents in patients with malignant common duct strictures. Gut. 2000; 46 (3): 395–400

Galandi D, Schwarzer G, Bassler D, Allgaier HP. Ursodeoxycholic acid and/or antibiotics for

prevention of biliary stent occlusion. Cochrane Database of Systematic Reviews. 2002; (3): 23

Garg P, Singh U, Mishra C, Nagpal R, Tyagi S, Sinha D. Comparison of antimicrobial efficacy of propolis, Morinda citrifolia, Azadirachta indica (Neem) and 5% sodium hypochlorite on Candida albicans biofilm formed on tooth substrate: An in-vitro study. Journal of Conservative Dentistry. 2013; 16 (6): 532

Getzin S, Wiegand T, Wiegand K, He F. Heterogeneity influences spatial patterns and demographics in forest stands. Journal of Ecology. 2008; 96 (4): 807–20

Gibaud S, Jaouen G. Arsenic-Based Drugs: From Fowler's Solution to Modern Anticancer Chemotherapy. In: Topics in Organometallic Chemistry. 2010. p. 1–20

Gill P, Musaramthota V, Munroe N, Datye A, Dua R, Haider W, et al. Surface modification of Ni–Ti alloys for stent application after magnetoelectropolishing. Materials Science and Engineering: C. 2015; 50: 37–44

Goc A, Niedzwiecki A, Rath M. In vitro evaluation of antibacterial activity of phytochemicals and micronutrients against Borrelia burgdorferi and Borrelia garinii. Journal of Applied Microbiology. 2015; 119 (6): 1561–72

Groen AK, Out T, Huibregtse K, Delzenne B, Hoek FJ, Tytgat GNJ. Characterization of the Content of Occluded Biliary Endoprostheses. Endoscopy. 1987; 19 (02): 57–59

Guaglianone E, Cardines R, Vuotto C, Di Rosa R, Babini V, Mastrantonio P, et al. Microbial biofilms associated with biliary stent clogging. FEMS Immunology & Medical Microbiology. 2010; 59 (3): 410–20

Guggenheim S, Adams JM, Bain DC, Bergaya F, Brigatti MF, Drits VA, et al. Corrigenda. Clays and Clay Minerals. 2007; 55 (6): 646–47

Haile T, Nakhla G. The inhibitory effect of antimicrobial zeolite on the biofilm of Acidithiobacillus thiooxidans. Biodegradation. 2010; 21 (1): 123–34

Harjai K, Bala A, Gupta RK, Sharma R. Leaf extract of Azadirachta indica (neem): a potential antibiofilm agent for Pseudomonas aeruginosa. Pathogens and Disease. 2013; 69 (1): 62–65

Hlaváč D, Klushina D, Tokarský J. Interaction of antitumoral drug erlotinib with biodegradable triblock copolymers: a molecular modeling study. Chemical Papers. 2018; 72 (8): 2023–34.

Hoffman AS. Hydrogels for biomedical applications. Advanced Drug Delivery Reviews. 2012; 64: 18–23

Hosterman JW, Patterson SH. Bentonite and fuller's earth resources of the United States. US Geological Survey Professional Paper. 1992; 1522

Hurdle JG, Yendapally R, Sun D, Lee RE. Evaluation of Analogs of Reutericyclin as Prospective Candidates for Treatment of Staphylococcal Skin Infections. Antimicrobial Agents and Chemotherapy. 2009; 53 (9): 4028–31

Inaba K. X-ray thin-film measurement techniques I. overview. The Rigaku Journal. 2008; 24 (1): 10–15

Jacqueline C, Caillon J. Impact of bacterial biofilm on the treatment of prosthetic joint infections. Journal of Antimicrobial Chemotherapy. 2014; 69 (suppl 1): i37–40

Jakobsen TH, Bragason SK, Phipps RK, Christensen LD, van Gennip M, Alhede M, et al. Food as a Source for Quorum Sensing Inhibitors: Iberin from Horseradish Revealed as a Quorum Sensing Inhibitor of Pseudomonas aeruginosa. Applied and Environmental Microbiology. 2012; 78 (7): 2410–21

Jaleh B, Fakhri P. Infrared and Fourier transform infrared spectroscopy for nanofillers and their nanocomposites. In: Spectroscopy of Polymer Nanocomposites. Elsevier; 2016. p. 112–29

Kadakia SC, Starnes E. Comparison of 10 French gauge stent with 11.5 French gauge stent in patients with biliary tract diseases. Gastrointestinal Endoscopy. 1992; 38 (4): 454–59

Kavanaugh NL, Ribbeck K. Selected Antimicrobial Essential Oils Eradicate Pseudomonas spp. and Staphylococcus aureus Biofilms. Applied and Environmental Microbiology. 2012; 78 (11): 4057–61

Kim H-S, Park H-D. Ginger Extract Inhibits Biofilm Formation by Pseudomonas aeruginosa PA14. PLoS ONE. 2013; 8 (9): e76106

Kokabi M, Sirousazar M, Hassan ZM. PVA-clay nanocomposite hydrogels for wound dressing. European Polymer Journal. 2007; 43 (3): 773–81

Lee TH, Jang BS, Jung MK, Pack CG, Choi J-H, Park DH. Fabrication of a silver particle-integrated silicone polymer-covered metal stent against sludge and biofilm formation and stent-induced tissue inflammation. Scientific Reports. 2016; 6 (1): 35446

Leem SH, Park JE, Kim IS, Chae JY, Sugino A, Sunwoo Y. The possible mechanism of action of ciclopirox olamine in the yeast Saccharomyces cerevisiae. Molecules and Cells. 2003; 15 (1): 55–61

Lendlein A, Sisson A. Handbook of Biodegradable Polymers. Handbook of Biodegradable Polymers: Isolation, Synthesis, Characterization and Applications. Weinheim, Germany: Wiley-VCH Verlag GmbH & Co. KGaA; 2011

Leung JWC, Ling TKW, Kung JLS, Vallance-Owen J. The role of bacteria in the blockage of biliary stents. Gastrointestinal Endoscopy. 1988; 34 (1): 19–22

Leung JW, Liu Y, Chan RCY, Tang Y, Mina Y, Cheng AF, et al. Early attachment of anaerobic bacteria may play an important role in biliary stent blockage. Gastrointestinal Endoscopy. 2000; 52 (6): 725–29

Lewandowski Z. Structure and Function of Biofilms. In: Biofilms Recent Advences in Their Study and Control. 2000. p. 1–17

Liu Q, Niu H, Zhang W, Mu H, Sun C, Duan J. Synergy among thymol, eugenol, berberine, cinnamaldehyde and streptomycin against planktonic and biofilm-associated food-borne pathogens. Letters in Applied Microbiology. 2015; 60 (5): 421–30

Lu J, Turnbull L, Burke CM, Liu M, Carter DA, Schlothauer RC, et al. Manuka-type honeys can eradicate biofilms produced by Staphylococcus aureus strains with different biofilm-forming abilities. PeerJ. 2014; 2: e326

Lübbert C, Wendt K, Feisthammel J, Moter A, Lippmann N, Busch T, et al. Epidemiology and Resistance Patterns of Bacterial and Fungal Colonization of Biliary Plastic Stents: A Prospective Cohort Study. PLOS ONE. 2016; 11 (5): e0155479

Magesh H, Kumar A, Alam A, Priyam, Sekar U, Sumantran VN, et al. Identification of natural compounds which inhibit biofilm formation in clinical isolates of Klebsiella pneumoniae. Indian Journal of Experimental Biology. 2013; 51 (9): 764–72

Mangiavillano B. Outcome of stenting in biliary and pancreatic benign and malignant diseases: A comprehensive review. World Journal of Gastroenterology. 2015; 21 (30): 9038

Mecikoglu M, Saygi B, Yildirim Y, Karadag-Saygi E, Ramadan SS, Esemenli T. The Effect of Proteolytic Enzyme Serratiopeptidase in the Treatment of Experimental Implant-Related Infection. The Journal of Bone & Joint Surgery. 2006; 88 (6): 1208–14

Merckoll P, Jonassen TØ, Vad ME, Jeansson SL, Melby KK. Bacteria, biofilm and honey: A study of the effects of honey on 'planktonic' and biofilm-embedded chronic wound bacteria. Scandinavian Journal of Infectious Diseases. 2009; 41 (5): 341–47

Middleton G, Church MJ, Coniglio M, Hardie LA, Longstaffe FJ, MacNaughton RB, et al. Encyclopaedia of Sediments and Sedimentary Rocks. Geoscience Canada. 2003. 821 p

Middleton JC, Tipton AJ. Synthetic biodegradable polymers as orthopedic devices. Biomaterials. 2000; 21 (23): 2335–46

Miller MB, Bassler BL. Quorum Sensing in Bacteria. Annual Review of Microbiology. 2001; 55 (1): 165–99

Murugan K, Selvanayaki K, Al-Sohaibani S. Antibiofilm activity of Andrographis paniculata against cystic fibrosis clinical isolate Pseudomonas aeruginosa. World Journal of Microbiology and Biotechnology. 2011; 27 (7): 1661–68

Musk DJ, Banko DA, Hergenrother PJ. Iron Salts Perturb Biofilm Formation and Disrupt Existing Biofilms of Pseudomonas aeruginosa. Chemistry & Biology. 2005; 12 (7): 789–96

Naber CK. Staphylococcus aureus Bacteremia: Epidemiology, Pathophysiology, and Management Strategies. Clinical Infectious Diseases. 2009; 48 (s4): S231–37

Navarro M, Michiardi A, Castaño O, Planell J. Biomaterials in orthopaedics. Journal of The Royal Society Interface. 2008; 5 (27): 1137–58

Nguyen PTM, Falsetta ML, Hwang G, Gonzalez-Begne M, Koo H. α-Mangostin Disrupts the Development of Streptococcus mutans Biofilms and Facilitates Its Mechanical Removal. PLoS ONE. 2014; 9 (10): e111312

Niewerth M, Kunze D, Seibold M, Schaller M, Korting HC, Hube B. Ciclopirox Olamine Treatment Affects the Expression Pattern of Candida albicans Genes Encoding Virulence Factors, Iron Metabolism Proteins, and Drug Resistance Factors. Antimicrobial Agents and Chemotherapy. 2003; 47 (6): 1805–17

Nostro A, Procopio F, Pizzimenti FC, Cannatelli MA, Bisignano G, Marino A, et al. Effects of oregano, carvacrol and thymol on Staphylococcus aureus and Staphylococcus epidermidis biofilms. Journal of Medical Microbiology. 2007; 56 (4): 519–23

O'Neill J. Antimicrobial Resistance : Tackling a crisis for the health and wealth of nations. Review on

Antimicrobial Resistance. 2016; (December): 1–16

O'Toole G, Kaplan HB, Kolter R. Biofilm Formation as Microbial Development. Annual Review of Microbiology. 2000; 54 (1): 49–79

Olson ME, Ceri H, Morck DW, Buret AG, Read RR. Biofilm bacteria: Formation and comparative susceptibility to antibiotics. Canadian Journal of Veterinary Research. 2002; 66 (2): 86–92

Ozdil D, Aydin HM. Polymers for medical and tissue engineering applications. Journal of Chemical Technology & Biotechnology. 2014; 89 (12): 1793–1810

Pandit S, Cai JN, Song KY, Jeon JG. Identification of anti-biofilm components in Withania somnifera and their effect on virulence of Streptococcus mutans biofilms. Journal of Applied Microbiology. 2015; 119 (2): 571–81

Paul DR, Robeson LM. Polymer nanotechnology: Nanocomposites. Polymer. 2008; 49 (15): 3187–3204

Pavlidou S, Papaspyrides CD. A review on polymer-layered silicate nanocomposites. Progress in Polymer Science (Oxford). 2008

Pejin B, Ciric A, Markovic J, Glamoclija J, Nikolic M, Stanimirovic B, et al. Quercetin Potently Reduces Biofilm Formation of the Strain Pseudomonas aeruginosa PAO1 in vitro. Current Pharmaceutical Biotechnology. 2015; 16 (8): 733–37

Percival SL, Walker JT. Potable water and biofilms: A review of the public health implications. Biofouling. 1999; 14 (2): 99–115

Percival SL, McCarty SM, Lipsky B. Biofilms and Wounds: An Overview of the Evidence. Advances in Wound Care. 2015; 4 (7): 373–81

Percival SL, Thomas JG, Williams D. Microbiology of Wounds. Microbiology of Wounds. CRC Press; 2010. 271–292 p

Pfau PR, Pleskow DK, Banerjee S, Barth BA, Bhat YM, Desilets DJ, et al. Pancreatic and biliary stents. Gastrointestinal Endoscopy. 2013; 77 (3): 319–27

Piddock LJ V. Techniques used for the determination of antimicrobial resistance and sensitivity in bacteria. Journal of Applied Bacteriology. 1990; 68 (4): 307–18

Poupon R. Primary biliary cirrhosis: A 2010 update. Journal of Hepatology. 2010; 52 (5): 745–58

Radoslovich EW, Norrish K. The cell dimensions and symmetry of layer-lattice silicates: I. Some structural considerations. American Mineralogist. 1962; 47 (5–6): 599–616

Raijman I. Biliary and pancreatic stents. Gastrointestinal Endoscopy Clinics of North America. 2003; 13 (4): 561–92

Raja AF, Ali F, Khan IA, Shawl AS, Arora DS, Shah BA, et al. Antistaphylococcal and biofilm inhibitory activities of acetyl-11-keto-β-boswellic acid from Boswellia serrata. BMC Microbiology. 2011; 11 (1): 54

Rajiv S, Drilling A, Bassiouni A, James C, Vreugde S, Wormald P-J. Topical colloidal silver as an anti-biofilm agent in a Staphylococcus aureus chronic rhinosinusitis sheep model. International Forum of Allergy & Rhinology. 2015; 5 (4): 283–88

Ratnavel RC, Squire RA, Boorman GC. Clinical efficacies of shampoos containing ciclopirox olamine (1.5%) and ketoconazole (2.0%) in the treatment of seborrhoeic dermatitis. Journal of Dermatological Treatment. 2007; 18 (2): 88–96

Reid G, Hsiehl J, Potter P, Mighton J, Lam D, Warren D, et al. Cranberry juice consumption may reduce biofilms on uroepithelial cells: pilot study in spinal cord injured patients. Spinal Cord. 2001; 39 (1): 26–30

Rosenblatt J, Reitzel RA, Raad I. Caprylic Acid and Glyceryl Trinitrate Combination for Eradication of Biofilm. Antimicrobial Agents and Chemotherapy. 2015; 59 (3): 1786–88

Rosiak J, Olejniczak J, Burczak K. Polymer materials for biomedical use obtained by radiation methods. III. Radiation cross-linking of acrylamide and N-vinylpyrrolidone. Polimery w medycynie. 1989; 19 (3–4): 69–92

Roy S, Singha NR. Polymeric nanocomposite membranes for next generation pervaporation process: Strategies, challenges and future prospects. Membranes. 2017

Sadowska B, Budzy ska A, Wi ckowska-Szakiel M, Paszkiewicz M, Stochmal A, Moniuszko-Szajwaj B, et al. New pharmacological properties of Medicago sativa and Saponaria officinalis saponin-rich fractions addressed to Candida albicans. Journal of Medical Microbiology. 2014; 63 (Pt_8): 1076–86

Sarkisian SA, Janssen MJ, Matta H, Henry GE, LaPlante KL, Rowley DC. Inhibition of Bacterial

Growth and Biofilm Production by Constituents from Hypericum spp. Phytotherapy Research. 2012; 26 (7): 1012–16

Sawas T, Al Halabi S, Parsi MA, Vargo JJ. Self-expandable metal stents versus plastic stents for malignant biliary obstruction: a meta-analysis. Gastrointestinal Endoscopy. 2015; 82 (2): 256-267.e7

Schaller K. In vitro Antibacterial Activity of Different Clotrimazole Formulations. Chemotherapy. 1982; 28 (1): 32–36

Schierholz JM, Beuth J. Implant infections: A haven for opportunistic bacteria. Journal of Hospital Infection. 2001; 49(2): 87-93

Schindler A, Doedt M, Gezgin Ş, Menzel J, Schmölzer S. Identification of polymers by means of DSC, TG, STA and computer-assisted database search. Journal of Thermal Analysis and Calorimetry. 2017; 129 (2): 833–42

Serruys PW, Kutryk MJB, Ong ATL. Coronary-Artery Stents. New England Journal of Medicine. 2006; 354 (5): 483–95

Shatzel J. Drug eluting biliary stents to decrease stent failure rates: A review of the literature. World Journal of Gastrointestinal Endoscopy. 2016; 8 (2): 77

Shuford JA, Steckelberg JM, Patel R. Effects of Fresh Garlic Extract on Candida albicans Biofilms. Antimicrobial Agents and Chemotherapy. 2005; 49 (1): 473–473

Silva-Dias A, Palmeira-de-Oliveira A, Miranda IM, Branco J, Cobrado L, Monteiro-Soares M, et al. Anti-biofilm activity of low-molecular weight chitosan hydrogel against Candida species. Medical Microbiology and Immunology. 2014; 203 (1): 25–33

Simha Martynková G, Valášková M, Čapková P, Matějka V. Structural ordering of organovermiculite: Experiments and modeling. Journal of Colloid and Interface Science. 2007; 313 (1): 281–87

Sinha Ray S, Okamoto M. Polymer/layered silicate nanocomposites: a review from preparation to processing. Progress in Polymer Science. 2003; 28 (11): 1539–1641

Speer AG, Cotton PB, MacRae KD. Endoscopic management of malignant biliary obstruction: stents of 10 French gauge are preferable to stents of 8 French gauge. Gastrointestinal Endoscopy. 1988; 34 (5): 412–417

Šupová M, Martynková GS, Barabaszová K. Effect of Nanofillers Dispersion in Polymer Matrices: A Review. Science of Advanced Materials. 2011; 3 (1): 1–25

Takahashi N, Kuroda K. Materials design of layered silicates through covalent modification of interlayer surfaces. Journal of Materials Chemistry. 2011; 21 (38): 14336

Terruzzi V, Comin U, De Grazia F, Toti GL, Zambelli A, Beretta S, et al. Prospective randomized trial comparing Tannenbaum Teflon and standard polyethylene stents in distal malignant biliary stenosis. Gastrointestinal Endoscopy. 2000; 51 (1): 23–27

Theophilus PAS, Victoria MJ, Socarras KM, Filush KR, Gupta K, Luecke DF, et al. Effectiveness of Stevia rebaudiana whole leaf extract against the various morphological forms of Borrelia burgdorferi in vitro. European Journal of Microbiology and Immunology. 2015; 5 (4): 268–80

Tian H, Tang Z, Zhuang X, Chen X, Jing X. Biodegradable synthetic polymers: Preparation, functionalization and biomedical application. Progress in Polymer Science. 2012; 37 (2): 237–80

Valaskova M, SIMHA MARTYNKOVA G, MATEJKA V, BARABASZOVA K, PLEVOVA E, MERINSKA D. Organovermiculite nanofillers in polypropylene. Applied Clay Science. 2009; 43 (1): 108–12

Valášková, M., Simha Martynková G, Lešková J, Čapková P, Klemm V, Silver nanoparticles/montmorillonite composites prepared using nitrating reagent at water and glycerol, Journal of nanoscience and nanotechnology. 2008, 8 (6), 3050-3058

Vikram A, Jayaprakasha GK, Jesudhasan PR, Pillai SD, Patil BS. Suppression of bacterial cell-cell signalling, biofilm formation and type III secretion system by citrus flavonoids. Journal of Applied Microbiology. 2010; 109 (2): 515–27

Vitale GC, Tran TC, Davis BR, Vitale M, Vitale D, Larson G. Endoscopic Management of Postcholecystectomy Bile Duct Strictures. Journal of the American College of Surgeons. 2008; 206 (5): 918–23

Vroman I, Tighzert L. Biodegradable Polymers. Materials. 2009; 2 (2): 307–44

Wang EW, Agostini G, Olomu O, Runco D, Jung JY, Chole RA. Gentian Violet and Ferric Ammonium Citrate Disrupt Pseudomonas Aeruginosa Biofilms. The Laryngoscope. 2008; 118 (11): 2050–56

Wang X, Yao X, Zhu Z, Tang T, Dai K, Sadovskaya I, et al. Effect of berberine on Staphylococcus epidermidis biofilm formation. International Journal of Antimicrobial Agents. 2009; 34 (1): 60–66

Wirtanen G. SURFACE MICROBIOLOGY Biofilm Formation & Its Elimination Example : Poor hygienic design Example : Poor hygienic design Surface Profiles of Various Stainless Surfaces. 2015; 1 (December): 1–21

Wu C, Labrie J, Tremblay YDN, Haine D, Mourez M, Jacques M. Zinc as an agent for the prevention of biofilm formation by pathogenic bacteria. Journal of Applied Microbiology. 2013; 115 (1): 30–40

Wu T, Xie A-G, Tan S-Z, Cai X. Antimicrobial effects of quaternary phosphonium salt intercalated clay minerals on Escherichia coli and Staphylococci aureus. Colloids and Surfaces B: Biointerfaces. 2011; 86 (1): 232–36

Yang B, Zhang J. Nanoparticles: Synthesis in Polymer Substrates. In: Dekker Encyclopedia of Nanoscience and Nanotechnology, Seven Volume Set. 3rd ed. New York; 2009. p. 11

Yang K, Ren Y. Nickel-free austenitic stainless steels for medical applications. Science and Technology of Advanced Materials. 2010; 11 (1): 014105 (13 pp)

Yeum JH, Sun Q, Deng Y. Poly(vinyl acetate)/Silver Nanocomposite Microspheres Prepared by Suspension Polymerization at Low Temperature. Macromolecular Materials and Engineering. 2005; 290 (1): 78–84

Yu J-L, Andersson R, Ljungh Å. Protein Adsorption and Bacterial Adhesion to Biliary Stent Materials. Journal of Surgical Research. 1996; 62 (1): 69–73

Zapotoczna M, McCarthy H, Rudkin JK, O'Gara JP, O'Neill E. An Essential Role for Coagulase in Staphylococcus aureus Biofilm Development Reveals New Therapeutic Possibilities for Device-Related Infections. Journal of Infectious Diseases. 2015; 212 (12): 1883–93

Zeng QH, Yu AB, Lu GQ. Multiscale modeling and simulation of polymer nanocomposites. Progress in Polymer Science. 2008; 33 (2): 191–269

Zorofchian Moghadamtousi S, Abdul Kadir H, Hassandarvish P, Tajik H, Abubakar S, Zandi K. A Review on Antibacterial, Antiviral, and Antifungal Activity of Curcumin. BioMed Research International. 2014; 2014:1-12.

LIST OF FIGURES

LIST OF TABLES

PUBLICATIONS

Pakseresht S, Alogaili AWM, Akbulut H, Placha D, Pazdziora E, Klushina D, et al. Silver/Chitosan Antimicrobial Nanocomposites Coating for Medical Devices: Comparison of Nanofiller Effect Prepared via Chemical Reduction and Biosynthesis. Journal of Nanoscience and Nanotechnology. 2019; 19 (5): 2938–42.

Hlaváč D, Klushina D, Tokarský J. Interaction of antitumoral drug erlotinib with biodegradable triblock copolymers: a molecular modeling study. Chemical Papers. 2018; 72 (8): 2023–34.

Lazecky M, Lhota S, Penaz T, Klushina D. Application of Sentinel-1 satellite to identify oil palm plantations in Balikpapan Bay. IOP Conference Series: Earth and Environmental Science. 2018; 169: 012064.

Klushina D, Martynková GS, Plachá D. Polymeric Nanocomposite with Antibacterial and Antitumoral Particles. Advanced Science Letters. 2016; 22 (3): 685–87.

Klushina D, Martynkova G.S. Preparation of Polymeric nanocomposites with antimicrobial properties, Den doktorandů 2017. Abstract.

Klushina D. The development of a polymeric nanocomposite with antibacterial and antitumoral properties; International Conference on Dermal Drug Delivery by Nanocarriers 14.-16.03.2016, Berlin, p.91

Klushina D, Martynkova GS, PEG A PGA MATRICE PRO NANOKOMPOZIT S ANTIBAKTERIÁLNÍMI A LÉČIVÝMI VLASTNOSTMI, Den doktorandů 2015, ISBN 978-80-248-3856-4

Kryukova M, Tamarkin M, Klushina D, Lisov A, Lipkin A, Kachalova G. Research of the n-terminal tags influence on the autoubiquitination E3 ubiquitin ligase Parkin and its TV7 splice variant; Int. conference “Biology – the Science of the XXI Century”, Moscow, 2014

Lazecka D, International conference «NanoOstrava 2019», Ostrava, Czech Republic.
Abstract “Polymeric nanocomposites as a prevention of biofilm formation”. Oral presentation

Klushina D, International conference ‘INASCON 2018’, Trondheim, Norway.
Abstract ‘The study of polymeric nanocomposites with antimicrobial properties’. Poster

Klushina D, International conference «NanoOstrava 2017», Ostrava, Czech Republic.
Abstract ‘Polymeric nanocomposite thin films with modified clay minerals with antimicrobial properties’. Poster

ANNEX

Natural biofilm disruptors:

Foods

- Linoleic acid (omega-6) (Magesh et al., 2013) (Pandit et al., 2015)

Oleic Acid/Olive Oil (Pandit, 2015)

- Honey (Merckoll et al., 2009)
- Propolis (candida biofilm) (Garg et al., 2013)
- Apple Cider Vinegar (Bjarnsholt, 2015)- physiologically tolerable concentrations of acetic acid can completely eradicate bacteria in mature biofilms in vitro.
- Caprylic acid (G+,-, fungal) (Rosenblatt et al., 2015)
- Stevia (Theophilus et al., 2015)
- Xylitol (Alves et al., 2013)
- Garlic (Shuford et al., 2005)
- Manuka (Lu et al., 2014)
- Ginger (Kim et al., 2013) (G+,-)
- Cranberry (Reid et al., 2001)

Non-Herbal Biofilm Disruptors

- Chitosan (Silva-Dias et al., 2014), (Magesh, 2013)
- N-acetylcysteine (NAC) (Dinicola et al., 2014)
- Lactoferrin (Alves, 2013), (Ammons et al., 2013)
- EDTA (Banin et al., 2006) – EDTA likely exerts antimicrobial activity by chelating magnesium and calcium – minerals which are necessary for growth and membrane stability and may also display anti-biofilm activity by reducing biofilm material (EPS) production and/or enhancing the detachment of bacterial cells from the biofilm. Magnesium, calcium, iron, zinc, and manganese appear to stabilize the biofilm matrix of a

variety of organisms by enhancing structural integrity through electrostatic interactions that serve to cross-link the matrix (Cavaliere et al., 2014)

- Zinc (Wu et al., 2013)
- Iron (Musk et al., 2005)
- Manganese (Cavaliere, 2014)
- Monolaurin (Goc et al., 2015)
- Colloidal Silver (Rajiv et al., 2015)
- Zeolite (Acidithiobacillus thiooxidans) (Haile et al., 2010)
- L Reuteri (Hurdle et al., 2009)
- Citrates (Bosma et al., 2010)– Calcium Citrate, Magnesium Citrate
- Norspermidine (found in chlorella) (Böttcher et al., 2013)

Enzymes

- Trypsin (Chaignon et al., 2007)
- Serratiopeptidase (Mecikoglu et al., 2006)
- Nattokinase (Zapotoczna et al., 2015)

Herbal Biofilm Disruptors

- Andrographis (Murugan et al., 2011)
- Curcumin (Zorofchian Moghadamtousi et al., 2014)
- Berberine (Wang et al., 2009)
- Cinnamon/Cinnamaldehyde (Liu et al., 2015) and Cinnamon essential oil (Kavanaugh et al., 2012)
- Black cumin oil/Thymoquinone (Chaieb et al., 2011)
- Boswellia (Raja et al., 2011)
- Vanilla
- Ginkgo

- Oregano Oil (carvacrol+thymol) (Nostro et al., 2007)
- Quercetin (Pejin et al., 2015)
- Apigenin, Naringenin, Kaempferol (Vikram et al., 2010)
- St John's Wort (Sarkisian et al., 2012)
- Baicalein (Goc, 2015)
- Neem (Garg, 2013), (Harjai et al., 2013)
- Gentian violet (Wang et al., 2008)
- Mangosteen (streptococcus) (Nguyen et al., 2014)
- Alfalfa (Sadowska et al., 2014)
- Eugenol (Liu, 2015) (Magesh, 2013) (Kavanaugh, 2012) – found in Tulsi, clove essential oil and cinnamon essential oil

Other

- Farnesol (Alves, 2013)
- D-Amino Acids (Böttcher, 2013)
- Reserpine (Magesh, 2013)
- Rifampicin (Jacqueline et al., 2014)